Stability studies of a novel amine blend for the capture of CO_2 generated from indirect co-combustion of natural gas and biomass

A Thesis

Submitted to the Faculty of Graduate Studies and Research

in Partial Fulfilment of the Requirements

for the Degree of

Master of Applied Science

in

Process Systems Engineering

University of Regina

By

Raymond Owiredu Asante

Regina, Saskatchewan

September, 2024

UNIVERSITY OF REGINA

FACULTY OF GRADUATE STUDIES AND RESEARCH

SUPERVISORY AND EXAMINING COMMITTEE

Raymond Owiredu Asante, candidate for the degree of **Master of Applied Science in Process Systems Engineering,** has presented a thesis titled, ***Stability studies of a novel amine blend for the capture of CO2 generated from indirect co-combustion of natural gas and biomass,*** in an oral examination held on **August 21, 2024**. The following committee members have found the thesis acceptable in form and content, and that the candidate demonstrated satisfactory knowledge of the subject material.

External Examiner:	Dr. SD Jacob Muthu, Energy and Industrial Systems Engineering
Supervisor(s):	Dr. Raphael Idem, Industrial & Process Systems Engineering
Committee Member:	Dr. Teeradet Supap, Adjunct Professor, Faculty of Engineering and Applied Science
Committee Member:	Dr. Paitoon (P.T.) Tontiwachwuthikul, Industrial & Process Systems Engineering
Chair of Defense:	Dr. Abu Bockarie, Faculty of education

ABSTRACT

The excessive release of CO_2 from human activities has led to global warming and climate change, becoming a critical global issue for many years. Data released by the Environment Protection Agency of United States in 2022 clearly shows that, CO_2 is the most emitted gas among other greenhouse gases. In response, numerous strategies have been developed to address this pressing problem. One particularly compelling approach is to use an optimal mix of fuels in combination with post-combustion capture technology to achieve net-zero or even negative CO_2 emissions. Over the past years, solvent absorption in post-combustion capture technology has shown significant reliability and efficiency in reducing CO_2 emissions. Despite this, investors face major challenges such as the cost of solvents, solvent loss, and the expenses involved in solvent regeneration.

Monoethanolamine (MEA) is the most extensively studied alkanolamine absorbent and serves as the benchmark for evaluating other absorbents. MEA is recognized for its high absorption rate, low cost, and low viscosity. However, MEA is prone to a high degradation rate, which leads to significant solvent loss. In the field of CO_2 capture, degradation refers to the diminished capacity of the solvent to effectively capture CO_2 as expected during the capture process. This degradation is primarily caused by undesirable side reactions between the absorbent and impurities in the flue gas, such as oxygen, NOx, SOx, particulate matter, and heavy metals. Degradation is an endothermic reaction so the process is favoured at high temperature in the presence of these flue gas impurities.

Solvent degradation is an important parameter to consider during solvent selection for commercial use in CO_2 capture process. It does not only lead to solvent loss but degradation products like carboxylic acids and heat stable salt (HSS) promotes corrosion. Also, nitrosamines emitted due to

some absorbent reaction with NOx poses threat to human health. There are chances of fouling and solvent foaming due to degradation. Least to mention is the increase in cost of operation due to increase in heat duty required for regeneration because of the presence of degradation products.

This work demonstrates the stability of 4M AMP:1-(2 HE) PRLD. The novel amine blend was subjected to some conditions mimicking CO_2 capture for flue gas generated from indirect co-combustion of natural gas and biomass. When it was compared with a known amine blend, thus, 5M MEA:DMAE under same conditions, 4M AMP:1-(2 HE) PRLD, proved to be inherently more stable. It had a 33% increase in its rate in degradation as against 80% increment when the oxygen partial pressure was doubled keeping all other conditions constant. This implies the novel amine blend is stable and can be used commercially for the capture of CO_2 from pretreated flue gas. The results highlight its resilience and potential for long-term application in environments where oxygen levels may fluctuate without succumbing easily to the degradation processes that typically affect similar compounds. A kinetic model was generated for the rate of degradation and it is of the form:

$$\mathbf{r}\left(\frac{\mathbf{M}}{\mathbf{hr}}\right) = \mathbf{6.8222} \times \mathbf{10^9} e^{\left(\frac{-50314.08}{8.314 \times T}\right)} [\boldsymbol{O_2}]^{\mathbf{1.3}}$$

ACKNOWLEDGEMENT

All glory be to the Lord Almighty for His boundless grace which was sufficient for me in accomplishing this academic journey successfully.

I am deeply grateful to my supervisor, Dr. Idem, for his invaluable patience, guidance, and particularly his financial support throughout this research. His patience during the early stages of the project was truly remarkable. This project would not have come to fruition without his supervision and unwavering assistance.

I also extend my heartfelt thanks to several key individuals: Dr. Teeradet Supap, Dr. Pailin Muchan, Dr. Paweesuda Natewong, Ms. Jessica Narku-Tetteh, and Mr. Foster Appiah. I am sincerely grateful for your steadfast support and encouragement during this journey.

I would also like to express my gratitude to my colleagues Thomas Boakye, Domfeh Adjei, Emma Brakwah, Patience Bekoe and Samuel Nii-Adjei Adjetey, who have provided immense support throughout this project. Your contributions and encouragement have been invaluable, and for that, I thank you.

Lastly, I wish to extend my heartfelt appreciation to the National Science and Engineering Research Council of Canada (NSERC), the Canada Foundation for Innovation (CFI), the Government of Saskatchewan, the Faculty of Graduate Studies and Research, and the Clean Energy Technologies Research Institute for their financial support throughout my graduate studies.

DEDICATION

This achievement is to my dad, Dennis Asante, my mum, Helina Asante, my brothers Rudolph and Roland, as well as Alexandra and finally Ruby of beloved memory.

Together, we have achieved this!!

TABLE OF CONTENTS

LIST OF TABLES

LIST OF FIGURES

LIST OF APPENDICES

LIST OF ABBREVIATIONS

1-(2-HE) PRLD 1-(2-hydroxyethyl) pyrrolidine

AAD Average absolute deviation

AMP 2-amino-2-methyl-1-propanol

DMAE Dimethylethanolamine

BECCS Bio-energy with Carbon Capture and Storage

CCSU Carbon Capture Storage and Utilization

DAC Direct Air Capture

MEA Monoethanolamine

NH_3 Ammonia

O_2 Oxygen

GC-MS Gas Chromatography-Mass Spectrometry

GHG Greenhouse Gases

PPE Personal Protective Equipment

PCC Post combustion capture

ppm part per million

WHMIS Workplace Hazardous Materials Information Systems

TRANSPARENCY STATEMENT

I solemnly declare to use ChatGPT 3.5 to rephrase some of my sentences as well as improve some grammar and sentence structure in Chapters 1,2 and 4 of this document. I acknowledge that the above-mentioned technology was the only one deployed and issues regarding biased, discriminatory, incomplete and inaccurate outputs have been corrected and some renounced. I also acknowledge that I am solely responsible for the accuracy and academic integrity of this thesis.

CHAPTER 1 INTRODUCTION

1.1 Global Warming and Climate Change

In recent times, the world has been grappling with a pivotal challenge, namely, global warming and climate change. The emergence of this concern stems from the undue emission of certain greenhouse gases mostly from human activities. According to the United States Environmental Protection Agency, the main greenhouse gases (GHGs) usually emitted as shown in Figure 1.1 and Figure 1.2 are, carbon dioxide (CO_2), methane (CH_4), nitrous oxide (N_2O) and several fluorine-containing halogenated substances (HFCs, PFCs, SF_6 and NF_3)(Camobreco et al., 2024). The emission of these heat-trapping gases has significantly impacted the environment and human communities. Their presence in the atmosphere has intensified flooding, forcing people to abandon their homes. It has also prolonged droughts, which have caused severe food shortages. Last but not least, it has promoted wildfires which have ravaged vegetation and wildlife habitats, leading to widespread ecological destruction.(Camobreco et al., 2024)

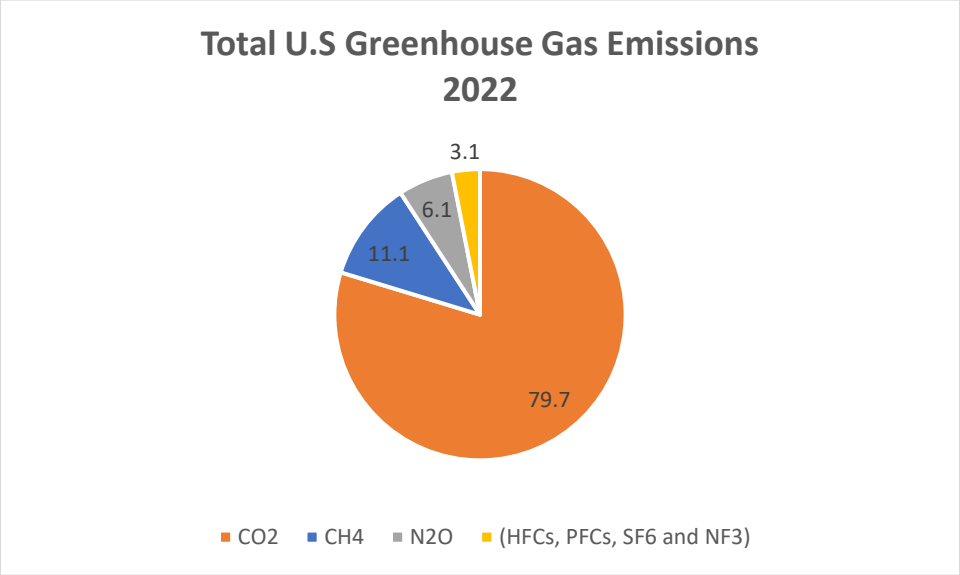

Figure 1.1: A chart of U.S GHGs emission in 2022(Camobreco et al., 2024)

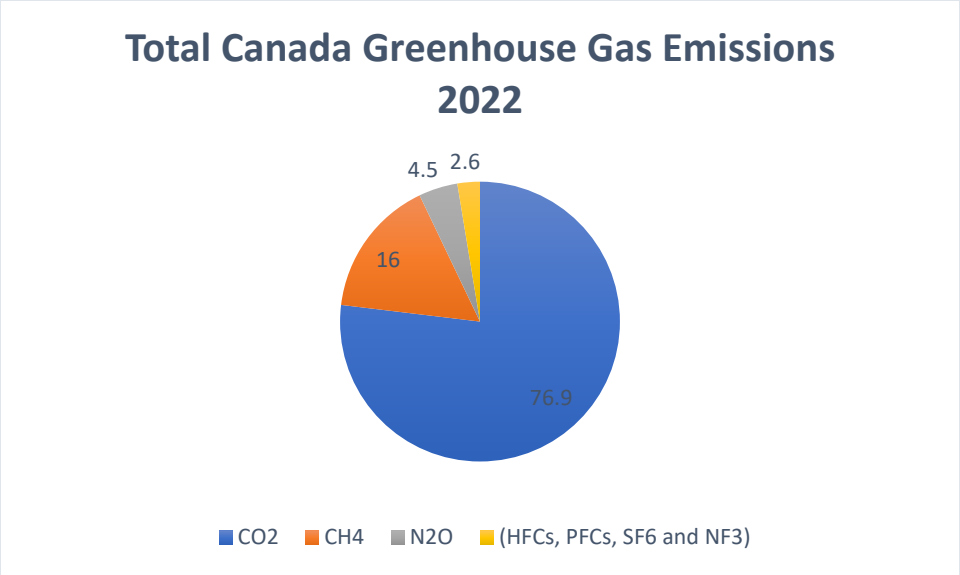

Figure 1.2: A chart of Canada GHGs emission in 2022(Camobreco et al., 2024)

1.2 CO_2 Emission

Worldwide, carbon dioxide is recognized as the most prevalent greenhouse gas released into the atmosphere. Since 2021, its levels have risen by 0.7%, a trend largely attributed to the burning of fossil fuels for energy production. This uptick highlights the ongoing reliance on coal, oil, and natural gas as primary energy sources(Camobreco et al., 2024; Natural Resources Canada, 2021). Compared to other greenhouse gases such as methane, carbon dioxide has a lower heat-trapping potential. However, CO_2 lingers in the atmosphere for hundreds of years, leading to prolonged warming effects. While methane exerts a stronger warming influence over a shorter period, the persistent presence of CO_2 in the atmosphere ultimately results in comparable long-term climate impacts(Camobreco et al., 2024). Sectors classified to be the sources CO_2 emission are; the industry sector, transportation sector, commercial sector and residential sector (Figure 1.3). A 2021 report from Natural Resources Canada indicates that approximately 81% of the nation's carbon dioxide emissions stem from burning fuels for energy production. This substantial contribution is

largely due to the country's expansive geographic area and dispersed population, necessitating extensive energy use for transportation and infrastructure. Additionally, the extreme cold temperatures experienced across the country drive increased heating demands, further elevating fuel consumption and CO_2 emissions(Natural Resources Canada, 2021).

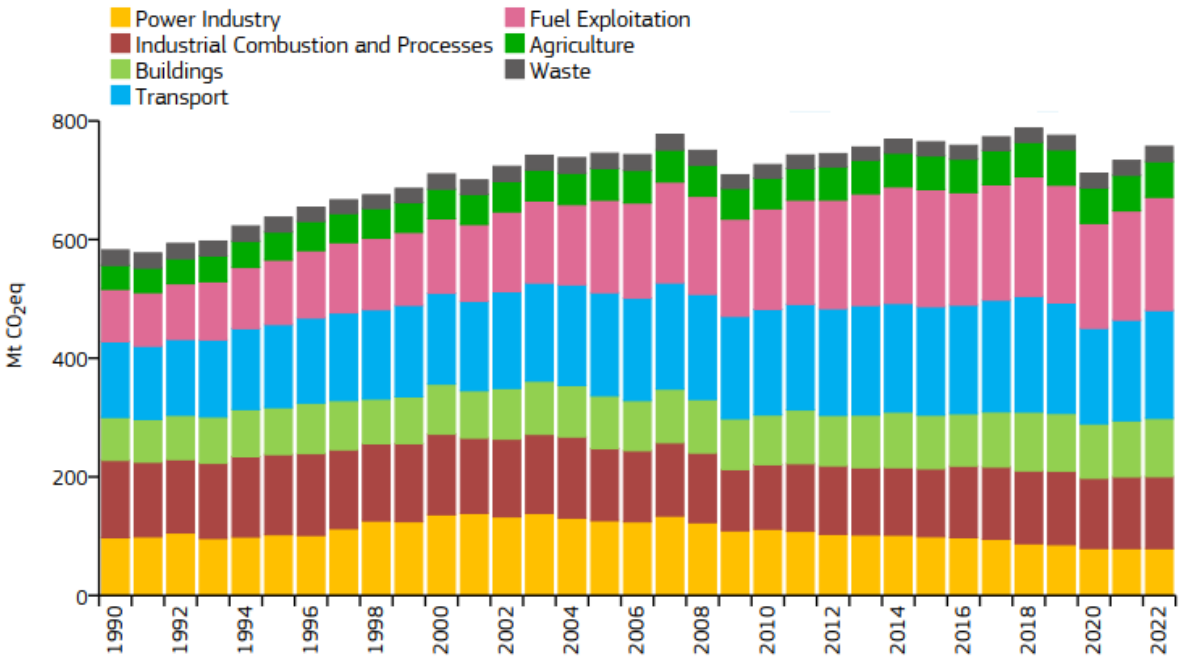

Figure 1.3: A chart of Canada Carbon emission from 1990-2022 in various sectors(Camobreco et al., 2024)

1.3 Carbon Capture Storage and Utilization (CCSU)

In the annals of industrial evolution, the concept of CCSU dates back to 1920s, where CO_2 together with other acid gases were removed from natural gas to form sweet gas. As time pressed forward, the oil and gas industry uncovered a use for the captured CO_2 by deploying it in reservoirs to increase the yield of oil explored. This pioneering technology was termed enhanced oil recovery

(EOR) and made its inaugural debut amidst the Texan landscape in the year 1977(IEAGHG, 2012). In order to mitigate the emission of carbon dioxide and curb the emission repercussions, extensive researches have been carried out to develop dependable processes and strategies.

1.4 Process and Strategies for CO_2 Mitigation

1.4.1 Mineralization of Carbon

This process involves the conversion gaseous carbon dioxide into solid state. The chemical reaction takes place between CO_2 and metals cations such as magnesium, calcium and iron to produce carbonates. The process can broadly categorise into two methods. These are; in situ mineralization also known as mineral trapping and ex situ mineralization(Avor et al., 2022; Romanov et al., 2015).

In situ mineralization is an aspect of geological sequestration in which CO_2 is injected into the ground at a suitable pressure to react with the alkaline minerals present within the earth crust to form solid carbonate species(Romanov et al., 2015).

In ex situ mineralization, the carbonation reaction occurs above ground, within a separate reactor or industrial process. The process was first developed within the 1990's at Los Alamos National Laboratory where calcium and magnesium bearing silicate minerals are reacted with CO_2(Romanov et al., 2015).

1.4.2 Afforestation and Reafforestation

Both the processes of afforestation and reafforestation culminate in the establishment of forested areas. However, their distinction lies in their origins: afforestation involves the creation of entirely new forests, while reafforestation focuses on the restoration of previously lost forests due to degradation or destruction. This process is regarded as a natural and economical means of sequestering CO_2 from the atmosphere.

In this natural orchestration, atmospheric CO_2 is harnessed by plants through the process of photosynthesis. During this intricate biochemical dance, green plants convert CO_2 into glucose and oxygen with the assistance of sunlight. The expansion, restoration, and adept management of forests facilitate increased CO_2 uptake from the atmosphere, thus contributing to efforts aimed at curbing atmospheric CO_2 levels.

However, this endeavour may inadvertently engender competition with agricultural lands and human settlements, potentially impacting food supplies and population growth. Furthermore, given the alarming rate at which CO_2 emissions are escalating due to human activities, reliance solely on this method may prove insufficient in effectively mitigating climate change.

1.4.3 Direct Air Capture (DAC)

This process involves capturing of CO_2 directly from the atmosphere. The captured CO2 can be either stored underground or utilized in various applications such as chemical synthesis, beverage production, or cement manufacturing. The process can either take a physical pathway or chemical pathway. Currently, the technologies used for DAC can classified into three types. These are; chemical, cryogenic and membrane(Avor et al., 2022; Guel et al., 2022; Sandalow et al., 2018).

Chemical method for DAC involves the capturing of CO_2 from ambient air by reacting it with either a chemical solvent or a solid sorbent. Subsequently, the captured CO2 is pressurized or

heated to concentrate it for underground storage or utilization in chemical synthesis, cement production, or beverage manufacturing.(Sandalow et al., 2018).

The cryogenic method of CO_2 capture in DAC is freezing CO_2 out of air. This method is deployed also in oxygen production to separate oxygen from CO_2(Sandalow et al., 2018).

On the other hand, membrane method of CO_2 capture in DAC uses ionic exchange membranes or reverse osmosis membranes which reflects the concepts plants and animals used to separate CO_2 during their biological processes(Sandalow et al., 2018).

1.4.4 Bio-energy with Carbon Capture and Storage (BECCS)

BECCS, or Bioenergy with Carbon Capture and Storage, represents a technique that utilizes biomass as a primary fuel source for generating energy(Avor et al., 2022). This process relies on the idea that no new CO_2 is formed or generated. This is because, during photosynthesis, plants absorb CO_2 from the atmosphere form the carbon content need for energy generation. Consequently, when these plants are combusted, the released CO_2 is essentially equivalent to the amount previously absorbed during photosynthesis. In this manner, achieving net-zero CO_2 emissions is attainable, as no additional CO_2 is introduced into the atmosphere. Moreover, when the released CO_2 is captured using a capture plant and securely stored away from the atmosphere, negative emissions can be realized. Hence, BECCS effectively enables the attainment of negative emissions by indirectly extracting CO_2 from the atmosphere(Avor et al., 2022).

However, challenges accompany this technology, primarily concerning the requirement for bioenergy crops. This demand may encroach upon land used for food production, potentially disrupting agricultural systems and altering ecosystems. Consequently, this could nullify the climate benefits of BECCS and exacerbate global food insecurity and ecosystem degradation(Avor et al., 2022).

1.4.5 Carbon Capture from Point Source

This process is usually used to reduce CO_2 emissions from large point-sources such flue gas from power generation plants, iron and steel industries, refinery industries and cement industries. Subsequently, the captured CO_2 from generated emissions is concentrated under suitable conditions, compressed, transported, stored under geological traps or utilization for enhanced oil recovery, fertilizers and other chemical syntheses(Appiah, 2021; Nakao et al., 2019; Narku-Tetteh et al., 2017). From literature, carbon capture has the potential to can cause a significant reduction of about ninety percent (90%) of CO_2 emitted from power plants (Song et al., 2018). This process technology can be classified into three broad types namely; post-combustion capture, pre-combustion capture and oxy-combustion capture. CO_2 concentration in flue gas stream, fuel type and the gas stream pressure are some of the important factors that should be considered before deciding on any of the options(Appiah, 2021; Narku-Tetteh et al., 2017; Vega et al., 2014a).

1.4.5.1 Pre-combustion capture

Pre-combustion capture is the removal of CO_2 from fuels before complete combustion. As shown in Figure 1.4, the primary fuel in a reactor is processed usually with steam and air or oxygen to produce syngas thus a mixture of hydrogen and carbon monoxide(Figueroa et al., 2008; Narku-Tetteh et al., 2017). Subsequently, with the same principle used in hydrogen production, water-gas shift reaction (WGSR), carbon monoxide is reacted with steam in a thermo-catalytic reaction to form carbon dioxide and hydrogen. The product from the WGSR is separated into streams of hydrogen and carbon dioxide either by absorption, adsorption or membrane. CO_2 captured can either be stored underground or used to produce cement, drinks or chemicals. Also, the hydrogen-rich stream can be used in various applications, such as reboilers, engines, gas turbines, and fuel cells. This technology is particularly effective for capturing CO_2 at high partial pressures, making it widely used in CO_2 capture from natural gas, hydrogen production, coal gasification plants for,

power, urea and ammonia production(Appiah, 2021; Avor et al., 2022; Figueroa et al., 2008; Institute, 2012; Nakao et al., 2019; Narku-Tetteh et al., 2017; Song et al., 2018). The intricate nature of the process, coupled with the high cost of equipment and the scarcity of gasification plants suitable for retrofitting, has constrained its widespread implementation (Figueroa et al., 2008).

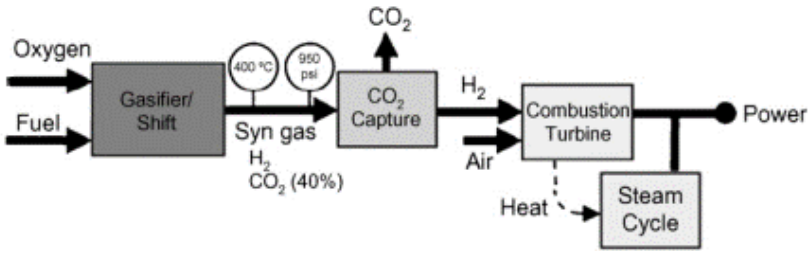

Figure 1.4: Schematic diagram illustrating pre-combustion capture (Figueroa et al., 2008)

1.4.5.2 Oxy-combustion capture

In the oxy-combustion process, fuel is burned in a pure oxygen environment. This involves using an air separation unit to extract nitrogen from the air, resulting in a high-purity oxygen stream for combustion, which primarily produces CO_2 and water (Figure 1.5). The air separation is achieved through a low-temperature process. While this technology can be retrofitted into existing plants, it comes with significant drawbacks, including the high capital cost of the air separation unit and the challenges associated with integrating this technique into existing facilities(Appiah, 2021; Figueroa et al., 2008; Narku-Tetteh et al., 2017; Song et al., 2018).

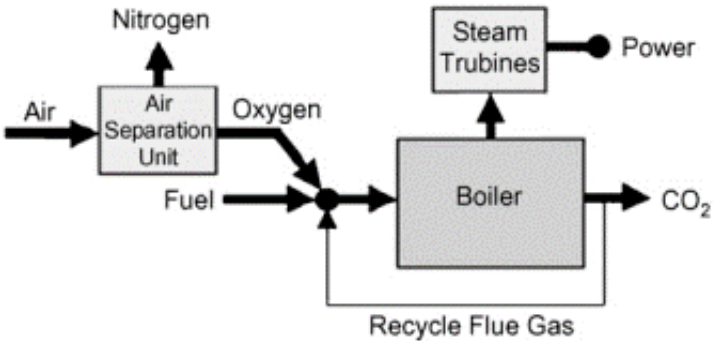

Figure 1.5: Schematic diagram illustrating oxy-combustion capture (Figueroa et al., 2008).

1.4.5.3 Post-combustion capture

In the post-combustion process, CO_2 is extracted after the fuel has been completely burned, similar to the oxy-combustion process, but without the need for a pure oxygen environment. This process technology uses techniques like absorption, adsorption, cryogenic separation, or membrane separation to capture the CO_2. The post-combustion approach is popular because it can be easily integrated into existing plants and also capture CO_2 in flues gas with low CO_2 partial pressure(Appiah, 2021; Figueroa et al., 2008; Nakao et al., 2019; Narku-Tetteh et al., 2017; Song et al., 2018).

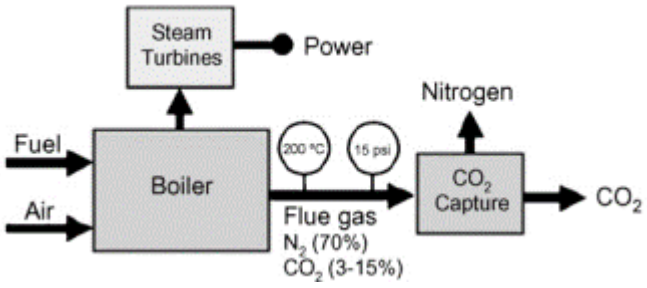

Figure 1.6: Schematic diagram illustrating post-combustion capture(Figueroa et al., 2008).

1.5 Techniques for CO_2 separation in Carbon Capture from Point Source

1.5.1 Cryogenic

The cryogenic technique for separating CO2 from flue gas involves extracting CO2 at extremely low temperatures. This technique leverages the distinct condensation and desublimation properties of different components within the flue gas. Typically, this separation is conducted under high-pressure conditions. The combination of very low temperatures and high pressures makes this process energy-intensive. Despite the high energy demands, the cryogenic separation method boasts a high CO2 capture efficiency, typically ranging from 90 to 95%.(Leung et al., 2014).

1.5.2 Adsorption

Adsorption is a technique for separating CO_2 from flue gas using solid sorbents. This method is particularly effective for flue gas streams with high partial pressure CO_2. The nature of the adsorption process can be either physical or chemical, depending on the type of solid sorbent used(Leung et al., 2014; Nakao et al., 2019).

- **Physical Adsorption**: In physical adsorption, the CO_2 molecules adhere to the surface of the sorbent through weak van der Waals forces. This type of interaction is generally reversible and can be managed through a process known as pressure swing adsorption (PSA), where changes in pressure facilitate the release of the adsorbed CO_2. Example of sorbents in this category are: zeolite and activated carbon(Nakao et al., 2019).

- **Chemical Adsorption**: Chemical adsorption involves the formation of strong chemical bonds between the CO_2 molecules and the sorbent. This interaction is more robust and typically requires a process called thermal swing adsorption (TSA) to release the CO_2, where heating the sorbent enables desorption. Example of sorbents in this category are: amine support inorganic porous material, lithium silicate and calcium oxide(Nakao et al., 2019).

Due to the differences in bonding strength, PSA is more suitable for physical adsorption, while TSA is more appropriate for chemical adsorption. Both methods are integral to efficiently managing the adsorption and subsequent desorption of CO_2, making the process adaptable to different operational needs and conditions. Some criteria for selecting an adsorbent are large specific surface area, high selectivity and high regeneration ability.

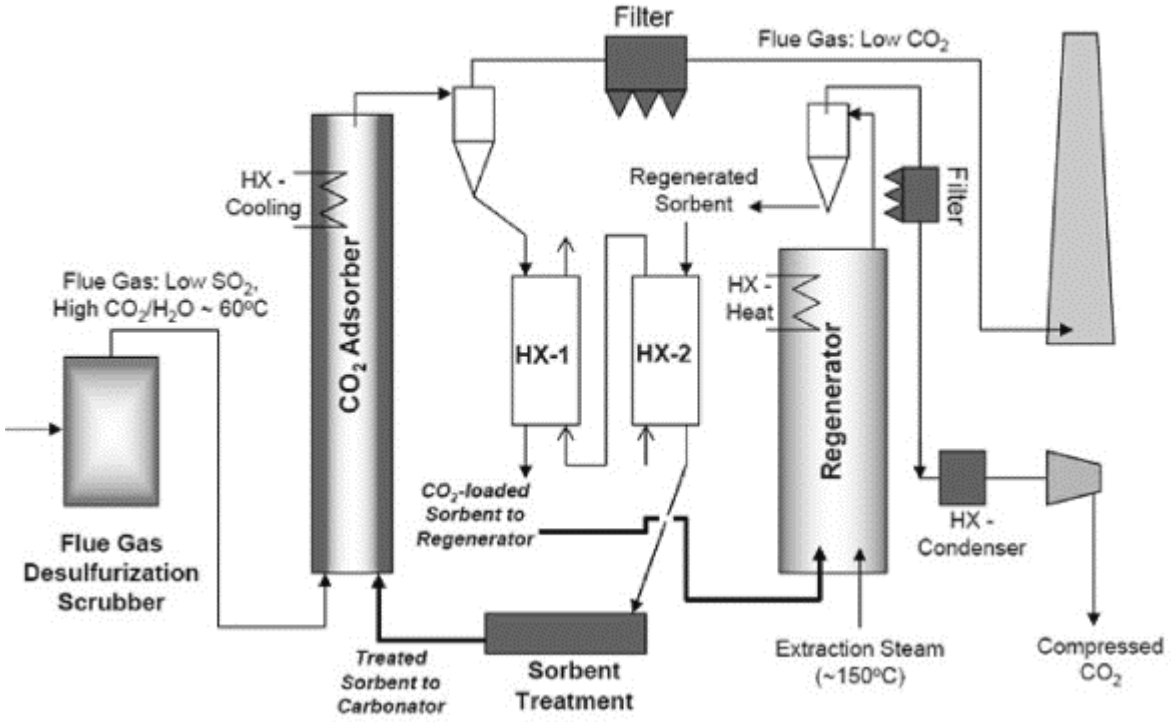

Figure 1.7: Post combustion process using adsorption technique(Nakao et al., 2019).

1.5.3 Membrane Separation

Membrane separation is one of the promising separation processes gaining much interest in recent times. Studies shows that, it is simply to operate and also energy efficient(Nakao et al., 2019). By far, two types that are advanced in research and utilization in gas separation is the conventional membrane and membrane contactor.

- **Conventional membrane:** This type of membrane can be utilized across all three primary classifications of carbon capture from point sources. In post-combustion and oxy-combustion scenarios, where CO_2 is separated from flue gas, a substantial portion of the membrane separation cost is attributed to operating the vacuum pump needed to clear the permeate side of the membrane. Conversely, in pre-combustion CO_2 separation, membrane technology can significantly lower CO_2 capture costs because high-pressure gas separations do not require a vacuum pump or compressor. Conventional membrane techniques depend largely on diffusion for gas separation by selective permeation through a membrane layer. The driving force for this separation is typically provided by flue gas compression, a sweep on the permeate side, application of a permeate-side vacuum, or a combination of these methods(Appiah, 2021; Nakao et al., 2019; Song et al., 2018).
- **Membrane contactor:** This type of membrane, unlike conventional ones, utilizes the partial pressure differences of each gas component across the membrane as the driving force for separation. It is versatile and can be applied to all three primary categories of carbon capture from point sources: post-combustion, pre-combustion, and oxy-combustion. However, a significant challenge in its application is the increased mass transfer resistance, particularly when the membranes become wetted. This wetting issue can hinder the efficiency of the gas separation process, making it a critical factor to address in practical applications.

1.5.4 Absorption

Absorption is a process used to capture CO_2 from flue gas by employing solvents. This method proves quite effective for flue gas streams where the CO_2 partial pressure is low. According to Henry's law, which asserts that the concentration of a dissolved gas in a solvent is directly proportional to the gas's partial pressure, we can predict the amount of CO_2 a solvent can absorbs(Nakao et al., 2019). This relationship allows us to calculate the CO_2 absorption capacity

of the solvent by knowing the partial pressure of CO_2 in the gas stream. In this procedure, the pre-treated flue gas interacts with a solvent in a counter-current flow within an absorption column, leading to the CO_2 being absorbed by the solvent(Appiah, 2021; Nakao et al., 2019; Song et al., 2018). Absorption is most effective at lower temperatures, with most industries employing this method typically operating in the 40°C to 60°C range(Narku-Tetteh et al., 2017). The solvent, now rich in CO_2, exits from the bottom of the absorber, while the cleaned gas leaves from the top. The CO_2-loaded solvent then undergoes regeneration, which can be achieved either by heating it or by reducing the pressure. The regenerated solvent, now depleted of CO_2, is cycled back to the absorber, allowing the capture process to continue. This regeneration step is commonly known as desorption and takes place in a desorption column(Appiah, 2021). This technique can be classified into two types, these are; physical absorption and chemical absorption(Nakao et al., 2019).

- **Physical absorption**: This technique involves the use of a physical solvent for CO_2 absorption. During this process, there is no chemical reaction between CO_2 and the solvent. Instead, the method relies primarily on mass transfer, driven by the concentration gradient between the gas and liquid phases. Because CO_2 is not chemically bonded to the solvent, regeneration is most often achieved by lowering the pressure of the CO_2-rich solvent. One major drawback of this method is the slow rate of CO_2 capture, which necessitates the construction of tall absorption columns to achieve high efficiencies, thereby increasing costs. Examples of physical solvents used in this process include methanol, water, and Selexol (dimethyl ether of polyethylene glycol)(Nakao et al., 2019; Narku-Tetteh et al., 2017; Song et al., 2018), (Henni, 2022).

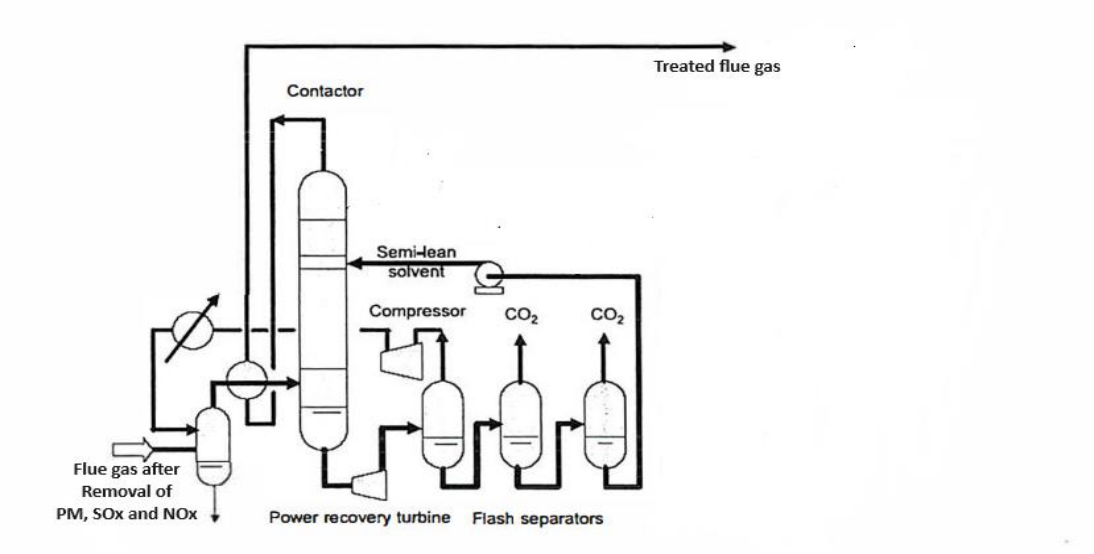

Figure 1.8: Flow diagram of physical absorption process (modified) (Henni, 2022)

- **Chemical absorption**: This technique on the other hand uses a chemical solvent for the capture of CO_2. The chemical solvent must be a base. Due to the chemical interaction that exist between the solvent and CO_2 during the capture process, the rate of CO_2 capture or loading into the solvent is influenced by both mass transfer and chemical reaction(Henni, 2022; Idem, 2021). However, because there is a stronger bond formed after the interaction, the regeneration of solvent usually achieved by heating. The challenge associated with this technique high cost in solvent regeneration due to high energy demand and also solvent degradation which leads to fouling, corrosion and solvent loss(Ofori et al., 2020; Song et al., 2018). Examples of chemical solvents used in this process include: potassium glycinate (KG), monoethanolamine (MEA) and sodium hydroxide (Appiah, 2021; Henni, 2022; Nakao et al., 2019; Narku-Tetteh et al., 2017; Song et al., 2018).

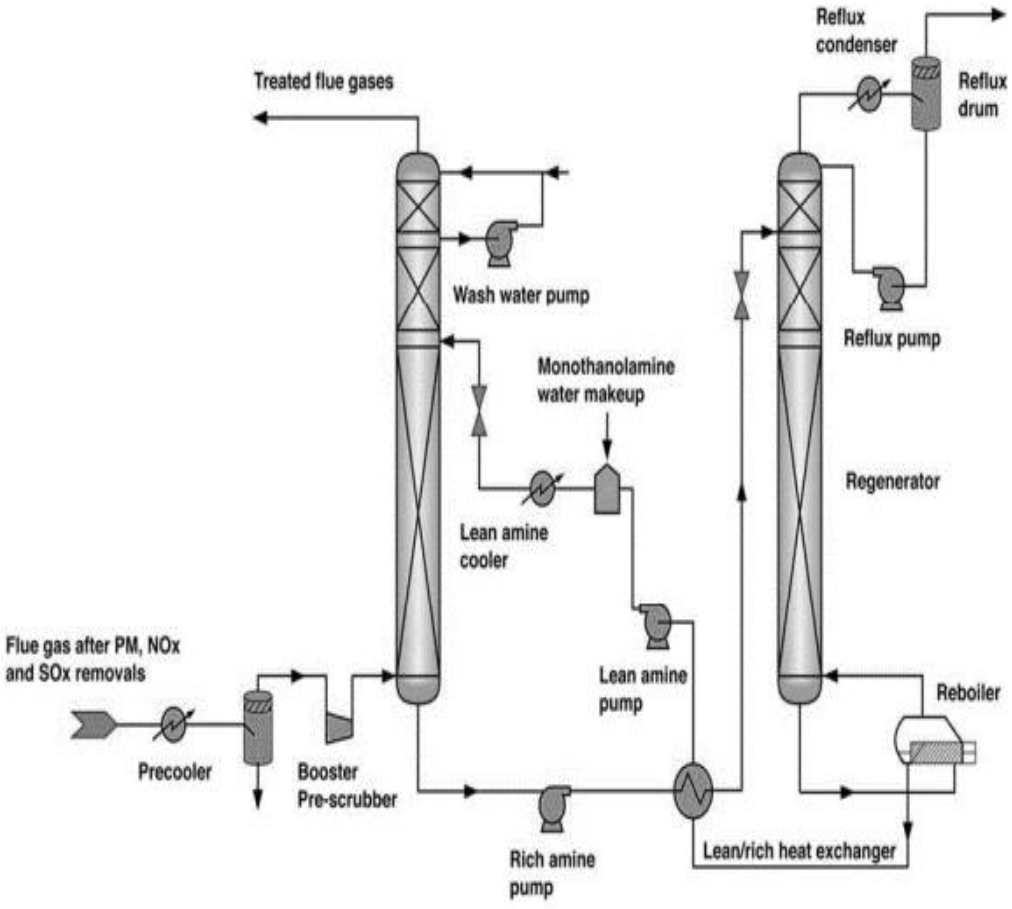

Figure 1.9: Flow diagram of chemical absorption process (Liang et al., 2011)

1.6 Research Problem

Amine degradation poses a significant challenge in amine-based post-combustion CO_2 capture. This degradation is unavoidable due to the presence of contaminants such as O_2, SOx, NOx, and metal oxides in the flue gas. Managing amine degradation is crucial for both economic efficiency and environmental safety.

The current best practices involve selecting or developing amine solvents that are more chemically stable and resistant to degradation, or using inhibitors to mitigate the degradation process. Additionally, pre-treating the flue gas to eliminate potential degradation agents is another approach. For example, electrostatic precipitators and membrane technologies can effectively remove metal oxides, while scrubbers can be employed for desulfurization and denitrification to eliminate SOx and NOx.

However, completely removing oxygen from flue gas remains unfeasible with current technologies. As a result, the degradation of amines due to oxygen will depend on the inherent stability of the specific amine used in the capture process and or chemically synthesised degradation inhibitors.

In 2022, Avor et al., formulated an amine solvent thus, a blend of 2-amino 2-methyl propanol (AMP) and 1-(2-hydroxyethyl) pyrrolidine (1-(2-HE) PRLD) in the ratio of 2:2 to form a concentration of 4M AMP: 1-(2-HE) PRLD. This solvent showed great potential in carbon capture by having a CO_2 removal efficiency of 31% (at desorption temperature 110^oC) higher than the benchmark solvent, 5M MEA(Avor et al., 2022). This same amine blend based on life cycle analyses (LCA) when used in CO_2 absorption promotes net zero CO_2 emission by using 6.3% less producer gas than the bench mark solvent(Avor et al., 2022). In this current study, the inherent

stability of this novel amine blend is examined by using conditions mimicking real time CO_2 capture plant of a pretreated flue gas.

1.7 Research Objectives

1.7.1 Main Objective

The main objectives of this research work are:

i. To determine the inherent stability of 4M AMP: 1-(2-HE) PRLD in the capture of CO_2 from a pretreated flue gas.
ii. To develop a kinetic model for the rate of degradation.
iii. To develop a relation between rate of degradation and ammonia emissions.

1.7.2 Specific Objectives

The specific objectives include:

i. Evaluate the stability of the novel blend under absorption conditions during CO_2 capture process.
ii. Evaluate the effect of temperature and partial pressure oxygen on the novel solvent
iii. Perform non-linear regression analysis on the experimental data to generate a kinetic model for the reaction between oxygen and the novel amine blend.
iv. Estimate the activation energy (E_a) for novel amine blend formulated.

1.8 Layout Out Thesis

Chapter 1 delves into carbon capture and storage technologies, discussing their advantages and disadvantages, and explaining the motivation behind the study.

Chapter 2 examines the current understanding of amine stability and emission pathways. It offers a comprehensive literature review on the chemistry of amine degradation and the role of oxygen in influencing this process.

Chapter 3 outlines the experimental methods used to achieve the research objectives. It includes a detailed description of the equipment and chemicals, the experimental procedures, and the analytical methods employed to assess solvent stability in a semi-batch mode.

Chapter 4 presents the experimental results and findings, elaborating on the data obtained from the experiments. It also includes a discussion on the observed data trends, providing justification for the results.

Chapter 5 concludes the research work, offering relevant recommendations for future studies.

CHAPTER 2 LITERATURE REVIEW

2.1 Solvents for CO_2 Capture

The utilization of amine compounds as chemical solvents to absorb carbon dioxide traces its origin back to the 1930s. This approach was implemented based on the recommendation of R.R. Bottoms, specifically for the purpose of eliminating acid gases from flue gas stream(Bottoms, 1930; Lidal, 1992). From that point onward, thorough investigations have been conducted on amines, with monoethanolamine (MEA) gaining widespread recognition as the benchmark to any other chemical solvent employed in capturing carbon dioxide (Avor et al., 2022; Narku-Tetteh et al., 2017).

In a broad sense, amines can be categorized into three groups based on the quantity of hydrogen atoms connected to the nitrogen atom within the amine molecule. These groups are primary amines, secondary amines and tertiary. There exist some special forms of amines namely the sterically hindered amine and the cyclic amines. Despite their classification further categories, these forms of amine can be placed under any one of the aforementioned three categories. Hence having gained recognition due to their distinctive characteristics observed during reactions involving amine-water-acid gas reaction systems(Muchan et al., 2021)(Narku-Tetteh et al., 2017).

2.2 Primary amines

These particular amines possess a chemical structure wherein two hydrogens are attached to the nitrogen atom. They are acknowledged as strong bases compared to the other two amine types. Typically, they exhibit a notable rapid rate of absorption initially and possess low vapor pressure, consequently resulting in a high boiling point. Nevertheless, primary amines exhibit a pronounced inclination to undergo some degradation when employed for CO2 capture in flue gas stream.

Moreover, during capture, the regeneration process demands substantial heat energy in order for the absorbed gas to be released from the chemical solvent for reuse. Examples of such amines include monoethanolamine (MEA) and diglycolamine (DGA)(Avor et al., 2022; Chowdhury et al., 2014)

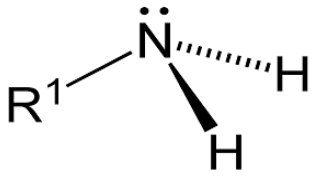

Figure 2.1: Structure of a primary amine

2.3 Secondary amines

Secondary amines on the other hand are amines that have one hydrogen attached to the nitrogen atom in its chemical structure. They are considered as mild bases relative to the other two types of amines. They are noted to mostly have intermediate properties between that of primary and tertiary amines. Some common examples are diethanolamine (DEA) and dimethylamine (DMA)(Avor et al., 2022; Chowdhury et al., 2014).

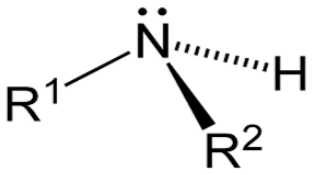

Figure 2.2: Structure of a secondary amine

2.4 Tertiary amine

These are amines that have no hydrogens attached to the nitrogen atom in its chemical structure. They are considered as weak base relative to the other two types of amines. Generally, they are noted to have low initial rate of absorption and high vapour pressure hence increasing the rate of solvent loss by vaporization. Nevertheless, tertiary amines exhibit minimal susceptibility to degradation when employed for CO2 capture in flue gas. Also, they require a relatively lower heat energy for regeneration during the capture process. Some common examples are triethanolamine (TEA) and methyldiethanolamine (MDEA)(Avor et al., 2022; Chowdhury et al., 2014).

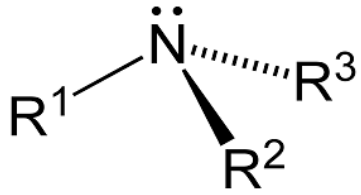

Figure 2.3: Structure of a tertiary amine

2.5 Amine Reaction with CO2 During Capture Process

Several published works on the reaction between amine and CO_2 have proven that, amines react with CO_2 to either form carbamate and or bicarbonate(Crooks & Donnellan, 1989; Narku-Tetteh et al., 2017),(Versteeg & van Swaaij, 1988),(Kim et al., 2016; Lv et al., 2015). This interaction between the aqueous amine and CO_2 can be classified under heterogenous reaction systems(Levenspiel, 1998). To form a carbamate and or a bicarbonate is dependent on the type of amine used in the capture of CO_2.

Generally, primary amines and secondary amines form carbamate and depending on the structure of the amine can go further to hydrolyse to form bicarbonate. For instance, MEA and DEA being a primary and secondary amine respectively forms a carbamate upon absorbing CO_2. However, a primary amine like 2-amino 2-methyl propanol (AMP) forms a carbamate which further undergoes hydrolysis to form bicarbonate due the steric hinderance inherent in its structure(Chakraborty et al., 1986; Sakwattanapong et al., 2009). Tertiary amines on the other form bicarbonate upon their interaction with CO_2.

2.6 Reaction Mechanism

As proposed by Caplow, Crooks and Donnellan, with regards to primary and second amines, there are indications from literature, leading to two potential reaction pathways with carbon dioxide (CO_2) namely, the zwitterion mechanism and the termolecular mechanism(Crooks & Donnellan, 1989; Kim et al., 2016). The termolecular reaction mechanism was first introduced by Crooks and Donnellan in 1989. They explained reaction to take place in a single step(Crooks & Donnellan, 1989).

$RNH + CO_2 + H_2O \leftrightarrow RNCOO^- + H_3O^+$

Nevertheless, the extensively employed zwitterion mechanism elucidates the reaction as a two-step process, incorporating an intermediate stage known as zwitterion formation, acknowledged as the rate-determining step. This conceptual framework was initially articulated by Caplow in 1968 and subsequently reintroduced with more comprehensive elaboration by Danckwerts in 1979 (Appiah, 2021; Kim et al., 2016).

$CO_2 + RNH_2 \leftrightarrow RN^+H_2COO^- + B$ (zwitterion formation)

$B + RN^{+}H_2COO^{-} \leftrightarrow BH^{+} + RNHCOO^{-}$ (carbamate formation).

Where the R species may be alkyl or alkanol chain and the base (B) can either be amine, OH^{-} or H_2O.

Sterically hindered primary amines have an additional step which leads to the bicarbonate formation through the process could hydrolysis(Chakraborty et al., 1986; Sakwattanapong et al., 2009).

$RNCOO^{-} + H_2O \leftrightarrow RNH + HCO^{-}_3$ (bicarbonate formation)

In the context of tertiary amines, the applicability of both the zwitterion and termolecular mechanisms is negated. This is attributed to the absence of a hydrogen atom linked to the nitrogen atom, preventing CO_2 displacement required for carbamate formation. Instead, tertiary amines exhibit a propensity for hydrolysis, leading to the generation of bicarbonate. The elucidation of this process as a base-catalysed hydrolysis was provided by Donald and Nguyen(Terrence & Yen, 1980).

$R_3N + H_2O \leftrightarrow R_3N^{+}H + OH^{-}$ (Protonation of amine)

$CO_2 + OH^{-} \leftrightarrow HCO^{-}_3$ (Hydrolysis of CO_2)

According to the assertions put forth by Shi in 2013, the preference for the base-catalysed hydrolysis of CO_2 into bicarbonates over carbamate formation is underscored by its comparatively lower regeneration energy demands(Shi, 2013). As a consequence of the reaction pathway outlined above, tertiary amines typically display a tendency to necessitate lower heat of desorption in general.

2.7 Amine Degradation

Amine degradation, pertains to the decline in the amine's efficacy to capture CO_2 as intended in the course of the capture process. Studies have shown that, this occurrence is caused by the molecular concentration reduction of the absorbent over time due to side reactions with flue gas components such as O_2, NO_x, SO_X and metal oxides. One other key factor that has been proven to aid in amine degradation is temperature. Supap et al., 2009 in their work demonstrated how temperature played a significant role in promoting MEA degradation. At an initial concentration of 5 kmol/m^3 MEA, the initial rate of degradation was noticed to be different for various set of experimental temperatures. The trend noticed was an increase in MEA degradation with increase experimental temperature(Supap et al., 2009).

Within the realm of CO_2 capture, there is a strong aversion towards degradation. This aversion stems from the adverse side effects resulting from interactions with the aforementioned flue gas components, giving rise to the production of specific byproducts. These byproducts, in turn, contribute to issues such as foaming, corrosion, and an elevation in the heat energy required for solvent regeneration. The substantial impact of degradation significantly contributes to an increase in operational expenses (Bello & Idem, 2005; Gouedard et al., 2012; Lepaumier et al., 2009; Supap et al., 2011).

In order to mitigate these adverse effects and the associated additional expenses that come with operation, certain industries employ the strategy of solvent reclamation. This involves the removal of degradation products through methods such as vacuum distillation and ion exchange [22]. Some sectors also opt for a preventive approach by eliminating flue gas components that contribute to degradation before reaching the capture plant. However, this method tends to be expensive, and the efficacy of the technologies employed has been less than optimal [22]. An alternative and

intriguing technology in use for degradation prevention is the incorporation of degradation inhibitors. These are chemical additives blended with the amine, undertaking side reactions on behalf of the amine while the latter concentrates exclusively on capturing CO_2 [23], [24].

2.7.1 Types of Amine Degradation

Amine degradation is commonly categorized into two primary types: oxidative degradation and thermal degradation. This classification from the literature can be linked to distinct stages within the capture process(Supap et al., 2011; Vega et al., 2014b).

2.7.1.1 Oxidative Degradation

This type of degradation occurs mainly in the absorber column. It is caused by the interaction between the amine and oxidizing agents such as O_2, NOx, SOx and metal oxides(Supap et al., 2011; Vega et al., 2014b). However, before there can be an interaction between the amine and the oxidizing agents, these oxidizing agents, present within the reaction stream need to first of all dissolve in the amine(Levenspiel, 1998; Nyarko, 2022; Vega et al., 2014b). This phenomenon can be elucidated through using the two-phase theory involving chemical reactions, wherein the solute, acting as the oxidizing agent, must surmount certain resistances related to mass transfer prior to engaging in solvent reaction(Levenspiel, 1998). This implies, the rate of oxidative degradation is dependent on both mass transfer and chemical interaction of the chemical structures involved (Levenspiel, 1998; Vega et al., 2014b). The diagram provided in Figure 2.4 offers a visual representation of the aforementioned conceptual framework (Idem, 2021). Thus research by Wang et al., 2013 demonstrated how the overall degradation of AMP and MEA increased with increase partial pressures of oxygen and temperature(Wang & Jens, 2013). Muchan et al.,2021 also demonstrated in her research how the various types of amines have different rates of oxidative degradation when exposed to similar conditions. Tertiary amines and sterically hindered amines

were found to exhibit very slow degradation rates relative to primary and secondary amines(Muchan et al., 2021). Supap et al., illustrated in their research how amines preloaded with CO_2 exhibit decreased oxidative degradation compared to those without CO_2 preloading. They associated their findings to the salting out effect that happens due to the presence of the CO_2.(Supap et al., 2009, 2011)

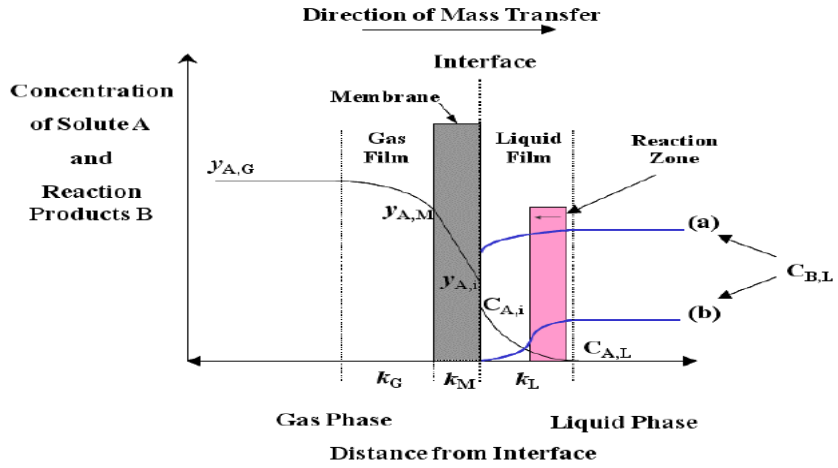

Figure 2.4: Two phase theory diagram(Idem, 2021)

2.7.1.2 Thermal Degradation

This type of degradation is used to describe degradation caused at high temperatures, typically within the operational range of a desorber and reboiler(Rochelle, 2012). In industrial operations, the optimal operating temperature for desorbers is contingent on thermal stability. Contrary to oxidative degradation, where CO_2 mitigates the rate of degradation, research indicate that, high partial pressure of CO_2 promotes thermal degradation(Gouedard et al., 2012; Lepaumier et al., 2009),(Buvik, Høisæter, et al., 2021). Davis et al., showed in their work how the rate of degradation of a primary amine, monoethanolamine (MEA), preloaded with CO_2 doubled when the CO_2 loading was doubled keeping other conditions constant(Davis et al., 2009). Mahmud et al., shared similar results when they studied the thermal stability of a tertiary amine, methyldiethanolamine

(MDEA). They observed a higher rate of degradation in the presence of CO_2 as compared to the absence of CO_2. According to several researches, a recognised method for mitigating thermal degradation is to reduce the amine hold up time at the bottom of the desorber where temperatures are usually at their peak(Rochelle, 2012).

2.8 Ammonia Emissions

During the process of capturing CO2 from flue gas using an amine solvent, various components within the flue gas interact with the amine to form a diverse range of by-products, some of which are highly volatile. Examples of these volatile by-products include ammonia, primary and secondary short-chain amines such as methylamine and ethylamine, as well as various acids, ketones, and aldehydes. These by-products can pose significant challenges in the capture process, potentially affecting efficiency and requiring additional handling and mitigation measures.(Gouedard et al., 2012; Sai-obodai, 2021; Spietz et al., 2018).

One of the significant concerns associated with amine-based CO2 capture technology is the release of emissions into the atmosphere from the capture plant. These emissions can lead to environmental and health problems upon their release. For example, certain by-products, such as nitrosamines, which are produced through side reactions between NOx present in the flue gas and the amine solvent, have been identified as carcinogenic. The presence of such harmful compounds in the atmosphere poses a risk to both human health and the environment, necessitating careful management and mitigation strategies to minimize their impact(Pradoo, 2021; Spietz et al., 2018).

To mitigate the emission of amines and volatile degradation products, the water wash technology was introduced in 1994(Kamijo et al., 2013; Spietz et al., 2018). This technology is used in

conjunction with demisters to effectively capture any entrained compounds leaving with the flue gas that interacts with the amines. A water wash section typically consists of a packed bed where water is continuously recycled. This recycled water serves to condense and absorb the volatile compounds, thereby significantly reducing their emissions. The combined use of water wash technology and demisters ensures that the amine solvent system operates more efficiently and with a lower environmental impact(Spietz et al., 2018).

Based on numerous reports on proposed amine degradation mechanisms, ammonia has been confirmed as one of the primary products of this reaction. The emission of ammonia during the CO_2 capture process is a key indicator of amine degradation. Typical methods for collecting and analysing these emissions in post-combustion capture plants include the use of boric acid impingers, H_2SO4 silica gel sorbents, and H_2SO4 on carbon beads. Analytical techniques such as indophenol blue absorption spectrophotometry, ion chromatography, and Fourier-transform infrared spectroscopy are employed to analyse these samples(Muchan et al., 2021; Nyarko, 2022; Pradoo, 2021; Sai-obodai, 2021).

The use of 0.05 M H_2SO4 as a trapping agent for ammonia was adapted from the Environmental Protection Agency (EPA) Method 5. This revised collection method has been widely adopted by industries and researchers and has proven to be effective in capturing and measuring ammonia emissions(Muchan et al., 2021; Nyarko, 2022; Pradoo, 2021; Sai-obodai, 2021).

2.9 Amine Degradation Kinetics, Mechanisms, Products and Inhibition

2.9.1 Degradation Kinetics

The main rationale for engaging in degradation kinetic analysis of a system is to develop a kinetic model that effectively forecasts the reaction patterns of the system across various conditions. The importance of kinetic models lies in their ability to efficiently conserve time and resources. Kinetic modelling enables the prediction of reaction rates, allowing for optimal reactor sizing without the necessity for extensive experimentation when conditions shift. In the case of amine degradation, it helps to know when the amine is no longer effective in capturing CO_2 under various conditions(Fogler, 2016; Levenspiel, 1998).

2.9.2 Kinetic Modelling

Up to this point, scholarly literature has offered limited coverage of kinetic models detailing the degradation of amines. The scarcity of such models can be linked to the meticulous and time-consuming nature of conducting experiments necessary to attain precise findings. Typically, the existing models demonstrate an average absolute deviation of about 25%(Vega et al., 2014b).

The two main types of kinetic modelling used are the power law model and mechanistic model approaches. While the power law model is known for its simplicity and straightforwardness, it has a drawback. It accurately predicts kinetics mainly within the specific conditions set during experimentation. Conversely, the mechanistic approach, albeit more complex and reliant on the reaction mechanism—including all intermediate steps—has the ability to forecast kinetics with a relatively higher precision, both within and beyond the predetermined experimental conditions(Fogler, 2016; Levenspiel, 1998).

2.9.3 Degradation Mechanism

The exploration of amine degradation mechanisms proves valuable when there is a need a need to develop an appropriate mechanistic model. Two prevailing pathways are followed, one, electron abstraction and two, hydrogen abstraction. These two stand as widely acknowledged mechanisms in this endeavour.

2.9.3.1 Hydrogen Abstraction Mechanism

The initiation step for hydrogen abstraction is the formation of the carbocation which is believe to be the rate determining step(Vega et al., 2014b),(Wang & Jens, 2014),(Ashenhurst, 2023). This mechanism usually ends up producing ammonia, formic acid, aldehydes and ketones as degradation products(Vega et al., 2014b; Wang & Jens, 2014). According the proposed mechanism by Wang et al., and an article released by Vega et al., the hydrogen abstraction usually takes place on the α-carbon. Bedell et al, also proposed a mechanism on hydrogen abstraction and suggested two pathways in which the abstraction can occur. Based on his discoveries, he suggested the plausibility of hydroxyl radical and organo-peroxy radical as potential molecules to facilitate the process of hydrogen abstraction within the amine compound. Below are figures illustrating amine degradation due to hydrogen abstraction.

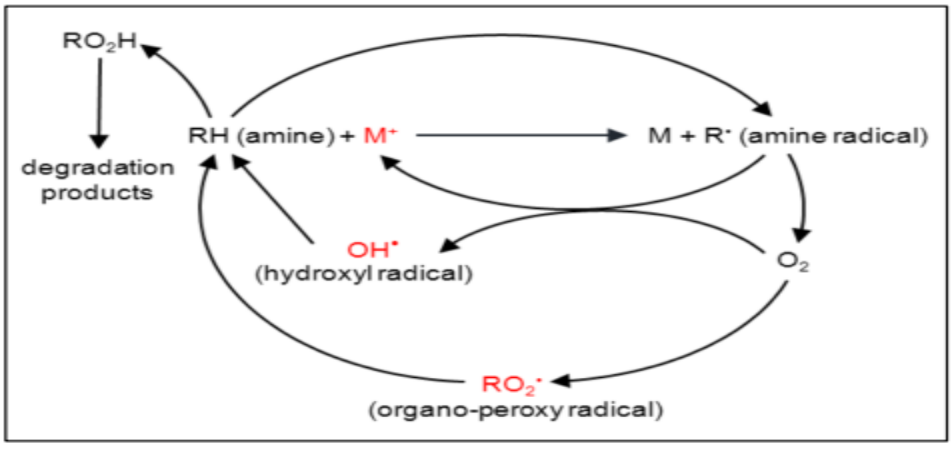

Figure 2.5: Bedell proposed hydrogen abstraction mechanism(Vega et al., 2014b)

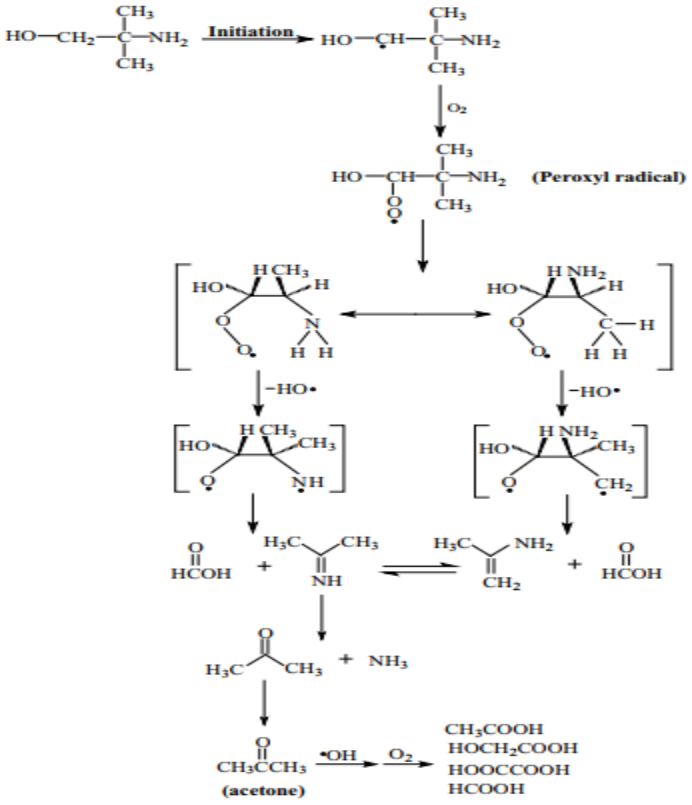

Figure 2.6: Wang et al., proposed AMP degradation with hydrogen abstraction mechanism(Wang & Jens, 2014)(Vega et al., 2014b)

2.9.3.2 Electron Abstraction Mechanism

Unlike the above talked about mechanism, electron abstraction's initiation step is the formation of aminium cation. This step however, according several authors is considered as the rate determining step(Chi & Rochelle, 2002; Fredriksen & Jens, 2013; Vega et al., 2014b). In the process, an electron is abstracted from the nitrogen atom within the amine compound, leading to the formation of the aminium cation. This oxidized form of the amine, the aminium cation, undergoes a reaction resulting in the generation of an imine radical. This radical subsequently releases a free radical, resulting in the formation of an imine(Sexton & Rochelle, 2009; Vega et al., 2014a). Some of the products form from this type of mechanism are ammonia, aldehyde and ketone(Chi & Rochelle, 2002; Sexton & Rochelle, 2009),(Fredriksen & Jens, 2013).

Chi et. al,2002 suggested and mechanism pathway for oxidative degradation of MEA to form an aldehyde and ammonia. Based on their suggested process, the ferric ion, acting as a catalyst for degradation, initiates the abstraction of an electron from MEA, resulting in the formation of an aminium radical. This radical subsequently undergoes further decomposition, leading to the generation of an imine radical. Dissolved oxygen then engages with the formed imine radical, yielding a peroxide radical. This peroxide radical subsequently decomposes to produce peroxide and imine. Ultimately, the imine undergoes hydrolysis, resulting in the formation of aldehydes and ammonia. A schematic representation of this proposed mechanism is illustrated in Figure 2.7 below.

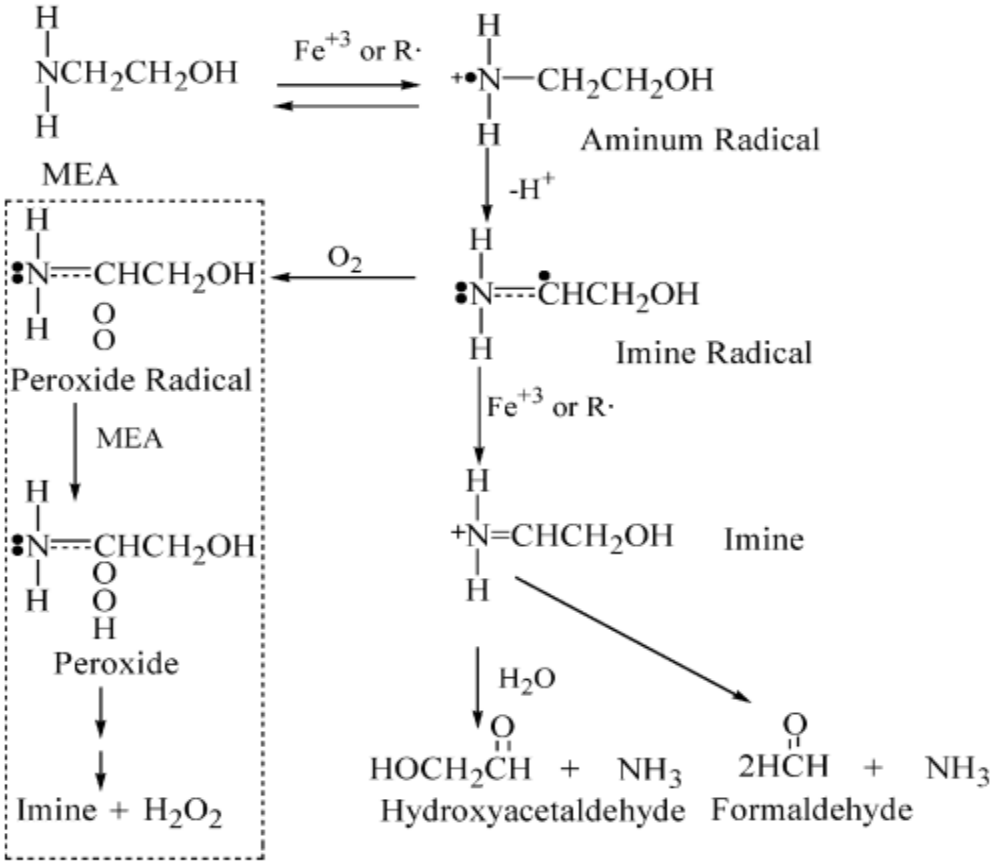

Figure 2.7: Schematic diagram of electron abstraction mechanism of MEA (Chi & Rochelle, 2002)

2.9.4 Degradation Products

There exist various equipment and analytical methods used to quantify and identify various degradation products. Supap et al. in 2006 published a research work focused on three analytical methods and equipment deployed for degradation studies. These were gas chromatography-mass spectrophotometer (GC-MS), high performance liquid chromatography-refractive index detection (HPLC-RID) and capillary electrophoresis-diode array detection (CE-DAD). Based on his findings, he concluded that both HP-35MS column (intermediate polarity) and HP-Innowax (high-polarity column) were needed for MEA degradation studies and product identification when using GC-MS. Additionally, he mentioned that the sole technique for the concurrent analysis of MEA degradation and the identification of degradation products was HPLC-RID employing a Nucleosil column along with a phosphate buffer. Other analytical methods and equipment, as corroborated by scholarly sources have also proven to be useful in amine degradation analysis. These include; gas chromatography-flame ionization detector (GC-FID), gas chromatography-atomic emission detection (GC-AED), ion chromatography (cation chromatography and anion chromatography), liquid chromatography-electrochemical detection (LC-ED) and liquid chromatography-mass spectrophometer(LC-MS)(Chi & Rochelle, 2002; Supap et al., 2006; Vega et al., 2014b).

Numerous research investigations have highlighted that specific acidic degradation by-products can react with amines, leading to the creation of heat-stable salts. These heat-stable salts are problematic as they contribute to a range of operational issues, including fouling, foaming, and corrosion within the system. The presence of these salts can significantly disrupt the capture process, necessitating more frequent and intensive maintenance. Consequently, this increases both operational and maintenance costs, impacting the overall efficiency and cost-effectiveness of the capture process.(Conway et al., 2015; Gouedard et al., 2012; Supap et al., 2011).

Table 2.1 is a summary of some identified degradation products identified when the degradation studies of selected amines were studied in accordance with literature findings.

Table 2.1: Some amines and its associated degradation product(Chi & Rochelle, 2002; Gouedard et al., 2012; Supap et al., 2011)

Amine	Some main degradation products
MEA (monoethylineamine)	2-oxazolidone Ammonia 4-methylmorpholine 1-amino-2-propanol 2-methyl-3-oxazolidine
AMP (2-amino 2-methyl propanol amine)	N,4,4-Trimethyloxazolini-2-one N,2,2-trimethylethanolamine 4,4-Dimethyloxazodin-2-one
MDEA (methyldiethanolamine)	Methanol Formic acid Ethyleneglycol Diethanolamine
MMEA (monomethylethanolamine)	N,N'-dimethyl imidazolidone N,N-dimethylpiperazine N-methyloxazolidone
DMEA (dimethyethanolamine)	N-methylethanolamine N-methyloxazolidone Ethyleneglycol
PZ (piperazine)	Ammonia Formic acid N-ethylpiperazine N-formylpiperazine
HEEDA (N-(2-Hydroxyethyl) ethylenediamine)	Monoethanolamine N,N-bis(2-hydroxyethyl)ethanodiamine

	2-oxazolidone

2.9.5 Degradation Inhibition

The idea of solving issues related to amine degradation led to the introduction of degradation inhibitors in carbon capture storage and utilization. The initial chemicals to be tested as a degradation inhibitor were tetrasodium salt of ethylenediaminetetraacetic acid (EDTA) and monosodium salt of N,N diethalnolglycine (DEG)(Blachly & Ravner, 1964; Buvik, Wanderley, et al., 2021). This investigation was initiated in 1964 by Blachy and Ravner, who examined the impact of these chelating agents on the stability of MEA in the presence and absence of metal ions. Their pioneering work inspired numerous subsequent researchers to delve deeply into this technology(Blachly & Ravner, 1964; Buvik, Wanderley, et al., 2021).

So far, degradation inhibitors can be generally classified into three groups namely; oxygen or peroxide scavengers, chelating agents and stable salts(Buvik, Wanderley, et al., 2021). Peroxide scavengers and chelating agents have demonstrated effectiveness as inhibitors. Nevertheless, research indicates that their inhibition capacity diminishes gradually during deployment, necessitating replacement. In contrast, stable salts like potassium chloride (KCl), potassium bromide (KBr), and potassium formate ($CHKO_2$) maintain their effectiveness without depleting over time, efficiently fulfilling their intended function(Buvik, Wanderley, et al., 2021)

CHAPTER 3 EXPERIMENTAL SECTION

The experimental section outlines the various procedures undertaken to achieve the research objectives. This section provides detailed information on the chemicals and equipment used for CO_2 absorption and desorption runs, degradation experiments, and emissions studies. Additionally, it lists the laboratory safety protocols followed to ensure a safe lab environment during the experiments.

The experiments were divided into two main categories. The first category involves CO_2 absorption and desorption runs to measure the CO_2 concentration in rich and lean amine solutions. These measurements were used to calculate the average CO_2 concentration for preloading the amine for stability studies.

The second category encompasses amine stability studies, which included degradation and emission experiments. These studies monitored the stability of amines under varying concentrations of oxygen and temperature. The amine stability experiments were conducted continuously for 21 days (504 hours) to thoroughly assess the stability of the amines.

3.1 Laboratory Health and Safety Precautions

Initially, comprehensive laboratory safety training was provided to underscore the potential hazards inherent in a research environment and to delineate the crucial safety precautions necessary to mitigate these risks. This training covered a range of important topics, including hazard identification, risk assessment, emergency procedures and proper use of personal protective equipment (PPE)

Following this foundational training, strict adherence to general laboratory safety rules was maintained throughout the research phase. This ensured a consistently safe environment for conducting experiments. The expectation is to apply the knowledge gained from the training sessions, implementing best practices and safety measures to minimize the risk of accidents and ensure the well-being of everyone in the lab. This dual approach—comprehensive initial training followed by vigilant adherence to safety protocols—was essential in fostering a safe and productive research environment.

Key safety precautions implemented throughout all experimental procedures include the following:

1. **Personal Protective Equipment (PPE):** Lab personnel were required to wear appropriate PPE, such as lab coats, safety goggles, gloves, and, when necessary, face shields.
2. **Chemical Handling:** Proper procedures for handling, storing, and disposing of chemicals were rigorously followed to prevent accidents and exposure.
3. **Ventilation:** Experiments involving volatile or hazardous substances were conducted in well-ventilated areas, such as fume hoods, to minimize inhalation risks.
4. **Spill Response:** Emergency protocols for dealing with chemical spills, including the availability of spill kits, were established and communicated to all lab personnel.
5. **Equipment Safety:** Regular maintenance and inspection of laboratory equipment were performed to ensure they were in proper working condition and to prevent malfunctions.
6. **Emergency Preparedness:** The lab was equipped with easily accessible emergency equipment, such as fire extinguishers, eyewash stations, and first aid kits. All personnel were trained in their use.

7. **Labelling and Signage:** All chemicals and solutions were clearly labelled and hazard signs were prominently displayed to inform and warn personnel of potential dangers.
8. **Proper Waste Disposal:** Hazardous waste was segregated and disposed of according to established protocols to prevent environmental contamination and ensure compliance with regulations.

These safety measures were diligently observed to create a secure laboratory environment for all experimental activities.

3.2 Equipment and Chemicals

The chemicals and equipment used for amine stability studies are well listed in this sub-section. 2-amino-2-methyl-1-propanol (BioXtra, ≥95%), 1-(2-hydroxyethyl) pyrrolidine (98%), purchased from Sigma Aldrich Co. Canada and TCI America respectively, MEA (Sigma Aldrich Co., Canada, CAS No.:141-43-5), DMAE (≥99.5%, Sigma Aldrich Co., Canada CAS No.:108-01-0), H_2SO4 (ACS Reagent, 95.0-98.0%, Sigma-Aldrich Co., Canada), HCl (1N Sigma Aldrich Co., Canada), Air tank (Class 2.2 Air Ultra Zero T, Linde Canada Inc.), Nitrogen Tank (Class 2.2 T Size UN1066, Linde Canada Inc), CO_2 Tank (Class 2.2 T Size UN1066, Linde Canada Inc) Masterflex Variable-Area Flowmeter (RK-03217-10, RK-03227-12, RK-03227-18 Cole-Palmer Co., Canada), Heating Immersion Circulator(Julabo CORIOTM CD,901200.02), Gas dispersion tubes (170 to 220 μm)- 12 mm O.D. Pyrex™ [39533-12EC], Recirculating chillers(196211010001, FisherbrandTM), Stainless steel Bath Tank (33L Julabo CORIOTM CD,9903433), Stainless steel seamless tubing(1/4" O.D, Swagelok, Canada), Chittick apparatus, GC-MS (Agilent Technologies),1/4"x3/8" Vinyl tubing (RK-06405-06, Cole-Palmer Co., Canada), 1/8" x 1/4" flexelene tubing (RK-06405-06, Cole-Palmer Co., Canada), Gas washing

bottles used as impingers(45/50 125 mL, ChemScience), Gas analyser (NOVA analytical system Inc.), 4 Station manifold(WWG2KHA9,AcklandsGrainger), Polypropylene floating ball (060301PolyScience), Flaks(threeneck,angled,250mL,24/40,Synthware), Thermometers(JUI14997,FisherbrandCanada),24/40Thermometeradapters(A522440SynthwareTM), 24/40 thermometer adapters with hose connection(A532440 SynthwareTM)

3.3 Chemical Preparation

1 litre of 4M ±0.2 AMP: 1-(2-HE) PRLD at the ratio 2:2 and 5M MEA:DMAE at the ratio 3:2 was prepared and standardized with 1 N HCl. The solution was stirred at a speed of 505 rpm to eliminate mass-transfer limitation.

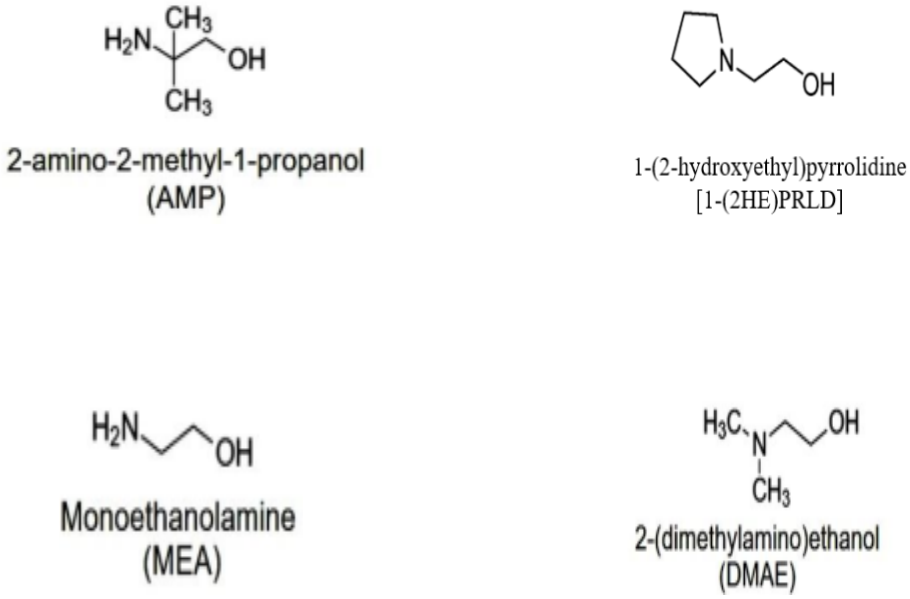

Figure 3.1:Chemical structure of amines studied (Avor et al., 2022; Muchan et al., 2021)

3.4 Experimental Procedure/Setup for Absorption

The CO_2 absorption experiment was carried out at 40±1°C, following the procedure outlined by (Singto et al., 2016). To begin the absorption run experiment, the heating oil was preheated to 40°C, with the stirrer set to 600 rpm. A 250 ml three-necked flask was filled with 100 ml of solvent, fitted with a condenser and a thermometer, and sealed with a glass cork in the third neck. The flask was then immersed in the preheated oil bath. Once the solvent temperature reached 40°C, 15% CO_2 balanced with nitrogen was mixed with 100% nitrogen in a proportion to attain 4.5% CO_2 (±5%). This composition was verified with a CO_2 gas analyser, with periodic checks made during the experiment via a bypass to the analyser. The mixed feed gas was introduced into the solvent at a pressure of 100kPa through a dispersion tube at a flow rate of 200 ml/min (±5%), and the timer was started.

Samples of the amine solvent, 1 ml each, were taken at 10-minute intervals for the first hour, at 30-minute intervals for the next two hours, and then at hourly intervals until equilibrium loading was confirmed, which typically took about 16 hours. The displacement volume was determined using the Chittick apparatus by measuring the volume displaced by CO_2 after titration with excess 1N HCl. The CO_2 loading for each sample was calculated using

$$CO_2 \text{ loading } \left(\text{mol}\frac{CO_2}{\text{mol}}\text{of amine}\right) = \frac{(\text{Vdisplacement} - \text{VHCl}) \times \text{Proom} \times 273.15\ \text{K}}{\text{Camine} \times \text{Vamine} \times \text{Troom} \times 760 \times 22.4}$$ (Narku-Tetteh et al., 2017)

where $V_{displacment}$ is the volume (mL) of the displacement in the gas measuring tube of the Chittick apparatus, V_{HCl} is the sum of the titre and excess volume (mL) of acid, P is the measured pressure of the room where the experiment is being done (mmHg), T is the measure temperature of the

room where the experiment is being done (K), Camine is the amine concentration (mol/L) and V is volume of the amine sample (mL).

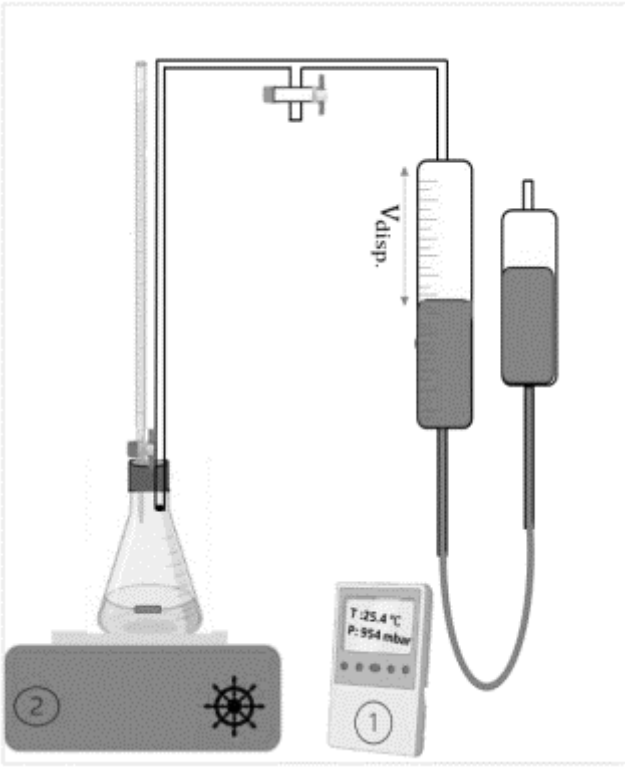

Figure 3.2: Diagram of the Chittick apparatus

The CO_2 loading (mol of CO_2 absorbed per mol of amine) was plotted against time to create an absorption profile. Using Minitab software, a model was developed to predict CO_2 loading at any given time during the experiment. Below is a schematic diagram of the absorption experimental setup.

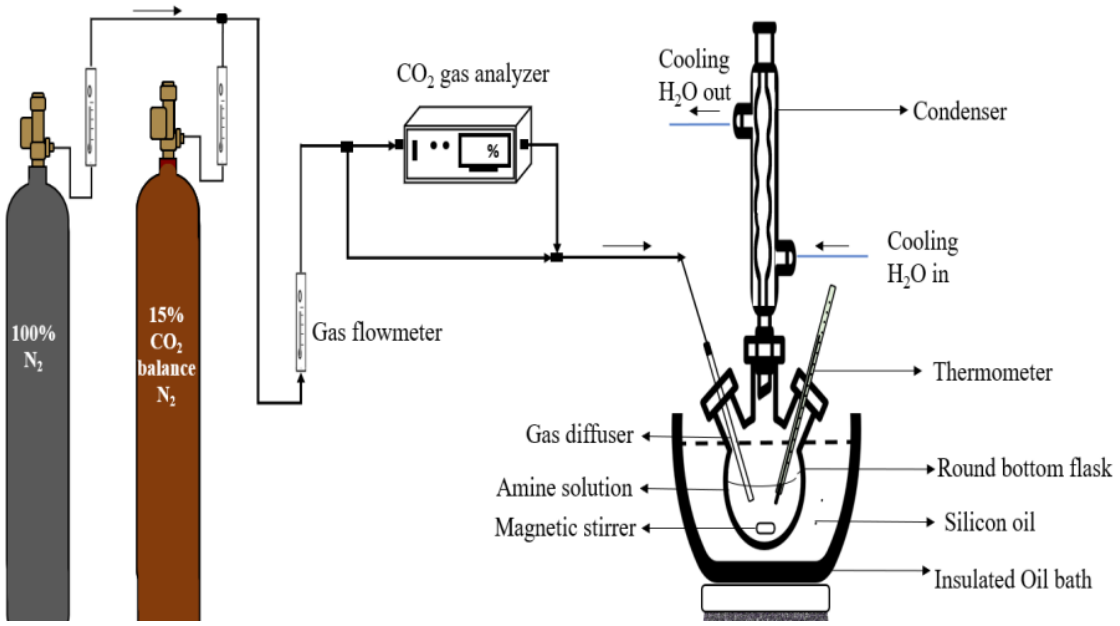

Figure 3.3: Schematic diagram for absorption setup(Avor et al., 2022).

3.5 Experimental Procedure/Setup for Desorption

The setup for the CO2 desorption experiment was similar to that of the absorption experiment, with the primary difference being the removal of the gas dispersion tube and sealing the flask with a glass cork. The desorption run utilized 75 ml of the amine solution loaded during the absorption experiment.

First, the condenser was supplied with cooling water at 5°C. The flask was then fully immersed in a preheated oil bath and allowed to reach a desorption temperature of 100°C. Samples were taken when the temperature of the solution reached 95°C and 100°C, with the corresponding times recorded. Additional samples were collected at intervals of 5, 7, 9, 11, 13, 15, and 20 minutes. Beyond 20 minutes, samples were taken every 10 minutes for the next 40 minutes.

As in the absorption experiment, the CO_2 loading per mole of amine for each sample was determined using CO_2 equation stated above following titration with the Chittick apparatus. To create a desorption profile for the amine solution, a plot of CO_2 loading per mole of amine versus time was generated. Utilizing the experimental data, Minitab software was employed to develop a model to predict the CO_2 loading per mole of amine at any given time. Below is a schematic diagram of the desorption experimental setup.

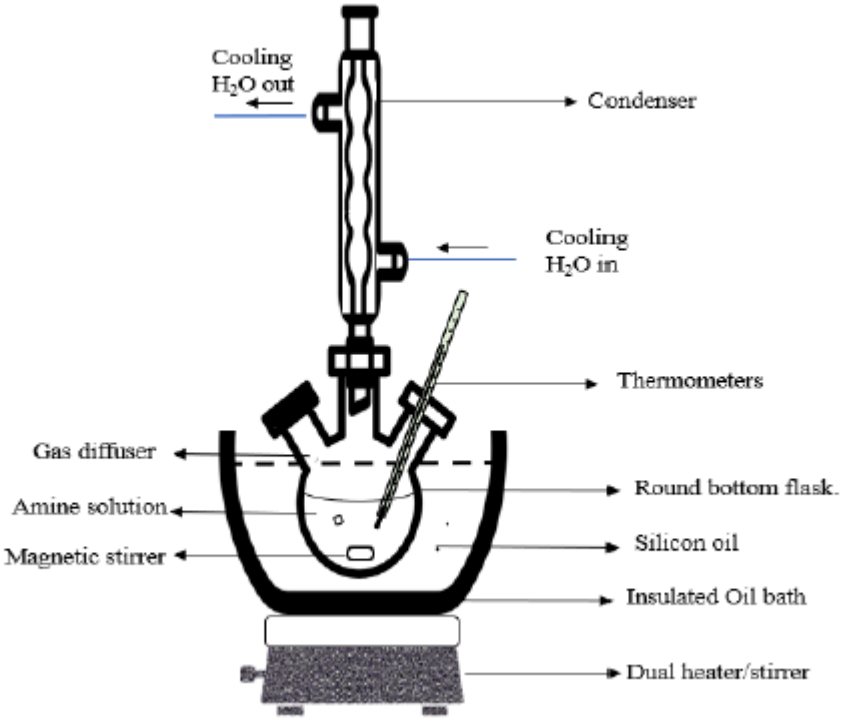

Figure 3.4: Schematic diagram for desorption setup(Avor et al., 2022).

3.6 Experimental Procedure/Setup for Preloading Amine blend

After attaining the rich and lean loading of the amine blend, just like the absorption test run, the oil bath was first heated to 40±1°C to accommodate a three-neck flask. Once the desired temperature was reached, 250 ml of the prepared amine blend was transferred into a 500 ml three-neck flask and placed in the oil bath. A condenser and a thermometer were fitted to two of the necks, while a gas delivery tube was attached to the third neck. A stirring speed of 600 rpm was maintained for all the test runs. to reach the desired absorption temperature. Then, a 100% CO_2 gas at a flow rate of 200 ml/min (±5 accuracy) was then bubbled into the solution through the dispersion tube. Samples were then taken at time intervals of 10 min in order to measure the CO2 loading using the Chittick apparatus until 0.25±0.2 mol CO_2/ mol amine was reached. If the CO_2 concentration exceeds the expected fresh amine blend is used to dilute it using the formula $C_1V_1 = C_2V_2$. Where C_1 is the concentration of the attained CO_2 and C2 is the concentration of expected CO_2, 0.25±0.2 mol CO_2/ mol amine, V_1 is the volume of the amine blend to be diluted, V_2 is the volume of the fresh amine blend to be used in dilution.

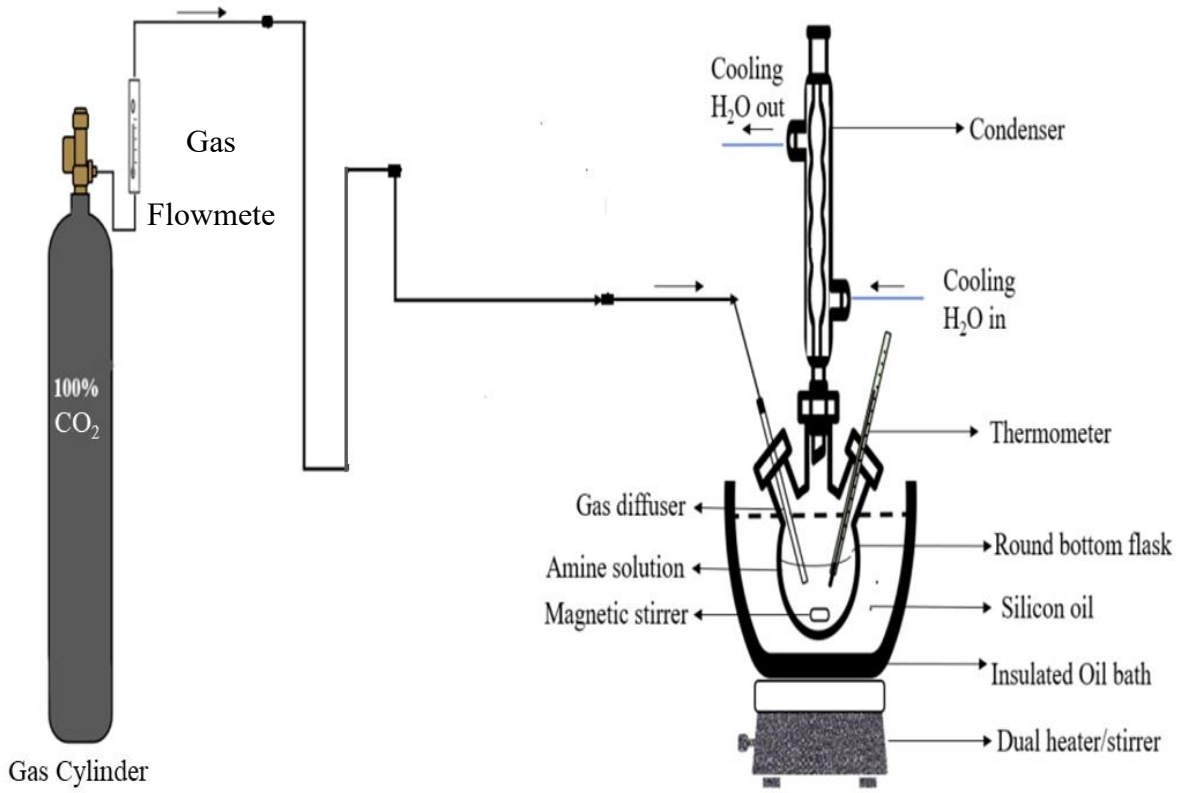

Figure 3.5: Schematic diagram for CO_2 preloading setup(Avor et al., 2022).

3.7 Experimental Setup for Stability

The experiment was setup in such a way that two different reaction flasks each containing 200 ml of the CO_2 preloaded amine blend was use simultaneously. This was done to check experimental repeatability and experimental errors. A simulated flue gas was directed through a manifold, splitting the gas into two lines which fed the two reactor cells with the same gas concentration at an atmospheric pressure. The gas flow rate in each line was regulated by a flow meter at 200 ±5 mL/min. Given that the gas provided from the cylinder lacked moisture, it was routed through a water saturator to pre-saturate the gas before coming into contact with the amine blend in each of the 500 ml reaction flasks. To further reduce the mass transfer limitation, a gas dispersion tube

was employed to introduce the gas into the solution, thereby increasing the contact area between the gas and liquid. The reaction flask containing the amine was submerged in a temperature-controlled water bath in which the temperature had been set to either 40, 50 or 60°C. It was noticed that the water in the bath evaporated due to the set temperature. Polypropylene floating ball cover was introduced to minimize the evaporation of water and to reduce heat loss. Make-up water was occasionally added to maintain the water level. A condenser was connected to the middle head of the reaction flask to avoid any loss of solvent and water due to evaporation. The temperature of the cooling water was set at 19 ℃ so that the outlet temperature of the off-gas would be equal to 24 ℃ which was the room temperature and the temperature of the water saturator. Since there are likely emission products the experiment was carried out in a fume hood(Muchan et al., 2021). Several runs were conducted by varying the temperature condition and the oxygen partial pressure condition. Every stability experiment run lasted for 21 days. The schematic diagram of the experimental setup is shown below in Figure 3.6

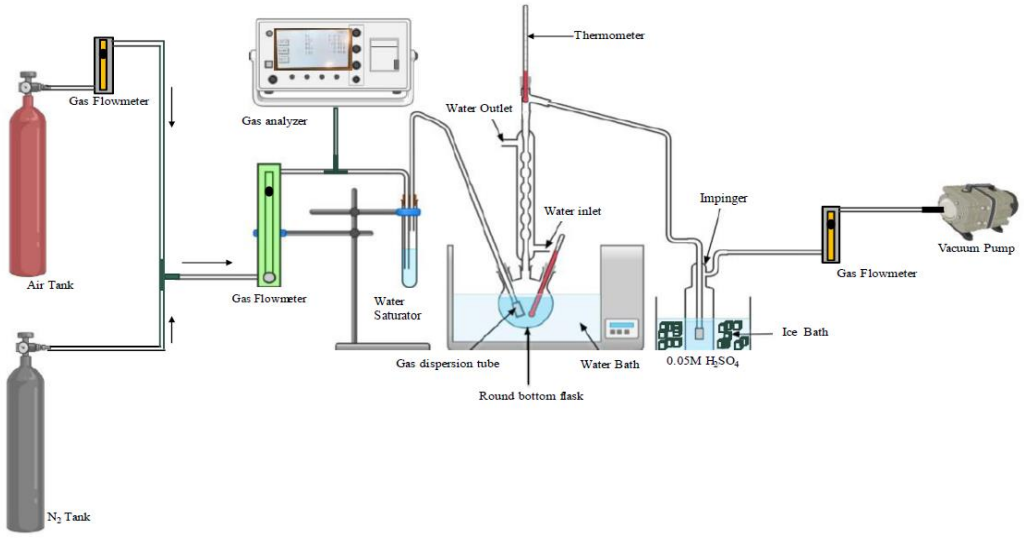

Figure 3.6: Schematic diagram of stability experimental setup (Pradoo 2021).

Figure 3.7: Picture of stability setup used in the lab

3.8 Amine Sampling

Amine was sampled every day by pipetting approximately 1 mL of each solution into a 2 ml sampling vial which was then immediately stored in a refrigerator to prevent further degradation caused by high temperature. The concentration of each collected sampled amine was analysed with gas chromatograph (Agilent 7890A) equipped with a capillary column of 5% diphenyl/95% siloxane (J&W Ttx_5 amine) and a mass spectrometer detector (Agilent 5975C inert XL MSD). UHP helium served as the carrier gas, maintaining a steady flow rate of 1.4 mL/min(Muchan et al., 2021). The operating condition of the GCMS was set as: 1 µl injection volume, split ratio 125:1; Oven Temperature 70°C and run time 11 minutes.

Before conducting the analysis with the GCMS, each amine sample was diluted with deionised water using a dilution factor of 10. The purpose of this action was to avoid overloading the column and improve the separation of components. The concentration of the amine solution was quantified by a calibration curve which was pre-made using different concentrations of standard amine solutions prepared.

To ascertain the precise amine blend concentration per time, emitted vapours during the run were collected twice every week for 6hrs and analysed with GCMS to know the amount amine blend loss by evaporation. Also, the final volume was measured and subtracted from the expected final volume after sampling to know the amount of water loss by evaporation.

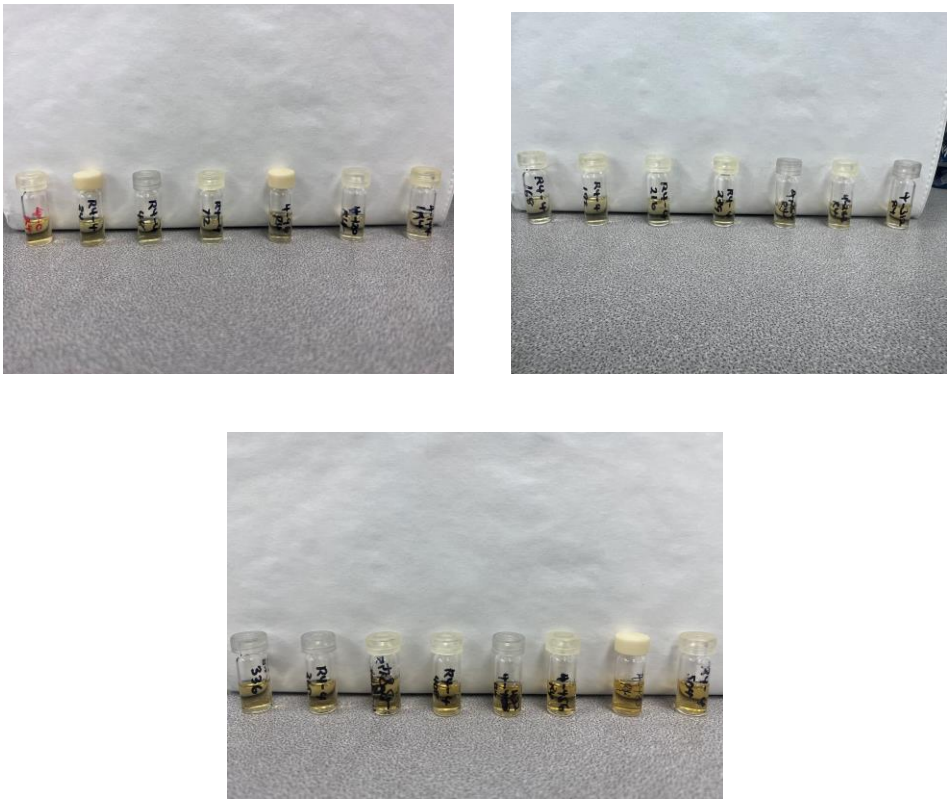

Figure 3.8: Picture of amine samples collected over 21 days of stability test run

3.9 Off-Gas Sampling

Off-gas sampling was done by connecting the emissions to an impinger containing 50ml of 0.05M H_2SO_4 at the 1st hour, 3rd hour, 18th hour, 24th hour and every other 24 hours after that till the end of the experiment run. The impinger connected to the off-gas was submerged in cold water at a temperature of 5±2℃ to enhance the solubility of the gas in the liquid (0.05M H_2SO_4). A vacuum pump was inserted at the exit of the last impinger to aid the off-gas flow at a flow rate of 200±10 mL/min for a sampling time of 60 minutes.

After sampling, the liquid content was transferred into a 100 mL volumetric flask and topped up with fresh 0.05M H_2SO_4 to the 100 ml mark. Samples are sent to Roy Romanow (Regina, Saskatchewan, Canada) to be analyzed for ammonia concentration using the Ammonia/Nitrate Analyzer (Timberline Model TL-2800). Concentrations are reported in mg/l but for emissions study converted to ppmV using:

$C_{ppmV} = \frac{C_{mg/l} \times 0.1 \times 24.04 \times 0.0001 \times 10^6}{V_T \times MW_{NH3}}$ (Muchan et al., 2021)

CHAPTER 4 RESULTS AND DISCUSSION

This chapter presents a detailed analysis of the experimental results from the stability tests. The discussion is organized into five sections:

1. **Solvent Performance in CO_2**: This section examines how the average CO_2 loading used for the stability studies was ascertained.
2. **Comparative Stability Analysis**: This section compares the stability of the new amine blend with a well-established amine blend, highlighting differences and similarities.
3. **Impact of Oxygen on AMP:1-(2-HE) PRLD**: The third section examines how exposure to oxygen affects the stability of the novel amine blend.
4. **Temperature Effect on AMP:1-(2-HE) PRLD**: This part explores the influence of temperature variations on the stability of the novel amine blend.
5. **Ammonia Emissions and Degradation**: The fifth section investigates the relationship between ammonia emissions and the degradation process of the amine blend.
6. **Kinetic Analysis on Stability**: Finally, the last section delves into the kinetic analysis of the stability of the novel amine blend, providing insights into its behaviour over time.

4.1 Solvent Performance

Avor. et al, 2022 in their work reported that 4M AMP:1-(2-HE) PRLD has a rich loading of 0.446 mol CO_2/mol amine at an absorption temperature of 40°C and a lean of 0.064 mol CO_2/mol amine at a desorption temperature of 100°C. The above work was carried out in a semi batch reactor.

Before the stability studies was carried out, a repetition of the absorption run and desorption run was done at the same conditions. By doing this, I confirmed the effectiveness of the semi-batch reactor, flow meters, and gas analyser for the stability test run. Also, the average CO_2 preloading to be used for the stability studies was attained. After the absorption run, I recorded a CO_2 loading of 0.406 CO_2/mol amine which was 8.7% lower than that reported in literature by Avor. et al., and after the desorption run, I recorded a CO_2 loading of 0.065 mol CO_2/mol amine which is 1.6% higher than that reported in literature by Avor. et al., 2022. These two results are very comparable and therefore went ahead to use an average of the lean and rich loadings of 0.25 ± 0.02 CO_2/mol amine as the CO_2 preloading value in the stability studies.

Several papers from literature carry out stability studies of amine either using fresh amine without preloading or preload the amine to attain its lean CO_2 state(Muchan et al., 2021; Nyarko, 2022; Supap et al., 2009, 2011; Uyanga & Idem, 2007). However, this research went ahead to use the average CO_2 just to mimic a reflection of CO_2 capture process where the degradation agents neither contact the amine when fresh nor when extremely lean.

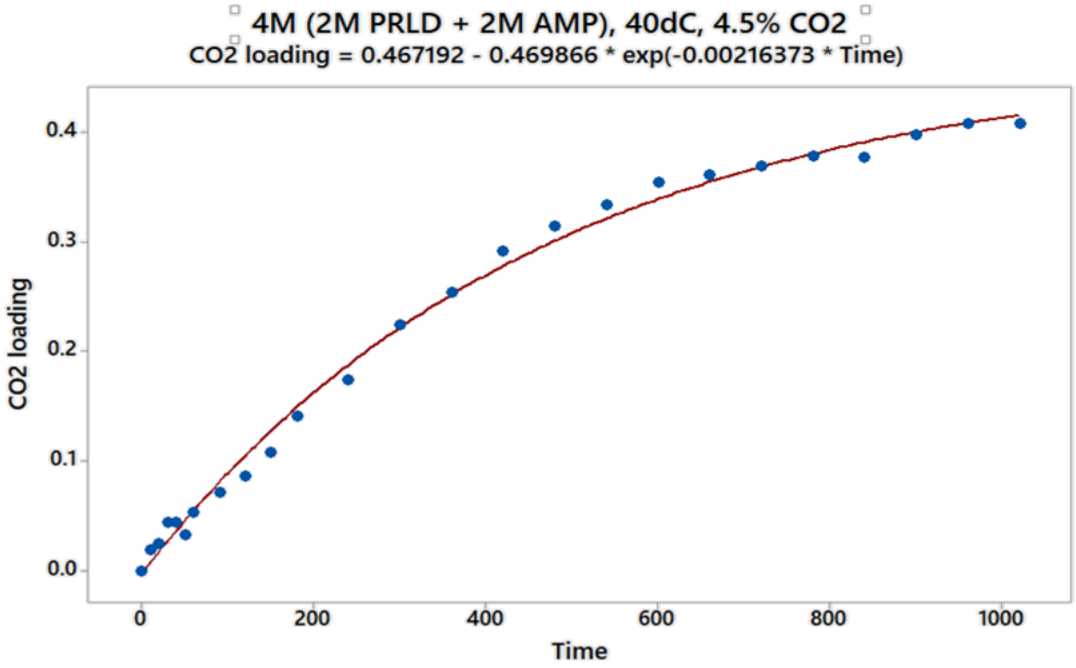

Figure 4.1: A graph showing the absorption run for 4M AMP:1-(2-HE) PRLD

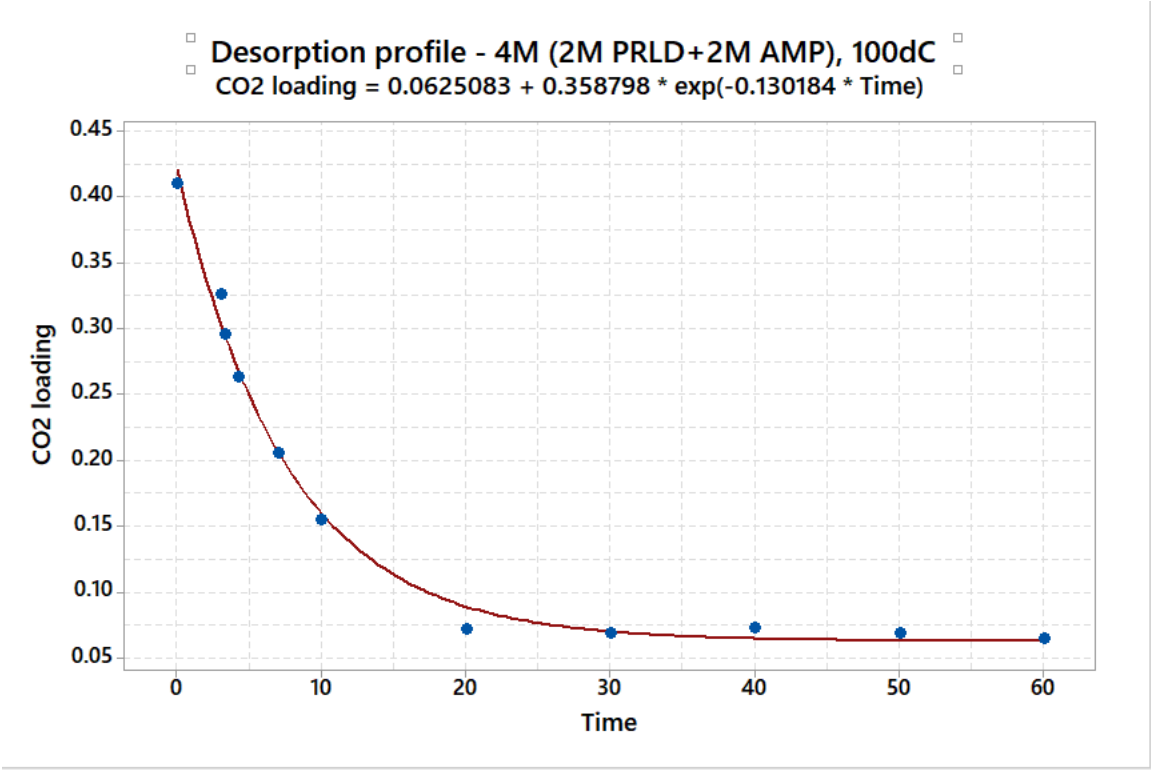

Figure 4.2: A graph showing the desorption run for 4M AMP:1-(2-HE) PRLD

4.2 Comparative Stability Analysis

In order to establish the inherent stability of the novel amine blend, 4M AMP:1-(2-HE) PRLD, it was compared with a known amine blend, 5M MEA: DMAE, at the same exposed condition. MEA:DMAE blend is a well-known amine blend to have great potential in CO_2 capture(Chen et al., 2020; Conway et al., 2015; Gao et al., 2017; Jiang et al., 2018; Nyarko, 2022). Similar to the novel amine blend (4M AMP:1-(2-HE) PRLD), 5M MEA: DMAE also features a combination of a primary amine and a tertiary amine. Also, even though AMP:1-(2-HE) PRLD is 4M and MEA: DMAE is 5M, the cyclic capacity both amine blends are very much similar(Avor et al., 2022; Nyarko, 2022). When these two unique amine blends were first exposed to a stability test run of 60°C and 6% oxygen partial pressure balanced with nitrogen, there was no significant difference with respect to their rate of degradation. 5M MEA:DMAE recorded a rate of degradation of -0.0005 M/hr while 4M AMP:1-(2-HE) PRLD recorded a rate of degradation of -0.0003 M/hr. When the oxygen partial pressure was doubled while keeping the temperature constant at 60°C, the degradation rate of the 5M MEA:DMAE surged by 80%. In contrast, the 4M AMP:1-(2-HE) PRLD exhibited a more modest increase in its degradation rate, rising by only 33%. This stark difference underscores the superior stability of the novel solvent under elevated oxidative conditions. The results highlight the solvent's robust stability, highlighting its resilience and potential for long-term application in environments where oxygen levels may fluctuate without succumbing easily to the degradation processes that typically affect similar compounds. This inherent or intrinsic resistance to breakdown ensures long-term reliability and efficiency in practical applications.

According to the 2008 publication by Singh et al. on structure and activity relationships, the inherent molecular structure of an amine can affect the rate of absorption. For example, their

research showed that adding an alkyl group to the α-carbon decreases the initial absorption rate due to steric hindrance (Singh et al., 2008). Narku-Tetteh et al. also emphasized in their research on how inherent characteristics such as electron density and the number of hydroxyl groups of an amine compound can influence CO_2 absorption rate(Narku-Tetteh et al., 2017).

When it comes to amine degradation, studies indicate that, the process typically follows two main pathways: electron abstraction and hydrogen abstraction. In the electron abstraction pathway, the rate-determining step involves the loss of an electron from the nitrogen atom of the amine group, leading to the formation of an aminium cation. Conversely, in the hydrogen abstraction pathway, the rate-determining step is the loss of a hydrogen atom, resulting in the formation of a carbocation(Chi & Rochelle, 2002; Fredriksen & Jens, 2013; Wang & Jens, 2014).

If the aminium cation formation pathway is taken, as shown below in Figure 4.3, AMP:1-(2-HE) PRLD blend has both individual compounds having more alkyl groups which are bulky in terms of molecular size surrounding the amino group preventing oxygen from easily accessing the electrons attached to the nitrogen. This steric hinderance slows the rate of reaction within the blend. On the other hand, DMAE has such comparable steric hinderance around the nitrogen of the amino. However, MEA has more hydrogen atoms which is relatively smaller in terms of atomic size surrounding the nitrogen of the amino group. This causes MEA to experience less steric hinderance. Therefore, AMP:1-(2-HE) PRLD blend is more likely to have a low rate of degradation relative to the MEA:DMAE blend considering the electron abstraction pathway.

If hydrogen abstraction pathway is considered, MEA, DMAE and 1-(2-HE) PRLD have similar structure on the α-carbon while AMP assumes a different structure configuration. With hydroxyl (OH^-) being an electron withdrawing compound and oxygen being more electronegative, the carbon atom attached to it becomes easily polarised. The polarization causes the carbon to be

slightly positive hence promoting the abstraction of the hydrogen atom attached to the carbon. However, because AMP has more electron donating groups and high electron density around the carbon attached to the hydroxyl group, it quickly neutralises the effect of being slightly positive. Thereby, the rate of hydrogen abstraction is reduced. In effect AMP:1-(2-HE) PRLD is more likely to have less rate of degradation in the hydrogen abstraction pathway than MEA:DMAE blend. In both mechanisms explained, AMP: 1-(2-HE) PRLD proves to be more stable and it was justified with the experimental results obtained from the rate of degradation.

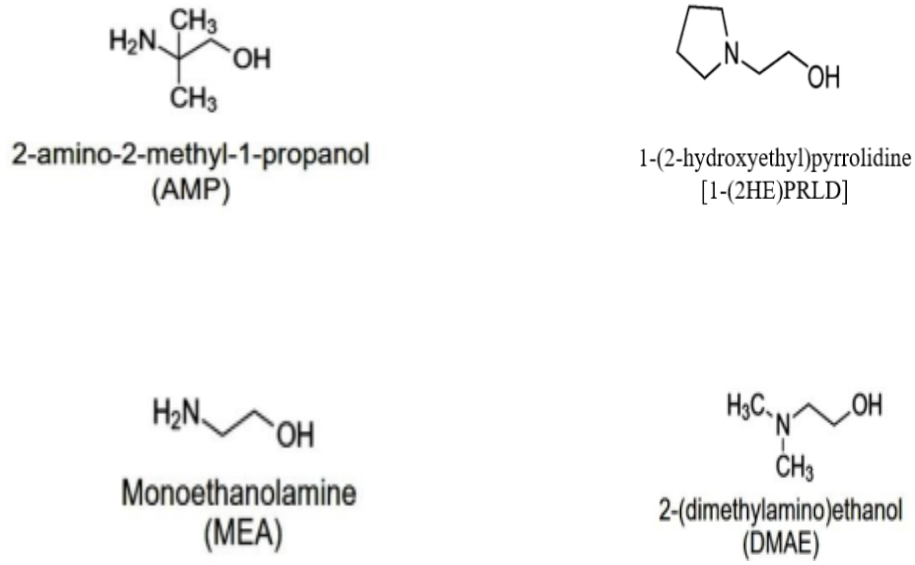

Figure 4.3: Chemical structures of amine blends(Avor et al., 2022; Muchan et al., 2021)

Spearman's correlation coefficient was used to ascertain the strength of the relationship regarding the change in concentration over time. MEA:DMAE blend had – 0.84 and -0.94 for 6% O_2 ;60° C and 12% O_2 ;60° C respectively while AMP:1-(2-HE) PRLD blend had -0.79 and -0.84 for 6% O_2 ;60° C and 12% O_2 ;60° C respectively. The higher the Spearman's correlation coefficient the stronger or higher the rate of degradation and the negative sign is an indicator that concentration

was indirectly proportional to time. Thus, as time increases the concentration of the amines reduced.

The rate of ammonia emissions was also analysed for both blends at each condition. The measured emission rate for MEA:DMAE blend were 3.72 ppmV/hr and 4.16 ppmV/hr for 6% O_2 ;60° C and 12% O_2 ;60° C respectively. While that of AMP:1-(2-HE) PRLD blend were 1.93 ppmV/hr and 2.11 ppmV/hr for 6% O_2 ;60° C and 12% O_2 ;60° C respectively. This was an expected outcome since AMP:1-(2-HE) PRLD blend had relatively showed a lower rate of degradation for each experimental condition.

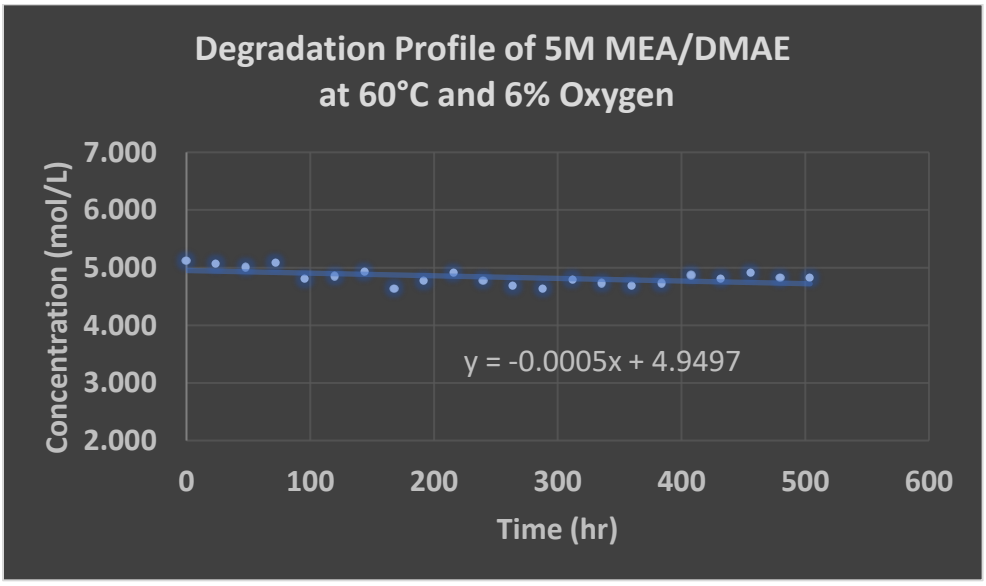

Figure 4.4: A graph concentration against time for 5M MEA/DMAE at 60°C and 6% oxygen

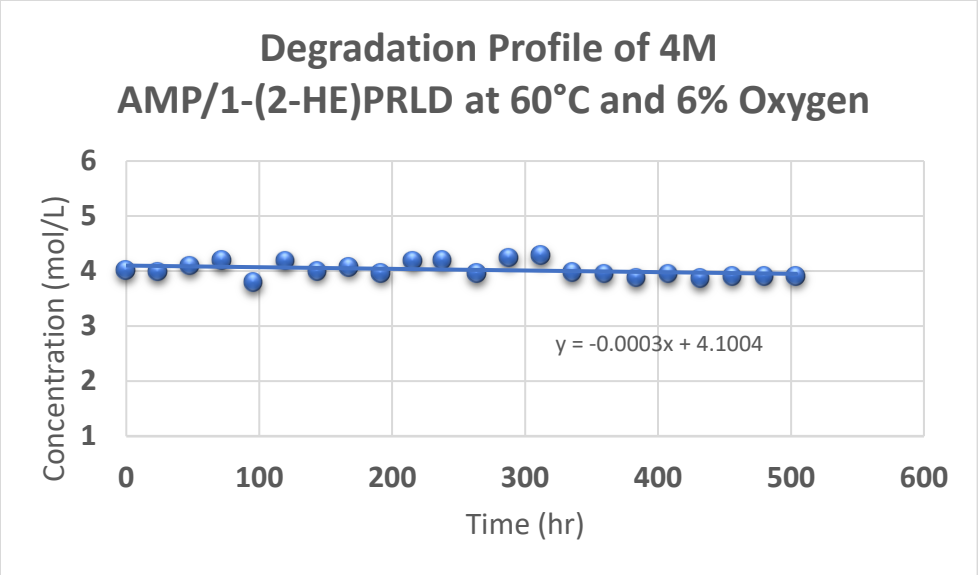

Figure 4.5: A graph concentration against time for 4M AMP: 1-(2 HE) PRLD at 60°C and 6% oxygen

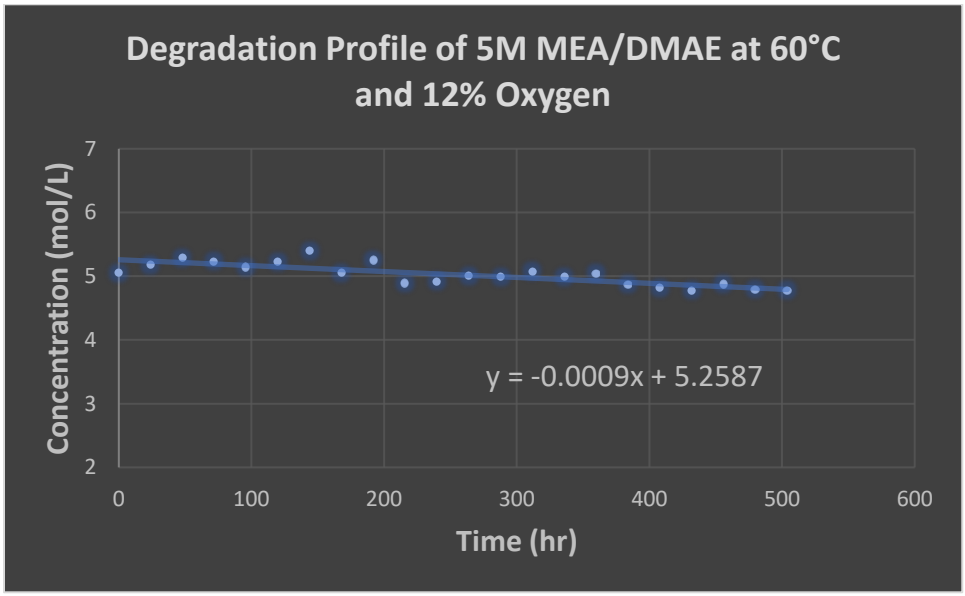

Figure 4.6: A graph concentration against time for 5M MEA/DMAE at 60°C and 12% oxygen

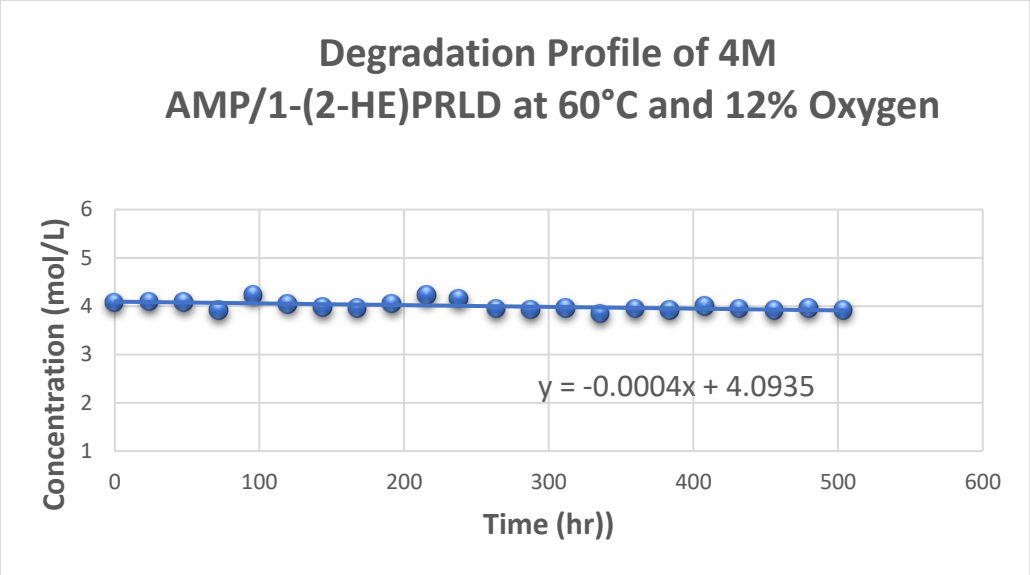

Figure 4.7: A graph concentration against time for 4M AMP: 1-(2 HE) PRLD at 60°C and 12% oxygen

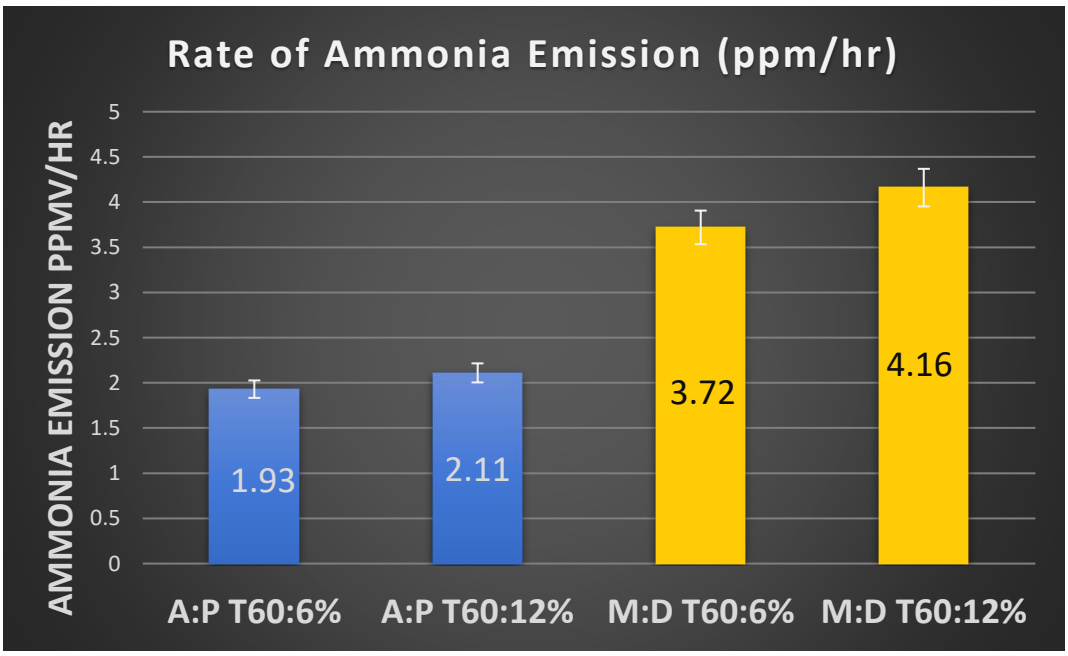

Figure 4.8: A graph of rate of ammonia emissions for AMP: 1-(2 HE) PRLD (A:P) and MEA:DMAE (M:D)

4.3 Oxygen Effect on AMP: 1-(2 HE) PRLD

Keeping all other conditions constant and varying the partial pressure of oxygen at 6%, 12% and 18% balanced with nitrogen we observed a trend. As the partial pressure increases, the rate of degradation increased. This occurs because increasing the partial pressure of oxygen results in a higher concentration of dissolved oxygen within the amine solution. This elevated level of dissolved oxygen enhances the frequency of molecular collisions. Consequently, the number of effective collisions that lead to degradation also increases. The results from this aligns with what literature says about oxygen being an agent of amine degradation during CO_2 capture process. 18% oxygen partial pressure had the highest rate of degradation followed 12% and the least is 6% oxygen partial pressure.

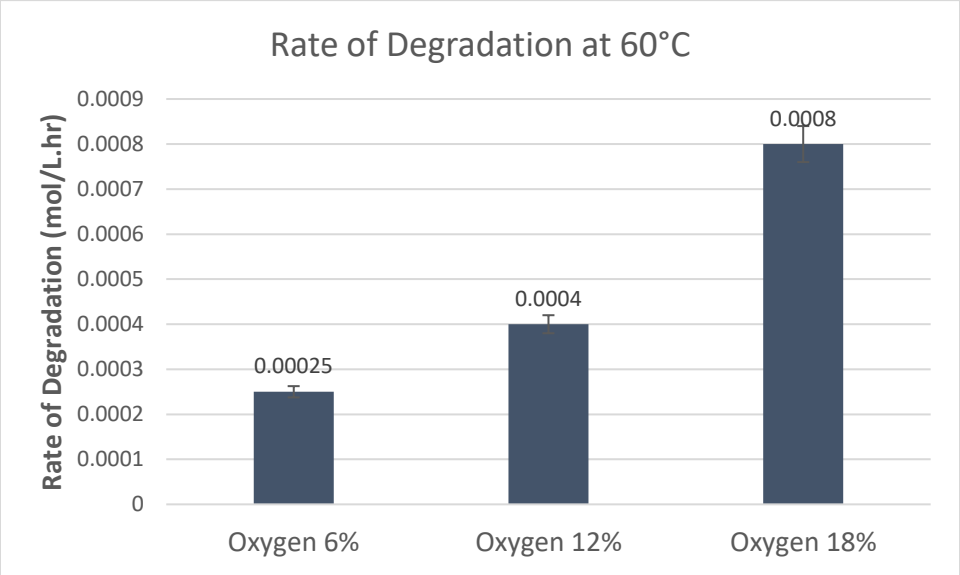

Figure 4.9: A graph of oxygen effect on 4M AMP: 1-(2 HE) PRLD at 60°C

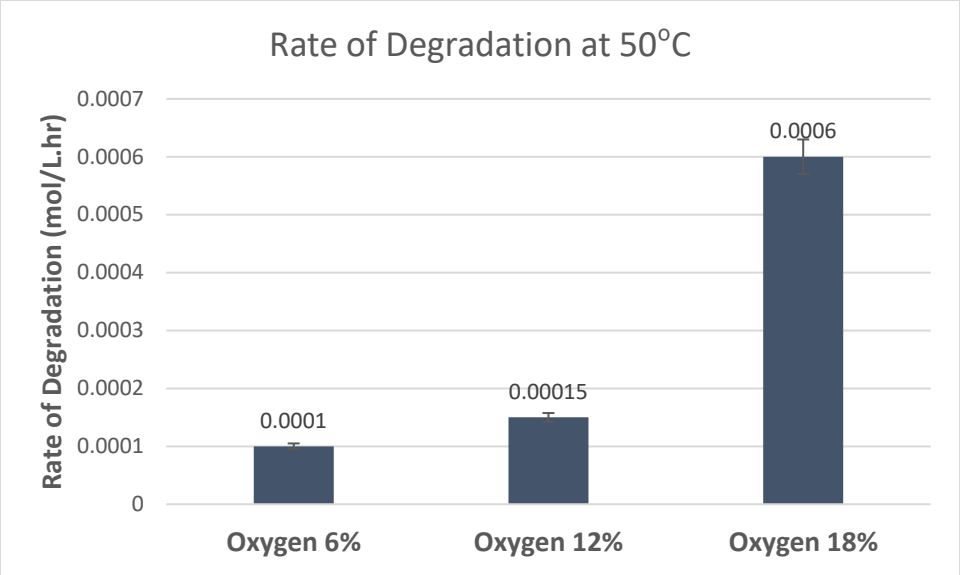

Figure 4.10: A graph of oxygen effect on 4M AMP: 1-(2 HE) PRLD at 50°C

4.4 Temperature Effect on AMP:1-(2-HE) PRLD

Similarly, all other variables were maintained constant to isolate the effect of temperature on the amine blend. It was noted that the degradation rate rose with increasing temperature; 60°C had the highest rate of degradation followed by 50°C and the least is 40°C. This finding aligns with literature suggesting that amine degradation is an endothermic process. Higher temperatures enhance the collision frequency among reacting molecules, thereby boosting the number of effective collisions and leading to increased degradation.

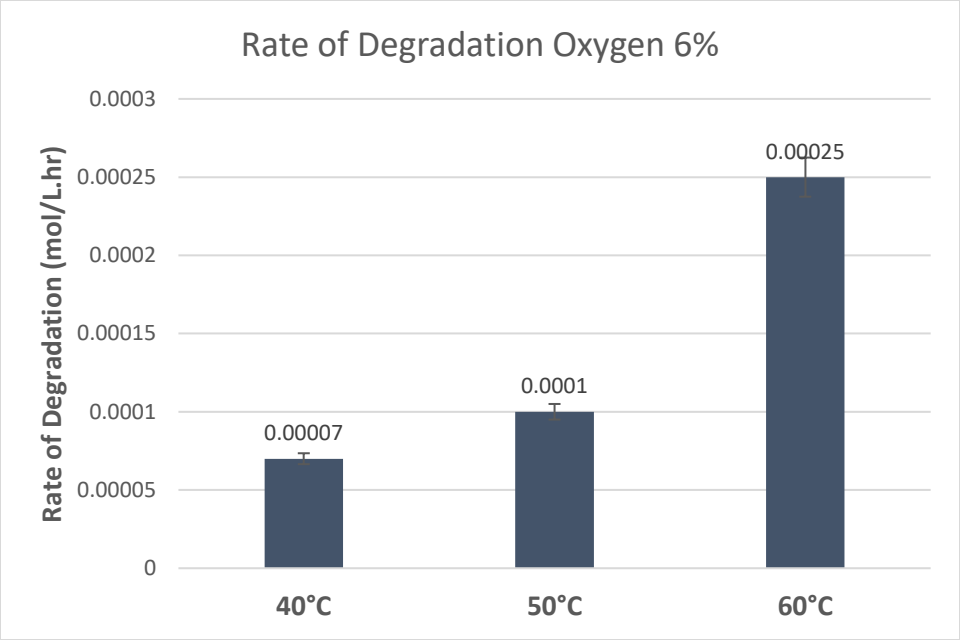

Figure 4.11: A graph of temperature effect on 4M AMP: 1-(2 HE) PRLD at 6% oxygen

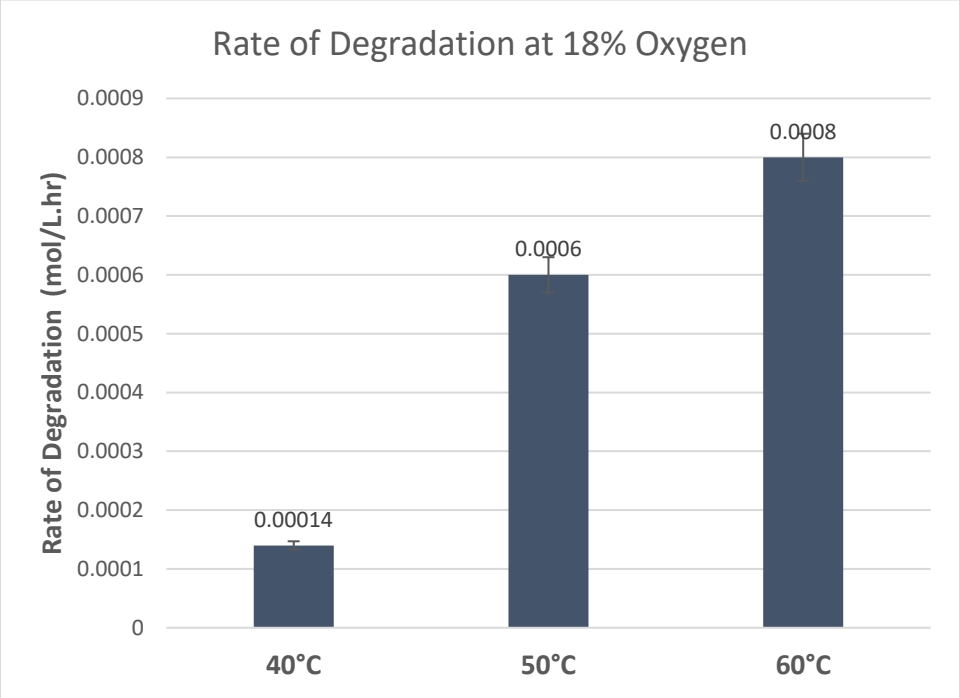

Figure 4.12: A graph of temperature effect on 4M AMP: 1-(2 HE) PRLD at 18% oxygen

4.5 Ammonia Emissions and Rate of Degradation

All proposed mechanisms for amine degradation reveals ammonia as one of the end products of the reaction pathway. As such, there was a need to relate the rate of degradation to rate of ammonia emission. The study by Muchan et al. indicates that there is typically a direct correlation between the rate of ammonia emissions and the degradation rate (Muchan et al., 2021). Even though there were instances the linear relation did not hold, it was made clear in the research work that some of the produced ammonia remained in the solvent as liquid ammonia and could not gain the required energy to transform into gaseous ammonia to be captured during the emission studies. In this work, from Figure 4.13, the linear relation was established with a regression coefficient of determination as 0.923. However, the accuracy of the model holds for when ‘x’ which represents the rate of ammonia emission in ppmV is greater than 0.75 ppmV where the rate of degradation ‘y’ will not be less than or equal to zero. The AAD for the linear model generated was calculated to be 25.3%. In the parity plot in Figure 4.14, the two points that stand out represent ammonia emissions analysed at 60°C with 6% and 12% oxygen. Despite having low degradation rates, the higher temperature condition allowed more ammonia to be released compared to the emissions at 40°C and 50°C, which also showed low degradation rates.

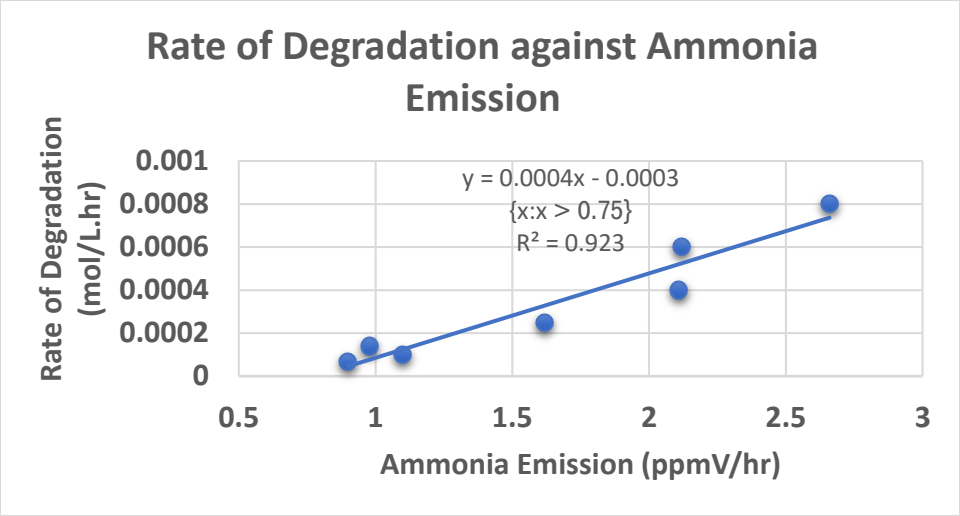

Figure 4.13: Graph of rate of degradation against rate of ammonia emission for 4M AMP: 1-(2 HE) PRLD.

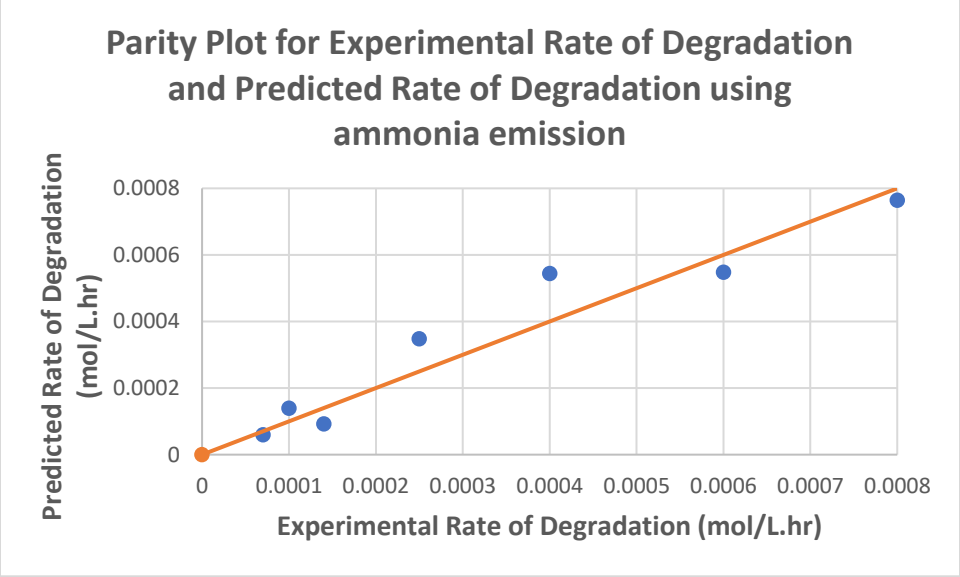

Figure 4.14: Parity plot of rate of degradation for 4M AMP: 1-(2 HE) PRLD using ammonia emission.

4.6 Kinetic Analysis on Stability

The reactants considered in this reaction are O_2 and the amine blend. This type of reaction is typically an example of gas-liquid reaction where the kinetics involves both mass transfer and chemical reaction. However, in order to develop the kinetic model for the reaction, assumptions such as no mass transfer limitation, no heat transfer resistance, reaction occurs only in the liquid phase, the chemical reaction is infinitely slow and the concentration of the amine blend exists in excess relative to that of the oxygen(Supap et al., 2009; Uyanga & Idem, 2007). Based on the above listed assumptions, the rate equation was derived using the power law model with excess method where the concentration of dissolved oxygen is now considered as the sole reactant the kinetic model is dependent. Also, the kinetic model is void of mass transfer since the chemical reaction is very slow and controlling the rate.

4.7 Oxygen Solubility in Amine

The concentration of dissolved oxygen was calculated using an equation derived by Rooney and Daniels,1998 and Xiang, et al., 2015 (Xiang et al., 2016),(Buvik, Høisæter, et al., 2021). This equation does not consider only the partial pressure of the gas but also takes into account the temperature of the solvent that dissolves the solute (oxygen gas). The equation is reported to have a regression coefficient of determination of 0.9992 and an error less than 1.63%. As shown in Table 4.1 and Figure 4.15, the values of oxygen calculated supports what literature reveals concerning the fact that absorption or solubility of gases in polar solvents favours low temperatures. Taking a constant partial pressure of oxygen, it can be seen that as the temperature increased the amount of oxygen in parts per million (pmm) level decreased. This is because, since the solubility is an exothermic reaction, Le Chatelier's principle suggests when temperature is

increased, the equilibrium position shifts to the left side of the reaction which leads to less of the oxygen in the aqueous phase being formed.

$$\text{solute(gas)} + \text{polar solvent (l)} \rightleftharpoons \text{solute(aq)} + \text{polar solvent(aq)} \quad \Delta H_{sol} < 0$$

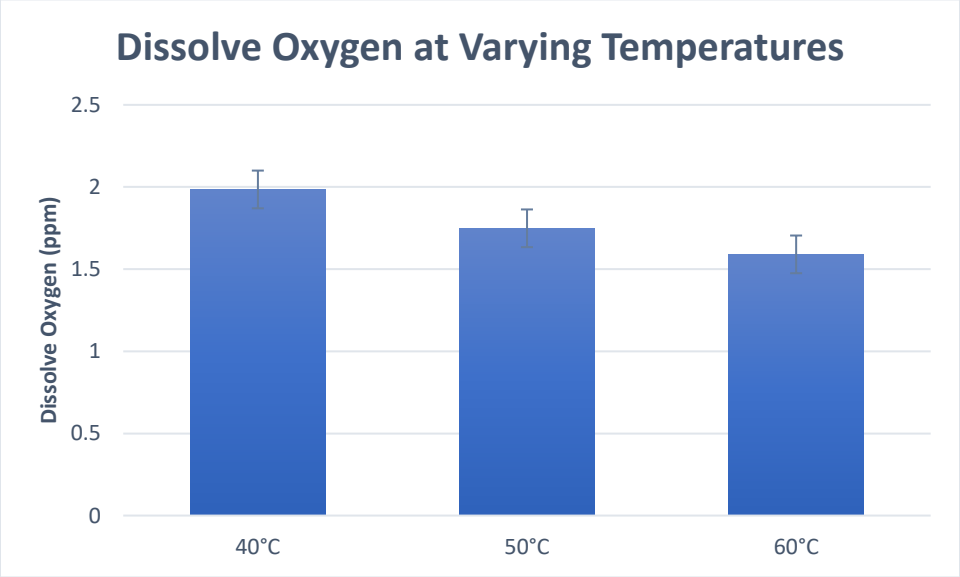

Figure 4.15: A graph of oxygen solubility at various temperatures for stability test

Table 4.1: Summary of dissolved oxygen at various temperatures and partial pressures

Run	Tempt°C	Total Pressure (atm)	O_2 %	Partial pressure, P (atm)	k	O_2 ppm
1	60	1	18	0.18	67088.78848	4.769798
2	40	1	18	0.18	53733.38953	5.955329
3	60	1	12	0.12	67088.78848	3.179866
4	60	1	6	0.06	67088.78848	1.589933

5	50	1	18	0.18	61001.67653	5.245757
6	50	1	6	0.06	61001.67653	1.748586
7	40	1	6	0.06	53733.38953	1.98511
8	60	1	18	0.18	67088.78848	4.769798
9	50	1	12	0.12	61001.67653	3.497172

4.8 Rate Equation and Parameters Estimation

The assumptions outlined earlier, which were employed to derive the power law model, are justified. Numerous studies involving similar reactors and experimental setups have demonstrated their validity(Liang et al., 2011; Naami et al., 2012; Narku-Tetteh et al., 2017; Supap et al., 2009, 2011). Research by Avor et al. (2022) and Narku-Tetteh et al. (2017) indicates that 2-amino-2-methylpropanol and 1-(2-hydroxyethyl) pyrrolidine exhibit low vapor pressures. This means both amines have strong force of cohesion and will not easily evaporate at a given temperature below their boiling point. That being said, the assumption that the reaction takes place in only in the liquid phase holds. Also, the assumption of no mass transfer limitation was supported by research carried out by Supap et al., 2009 and Amoako et al., 2021 where they found out that the degradation products does not change the viscosity of the amine throughout the experimental period. And since the viscosity remains constant, it is reasonable to conclude that the mass transfer limitation caused by the transfer of oxygen into the amine is negligible. Another assumption, that there was no heat transfer limitation, was based on the reactor being fully immersed in a water bath. Additionally, the reactor's good thermal conductivity and the effective bubbling caused by the gas delivery pressure through the diffuser ensured thorough mixing, thereby maintaining isothermal conditions. With regards to the slow rate of reaction and excess concentration of the amine blend assumption,

literature shows how tertiary amines and sterically hindered amines using have low rate of degradation and results from this research work after analysing the concentration of the amine blend after each condition aligns with literature. Additionally, the final concentration measured after the stability test run for the amine blend is so high compared to the dissolved oxygen that exist in parts per million (ppm) level.

Based on these justified assumptions, the power law for the rate of degradation of the amine blend was simplified to $-\frac{dC_A}{dt} = A_o e^{\left(\frac{-Ea}{RT}\right)} [O_2]^w$

Where:

- dC_A/dt is the rate of change in concentration over the time of the stability test run
- A_o is the collision factor or pre-exponential collision factor
- E_a is the activation energy
- R is the gas rate constant
- T is the temperature for the reaction or experimental run
- $[O_2]$ is the concentration of dissolved oxygen
- w is the order of the reaction with respect to oxygen

To help estimate the parameters which in this case 'A_o, E_a and w' non-linear regression method was employed. NL-REG version 6.3 was the software used to aid in the parameter estimations. The iteration was done at a confidence level interval of 95% and tolerance of 10^{-15}. The experimental data used can be found in Table 4.2

Table 4.2: Summary of experimental data for kinetic analysis

Experimental Rate of Degradation (mol/l.hr)	**Temperature (K)**	**Oxygen concentration (mol/l)**
0.0008	333.15	0.000149
0.00025	333.15	4.97E-05
0.0006	323.15	0.000164
0.0001	323.15	5.46E-05
0.00007	313.15	6.2E-05
0.001	333.15	0.000149

Table 4.3: Summary of estimated parameters

Parameter	**Estimated Value**
E_a	50,314.08 ±0.0001 J/mol
A_o	6.822×10^9 ±0.0001 $L^{0.3}/mol^{0.3}.hr$
W	1.3

Based on the estimated values, the accuracy of model derived,

$\mathbf{r_{AMP:PRLD}}\left(\frac{\mathbf{mol}}{\mathbf{L.hr}}\right) = \mathbf{6.8222 \times 10^9 e^{\left(\frac{-50314.08}{8.314 \times T}\right)}}\ [\boldsymbol{O_2}]^{\mathbf{1.3}}$, was examined by comparing it with experimental values and the AAD obtained was 17.9%. The low level of AAD calculated proves

the validity of all the assumptions made in generating the reaction model since the experimental data is close to the predicted data using the model generated as shown in Figure 4.16. However, the estimated activation energy of 50,314.08 J/mol represents the minimum amount of energy necessary for the reactants, amine and oxygen, to undergo a chemical reaction that leads to the formation of degradation products. This value indicates the energy barrier that must be overcome for these reactants to interact effectively, initiating the chemical process that results in the degradation.

Table 4.4: Experimental data and Predicted data

Experimental Rate of Degradation (mol/l.hr)	**Predicted Rate of Degradation (mol/l.hr)**	**AD**
0.0008	0.000905132	0.131415
0.00014	0.000216156	0.135376
0.0004	0.000584022	0.026629
0.00025	0.000139471	0.394712
0.0006	9.04868E-05	0.292668
0.0001	0.000905132	0.094868
AAD =		0.179278

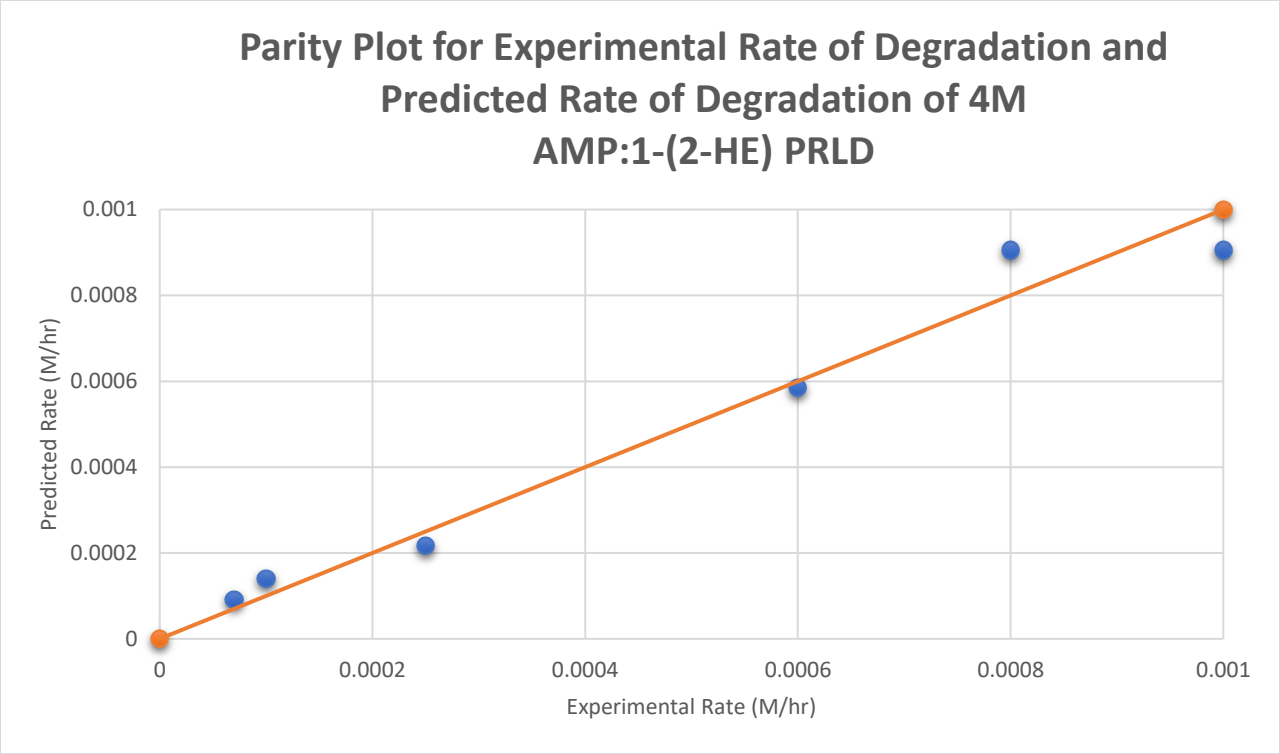

Figure 4.16: Parity plot of Experimental rate of degradation and predicted rate of degradation.

From the linear model derived from Figure 4.13 and power law model generated from the estimates in Table 4.3, an equation can be generated from substituting the rate of degradation in both models in order to relate the rate of ammonia, the activation energy, the collision factor and the order of reaction. Thus;

$$x = \frac{\mathbf{6.8222\times10^{9}}\boldsymbol{e}^{\left(\frac{\mathbf{-50314.08}}{\mathbf{8.314}\times\boldsymbol{T}}\right)}[\boldsymbol{O_2}]^{\mathbf{1.3}}\mathbf{+0.0003}}{\mathbf{0.0004}}$$

Where:

- x is the rate of ammonia emission in ppmV/hr
- O_2 is the concentration dissolved oxygen in mol/l
- T is the temperature of the reaction in K

The above equation relating rate of ammonia emission(x), dissolved oxygen (O_2) and temperature (T) when compared to experimental data as shown in Figure 4.17 gave an AAD of 17.4%.

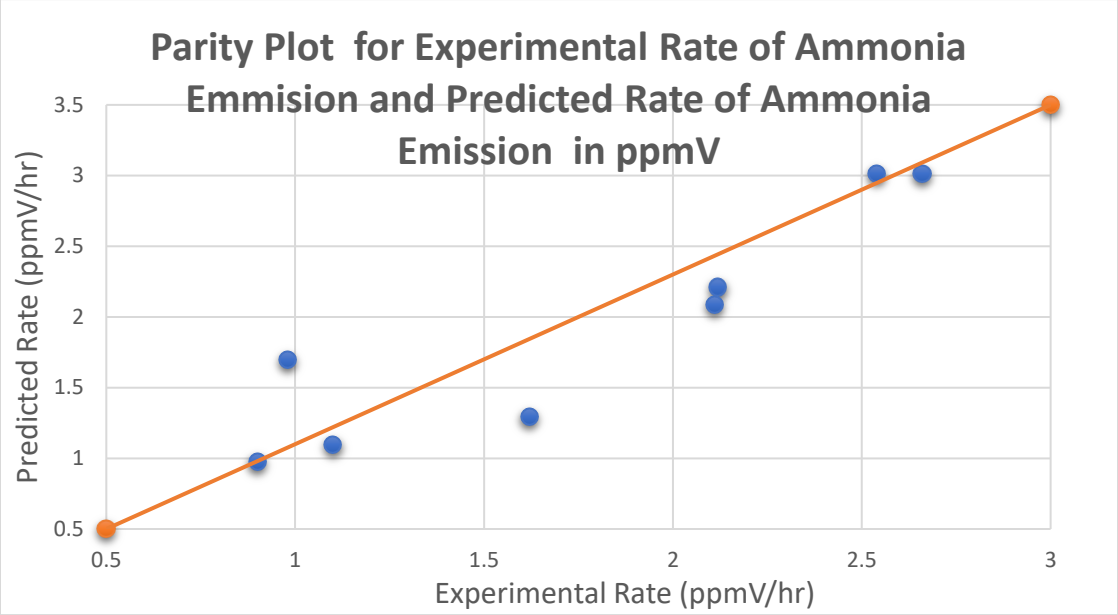

Figure 4.17: Parity Plot of Experimental and Predicted Rate of Ammonia Emission.

CHAPTER 5 CONCLUSIONS AND RECOMMENDATIONS

This chapter encapsulates the key findings and conclusions drawn from the present research. It does not only synthesize the outcomes of the study but also offers detailed recommendations for future research endeavours. These suggestions aim to broaden the scope of knowledge in the field and enhance the practical application of the research in commercial settings. By addressing both the theoretical and practical implications, this chapter seeks to provide a comprehensive overview that can guide further studies and promote the integration of research findings into industry practices.

5.1 Conclusions

In conclusion,

- ✓ 4M AMP:1-(2-HE) PRLD (2:2) is more stable than 5M MEA:DMAE (3:2) as it gave 33% increment as against 80% increment when the oxygen partial pressure was doubled at a constant temperature of 60°C. This results highlight's the solvent's intrinsic resistance to degradation.
- ✓ 4M AMP:1-(2-HE) PRLD (2:2) exhibits minimal degradation when exposed to oxygen having an order of reaction of 1.3. Also, the minimum amount of energy required to cause it to degrade is 50,314.08 J/mol.
- ✓ 4M AMP:1-(2-HE) PRLD (2:2) is stable and can be used commercially for CO_2 capture from pre-treated flue gas. It has the potential for long-term application in environments where oxygen levels may fluctuate without succumbing easily to the degradation processes that typically affect similar compounds.

- ✓ There is a strong relation between ammonia emission and rate of degradation. The correlation can be used as a quick check in determining the rate of degradation to give to a close to accurate value.

5.2 Recommendation

i. Stability studies should be scaled up and studied in a pilot plant level to know how flow dynamics can affect the rate of degradation.

ii. Degradation products should be investigated and other emissions due to degradation should be studied.

iii. Degradation of the novel amine blend should be studied under untreated flue gas conditions. Thus, in the presence of SOx, NOx and metal oxides.

iv. Degradation of AMP and PRLD should be studied separately so as come up with a reaction mechanism to aid in a mechanistic rate law equation

REFERENCES

Appiah, F. A. (2021). *Performance Studies of Novel Amine Blends in a Catalyst-Aided CO2 Capture Process*. University of Regina.

Ashenhurst, J. (2023). *3 Factors That Stabilize Carbocations*. Master Organic Chemistry. https://www.masterorganicchemistry.com/2011/03/11/3-factors-that-stabilize-carbocations/

Avor, E. P., Supap, T., Narku-Tetteh, J., Muchan, P., Natewong, P., & Idem, R. (2022). Achieving Net-Zero CO2 Emissions from Indirect Co-Combustion of Biomass and Natural Gas With Carbon Capture Using a Novel Amine Blend. *16th International Conference on Greenhouse Gas Control Technologies, GHGT-16, August*, 1–12.

Bello, A., & Idem, R. O. (2005). Pathways for the formation of products of the oxidative degradation of CO2-loaded concentrated aqueous monoethanolamine solutions during CO2 absorption from flue gases. *Industrial and Engineering Chemistry Research*, *44*(4), 945–969. https://doi.org/10.1021/ie049329+

Blachly, H. C., & Ravner, H. (1964). *The Stabilization of Monoethanolamine Solutions for Submarine Carbon Dioxide Scrubbers*.

Bottoms, R. R. (1930). *Process for separating acid gases* (Patent No. 486,918). UNITED STATES PATENT OFFICE.

Buvik, V., Høisæter, K. K., Vevelstad, S. J., & Knuutila, H. K. (2021). A review of degradation and emissions in post-combustion CO2 capture pilot plants. *International Journal of Greenhouse Gas Control*, *106*(December 2020). https://doi.org/10.1016/j.ijggc.2020.103246

Buvik, V., Wanderley, R. R., & Knuutila, H. K. (2021). Addition of potassium iodide reduces

oxidative degradation of monoethanolamine (MEA). *Chemical Engineering Science: X*, *10*(April), 100096. https://doi.org/10.1016/j.cesx.2021.100096

Camobreco, V., Roberts, S., Powers, J., Weitz, M., Sherry, C., Aepli, L., Desai, M., Steller, J., Rewcastle, K., Beaulieu, J., & Hall, A. (2024). Inventory of U.S. Greenhouse Gas Emissions and Sinks 1990-2022. *United States, Environmental Protection AgencY, EPA 430-R-*, 1–919. https://www.epa.gov/ghgemissions/inventory-us-greenhouse-gas-emissions-and-sinks

Chakraborty, A. K., Astarita, G., & Bischoff, K. B. (1986). CO2 absorption in aqueous solutions of hindered amines. *Chemical Engineering Science*, *41*(4), 997–1003. https://doi.org/10.1016/0009-2509(86)87185-8

Chen, S., Han, X., Sun, X., Luo, X., & Liang, Z. (2020). The comparative kinetics study of CO2 absorption into non-aqueous DEEA/MEA and DMEA/MEA blended systems solution by using stopped-flow technique. *Chemical Engineering Journal*, *386*(xxxx), 0–1. https://doi.org/10.1016/j.cej.2019.03.171

Chi, S., & Rochelle, G. T. (2002). Oxidative Degradation of Monoethanolamine. *Industrial & Engineering Chemistry Research*, *41*(17), 4178–4186. https://doi.org/10.1021/ie010697c

Chowdhury, F. A., Yamada, H., Matsuzaki, Y., Goto, K., Higashii, T., & Onoda, M. (2014). Development of Novel Synthetic Amine Absorbents for CO 2 Capture. *Energy Procedia*, *63*, 572–579. https://doi.org/10.1016/j.egypro.2014.11.062

Conway, W., Bruggink, S., Beyad, Y., Luo, W., Melián-Cabrera, I., Puxty, G., & Feron, P. (2015). CO2 absorption into aqueous amine blended solutions containing monoethanolamine (MEA), N,N-dimethylethanolamine (DMEA), N,N-diethylethanolamine

(DEEA) and 2-amino-2-methyl-1-propanol (AMP) for post-combustion capture processes. *Chemical Engineering Science*, *126*, 446–454. https://doi.org/10.1016/j.ces.2014.12.053

Crooks, J. E., & Donnellan, J. P. (1989). Kinetics and mechanism of the reaction between carbon dioxide and amines in aqueous solution. *Journal of the Chemical Society, Perkin Transactions 2*, *2*(4), 331–333. https://doi.org/10.1039/p29890000331

Davis, J. D., Rochelle, G., & Campion, A. (2009). *Thermal Degradation of Aqueous Amines Used for Carbon Dioxide Capture*. The University of Texas at Austin.

Dinh, H. H. T. (2010). *Analysis of ammonia and volatile organic amine emissions in a confined poultry facility*. Utah State University.

Figueroa, D., Fout, T., Plasynski, S., Mcilvried, H., & Srivastava, R. D. (2008). *Advances in CO 2 capture technology — The U . S . Department of Energy ' s Carbon Sequestration Program §*. *2*, 9–20. https://doi.org/10.1016/S1750-5836(07)00094-1

Fogler, H. S. (2016). *Elements of Chemical Reaction Engineering* (C. Vennema, A. Vennema, A. Arbor, & A. F. T. P. (University of Michigan) (eds.); Five). Pearson Education, Inc.

Fredriksen, S. B., & Jens, K. (2013). Oxidative degradation of aqueous amine solutions of MEA , AMP , MDEA , Pz : A review. *Energy Procedia*, *37*(1876), 1770–1777. https://doi.org/10.1016/j.egypro.2013.06.053

Gao, H., Wu, Z., Liu, H., Luo, X., & Liang, Z. (2017). Experimental Studies on the Effect of Tertiary Amine Promoters in Aqueous Monoethanolamine (MEA) Solutions on the Absorption/Stripping Performances in Post-combustion CO2 Capture. *Energy and Fuels*, *31*(12), 13883–13891. https://doi.org/10.1021/acs.energyfuels.7b02390

Gouedard, C., Picq, D., Launay, F., & Carrette, P. L. (2012). Amine degradation in CO2 capture. I. A review. *International Journal of Greenhouse Gas Control*, *10*, 244–270. https://doi.org/10.1016/j.ijggc.2012.06.015

Guel, T., Budins, S., & McCulloch, S. (2022). Direct Air Capture: A key technology for net zero. *International Energy Agency*, 1–76. www.iea.org

Henni, A. (2022). *Lecture note ENPC/ENIN 831 : Industrial Gas Processing Chapter 1*.

Idem, R. (2021). *Lecture Note: Mass Transfer With Chemical Reaction*.

IEAGHG. (2012). *A Brief History of CCS and Current Status*. 2.

Institute, G. C. (2012). CO2 Capture Technologies Pre Combustion Capture. *Gloabal CCS Institute*, *January*, 14. www.cdn.globalccsinstitute.com/sites/default/files/publications/29756/co2-capture-technologies-pre-combustion-capture.pdf.

Jiang, W., Luo, X., Gao, H., Liang, Z., Liu, B., Tontiwachwuthikul, P., & Hu, X. (2018). A comparative kinetics study of CO 2 absorption into aqueous DEEA/MEA and DMEA/MEA blended solutions. *AIChE Journal*, *64*(4), 1350–1358. https://doi.org/10.1002/aic.16024

Kamijo, T., Kajiya, Y., Endo, T., & Nagayasu, H. (2013). SO 3 impact on amine emission and emission reduction technology. *Energy Procedia*, *37*, 1793–1796. https://doi.org/10.1016/j.egypro.2013.06.056

Kim, S., Shi, H., & Lee, J. Y. (2016). CO2 absorption mechanism in amine solvents and enhancement of CO2 capture capability in blended amine solvent. *International Journal of Greenhouse Gas Control*, *45*, 181–188. https://doi.org/10.1016/j.ijggc.2015.12.024

Lepaumier, H., Picq, D., & Carrette, P. L. (2009). New amines for CO2 Capture. I. mechanisms

of amine degradation in the presence of CO2. *Industrial and Engineering Chemistry Research*, *48*(20), 9061–9067. https://doi.org/10.1021/ie900472x

Leung, D. Y. C., Caramanna, G., & Maroto-valer, M. M. (2014). An overview of current status of carbon dioxide capture and storage technologies. *Renewable and Sustainable Energy Reviews*, *39*, 426–443. https://doi.org/10.1016/j.rser.2014.07.093

Levenspiel, O. (1998). *Chemical reaction engineering*. 3ed., Wiley, T.

Liang, Z. H., Sanpasertparnich, T., & Tontiwachwuthikul, P. P. T. (2011). Part 1 : Design , modeling and simulation of post-combustion CO 2 capture systems using reactive solvents. In *Carbon Management* (pp. 265–288). Future Science Group.

Lidal, H. (1992). *Carbon dioxide removal in gas treating processes*. The University of Trondheim.

Lv, B., Guo, B., Zhou, Z., & Jing, G. (2015). Mechanisms of CO 2 Capture into Monoethanolamine Solution with Different CO 2 Loading during the Absorption/Desorption Processes. *Environmental Science & Technology*, *49*(17), 10728–10735. https://doi.org/10.1021/acs.est.5b02356

Muchan, P., Supap, T., Narku-tetteh, J., & Idem, R. (2021). Assessment of the Relationship between Degradation and Emission Activities of Carbon Capture Amines Based on their Chemical Structures. *15th International Conference on Greenhouse Gas Control Technologies, GHGT-15*, *March*, 1–12.

Naami, A., Edali, M., Sema, T., Idem, R., & Tontiwachwuthikul, P. (2012). Mass transfer performance of CO 2 absorption into aqueous solutions of 4-diethylamino-2-butanol,

monoethanolamine, and N-methyldiethanolamine. *Industrial and Engineering Chemistry Research*, *51*(18), 6470–6479. https://doi.org/10.1021/ie2008357

Nakao, S., Yogo, K., Goto, K., Kai, T., & Yamada, H. (2019). *Advanced CO2 Capture Technologies*. Springer International Publishing. https://doi.org/10.1007/978-3-030-18858-0

Narku-Tetteh, J., Muchan, P., Saiwan, C., Supap, T., & Idem, R. (2017). Selection of components for formulation of amine blends for post combustion CO2 capture based on the side chain structure of primary, secondary and tertiary amines. *Chemical Engineering Science*, *170*, 542–560. https://doi.org/10.1016/j.ces.2017.02.036

Natural Resources Canada. (2021). *Energy Fact Book 2021-2022*. 1–146.

Nyarko, C. (2022). *EFFECTS OF FLUE GAS IMPURITIES ON AMINE STABILITY IN CO2 CAPTURE*. University of Regina.

Ofori, D. A., Anjarwalla, P., Mwaura, L., Jamnadass, R., Stevenson, P. C., Smith, P., Koch, W., Kukula-Koch, W., Marzec, Z., Kasperek, E., Wyszogrodzka-Koma, L., Szwerc, W., Asakawa, Y., Moradi, S., Barati, A., Khayyat, S. A., Roselin, L. S., Jaafar, F. M., Osman, C. P., … Slaton, N. (2020). No 主観的健康感を中心とした在宅高齢者における 健康関連指標に関する共分散構造分析Title. *Molecules*, *2*(1), 1–12. http://clik.dva.gov.au/rehabilitation-library/1-introduction-rehabilitation%0Ahttp://www.scirp.org/journal/doi.aspx?DOI=10.4236/as.2017.81005%0Ahttp://www.scirp.org/journal/PaperDownload.aspx?DOI=10.4236/as.2012.34066%0Ahttp://dx.doi.org/10.1016/j.pbi.201

Pradoo, P. (2021). *Oxidative Degradation Of Diethanolamine Solvent Induced By Nitrogen*

Dioxide And Dissolved Materials In Post- Combustion Capture Of CO2 From Industrial Exhaust Gas Streams. University of Regina.

Rochelle, G. T. (2012). Thermal degradation of amines for CO 2 capture. *Current Opinion in Chemical Engineering*, *1*(2), 183–190. https://doi.org/10.1016/j.coche.2012.02.004

Romanov, V., Soong, Y., Carney, C., Rush, G. E., Nielsen, B., & O'Connor, W. (2015). Mineralization of Carbon Dioxide: A Literature Review. *ChemBioEng Reviews*, *2*(4), 231–256. https://doi.org/10.1002/cben.201500002

Sai-obodai, L. S. (2021). *A COMPREHENSIVE EVALUATION OF OFF-GAS EMISSIONS FROM A CATALYST- AIDED, AMINE-BASED, POST COMBUSTION CAPTURE OF CO2 FROM INDUSTRIAL EXHAUST GAS STREAMS* (Issue November). University of Regina.

Sakwattanapong, R., Aroonwilas, A., & Veawab, A. (2009). Reaction rate of CO2 in aqueous MEA-AMP solution: Experiment and modeling. *Energy Procedia*, *1*(1), 217–224. https://doi.org/10.1016/j.egypro.2009.01.031

Sandalow, D., Friedmann, J., Mccormick, C., & Mccoy, S. (2018). Direct Air Capture of Carbon Dioxide. *Innovation for Cool Earth Forum*, 1–43.

Sexton, A. J., & Rochelle, G. T. (2009). Catalysts and inhibitors for MEA oxidation. *Energy Procedia*, *1*(1), 1179–1185. https://doi.org/10.1016/j.egypro.2009.01.155

Shi, H. (2013). *Interactions for Studies of Vapour-Liquid Equilibrium and Catalyst Aided and Unaided Solvent Regeneration*.

Singh, P., Niederer, J. P. M., & Versteeg, G. F. (2008). *Structure and activity relationships for amine-based CO2 absorbents-II*. *7*(July), 135–144.

https://doi.org/10.1016/j.cherd.2008.07.014

Singto, S., Supap, T., Idem, R., Tontiwachwuthikul, P., Tantayanon, S., Al-marri, J., & Benamor, A. (2016). Synthesis of New Amines for Enhanced Carbon Dioxide (CO2) Capture Performance: The Effect of Chemical Structure on Equilibrium Solubility, Cyclic Capacity, Kinetics of Absorption and Regeneration, and Heats of Absorption and Regeneration. *SEPARATION AND PURIFICATION TECHNOLOGY*. https://doi.org/10.1016/j.seppur.2016.05.002

Song, C., Liu, Q., Ji, N., Deng, S., Zhao, J., Li, Y., & Song, Y. (2018). *Alternative pathways for e ffi cient CO 2 capture by hybrid processes — A review*. *82*(September 2017), 215–231. https://doi.org/10.1016/j.rser.2017.09.040

Spietz, T., Wilk, A., Tatarczuk, A., Wie, L., & Kro, A. (2018). *Ammonia emission from CO 2 capture pilot plant using aminoethylethanolamine*. 1085–1092. https://doi.org/10.1007/s13762-017-1475-z

Supap, T., Idem, R., Tontiwachwuthikul, P., & Saiwan, C. (2006). *Analysis of Monoethanolamine and Its Oxidative Degradation Products during CO 2 Absorption from Flue Gases : A Comparative Study of GC-MS , HPLC-RID , and CE-DAD Analytical Techniques and Possible Optimum Combinations*. 2437–2451.

Supap, T., Idem, R., Tontiwachwuthikul, P., & Saiwan, C. (2009). Kinetics of sulfur dioxide- and oxygen-induced degradation of aqueous monoethanolamine solution during CO2 absorption from power plant flue gas streams. *International Journal of Greenhouse Gas Control*, *3*(2), 133–142. https://doi.org/10.1016/j.ijggc.2008.06.009

Supap, T., Saiwan, C., Idem, R., & Tontiwachwuthikul, P. P. T. (2011). Part 2: Solvent

management: Solvent stability and amine degradation in CO 2 capture processes. *Carbon Management*, *2*(5), 551–566. https://doi.org/10.4155/cmt.11.55

Terrence, L. D., & Yen, N. N. (1980). *Carbon Dioxide Reaction Kinetics and Transport in Aqueous Amine Membranes*. *2*, 260–266.

Uyanga, I. J., & Idem, R. O. (2007). Studies of so2- and O2-induced degradation of aqueous MEA during CO2 capture from power plant flue gas streams. *Industrial and Engineering Chemistry Research*, *46*(8), 2558–2566. https://doi.org/10.1021/ie0614024

Vega, F., Sanna, A., Navarrete, B., Maroto-Valer, M. M., & Cortés, V. J. (2014a). Degradation of amine-based solvents in CO2 capture process by chemical absorption. *Greenhouse Gases: Science and Technology*, *4*(6), 707–733. https://doi.org/10.1002/ghg.1446

Vega, F., Sanna, A., Navarrete, B., Maroto-Valer, M. M., & Cortés, V. J. (2014b). Degradation of amine-based solvents in CO 2 capture process by chemical absorption. *Greenhouse Gases: Science and Technology*, *4*(6), 707–733. https://doi.org/10.1002/ghg.1446

Versteeg, G. F., & van Swaaij, W. P. M. (1988). On the kinetics between CO2 and alkanolamines both in aqueous and non-aqueous solutions-I. Primary and secondary amines. *Chemical Engineering Science*, *43*(3), 573–585. https://doi.org/10.1016/0009-2509(88)87017-9

Wang, T., & Jens, K. J. (2013). Oxidative degradation of AMP/MEA blends for post-combustion CO2 capture. *Energy Procedia*, *37*(1876), 306–313. https://doi.org/10.1016/j.egypro.2013.05.116

Wang, T., & Jens, K. J. (2014). Possible Pathways oxidative degradation of β-hydroxyl

alkanolamine for post-combustion CO2 capture. *Energy Procedia*, *51*(1876), 259–266. https://doi.org/10.1016/j.egypro.2014.07.030

Xiang, Y., Yan, W., & Wang, J. (2016). Solubility of oxygen in various alkanolamine–water solutions at low partial pressure. *Asia-Pacific Journal of Chemical Engineering*, *11*(1), 158–160. https://doi.org/10.1002/apj.1942

APPENDICES

APPENDIX A: Solvent Preparation Calculation

A.1: 4M AMP:1-(2-HE) PRLD Preparation

Basis of 1L 4M AMP: 1-(2-HE) PRLD (2:2) solvent

Mass of AMP (using 95% purity) needed for 2M AMP concentration is determined as

$$m_{AMP}=C_{AMP}\times V_{Total}\times Mwt_{AMP}$$

AMP molecular weight(Mwt_{AMP}) = 89.14 g/mol

$$m_{AMP}=\frac{1\times 2\times 89.14}{0.95}$$

$$= 187.66\ g$$

Mass of 1-(2-HE) PRLD (using 98% purity) needed for 2M 1-(2-HE) PRLD concentration is determined as

$$m_{1\text{-(2-HE) PRLD}}=C_{1\text{-(2-HE) PRLD}}\times V_{Total}\times Mwt_{1\text{-(2-HE) PRLD}}$$

1-(2-HE) PRLD molecular weight($Mwt_{1\text{-(2-HE) PRLD}}$) = 115.18 g/mol

$$m_{1\text{-(2-HE) PRLD}}=\frac{1\times 2\times 89.14}{0.98}$$

$$= 181.92\ g$$

A.2: 5M MEA:DMAE Preparation

Basis of 5M MEA-DMAE (3:2) solvent

DMAE needed for 2M DMAE concentration is determined as

$$m_{DMAE}=C_{DMAE}\times V_{Total}\times Mwt_{DMAE}$$

DMAE molecular weight(Mwt_{DMAE}) = 87.14 g/mol

$$m_{DMAE}=1\times 2\times 87.14$$

$$m_{DMAE}=174.28\ g$$

The amount of MEA needed for 3M is determined as

$$m_{MEA}=C_{MEA}\times V_{Total}\times Mwt_{MEA}$$

MEA molecular weight is 61.084 g/mol (Mwt_{MEA})

$$m_{_{MEA}}=3\times 1\times 61.08$$

$$m_{_{MEA}}=183.24\ g$$

A 1L volumetric flask is filled with 187.66 g of AMP and 181.92 1-(2-HE) PRLD and topped up with deionised water to the 1L mark. Also, another 1L volumetric flask is filled with 174.28 g of DMAE and 183.24 g of MEA and topped up with deionised water to the 1L mark. Both stock solutions are placed on magnetic stirrer and stirred for 30 mins.

A.3: Standardization of Prepared Stock Solution

The prepared solution was standardized using a titration procedure. 1ml of the solution was pipetted into a conical flask. Following the addition of 50 ml of distilled water, three drops of the methyl orange indicator (yellow colour observed) were added. The titration continued with IN HCl until reaching the endpoint was reached (pink colour observed). The titration was repeated at least twice to confirm the concentration of the prepared solution.

A.4: CO_2 Loading Determination for Loaded Samples

The Chittick apparatus (Figure 3.2) helps us to quantify the amount of CO_2 absorbed. Sine CO_2 is a weak acid, the strong acid, HCl, displaces it off during titration. The amount of displaced CO_2 gas is determined by recording the total displacement (VD) following the titration

The volume of gas (CO_2), $V_{gas}=V_D-V_{\text{total acid}}$

Here, V_m, P_s, and T_s are molar volume, pressure, and temperature at standard conditions respectively. On the other hand, P_{actual}, T_{actual} represents the actual pressure and temperature of the room in where analysis is taking place.

Using the concept of mole ratio from the balanced equation of HCl reacting with the amine $C_1V_1 = C_2V_2$, the concentration of amine at the reacted with the acid can be calculated.

$$CO_2\text{loading} = \frac{V_{gas}}{V_m V_{amine} C_{amine}} \left(\frac{P_{actual} T_s}{P_s T_{actual}}\right)$$

Calculation steps for sample analysis for CO_2 loading

Acid concentration = 1N HCl

Volume of amine = V_{amine} = 1 ml

The volume of acid at the endpoint = 4 ml

The volume of excess acid used = 2 ml

The total volume of acid added, $V_{total\ acid}$ = 6 ml

Total displacement after titration, V_D =46.9 ml

Volume of CO_2, $V_{gas} = V_D - V_{total\ acid} = 46.9 - 6 = 41.9$ ml

The concentration of amine calculated, C_{amine} = 4 M

Real-time pressure and temperature recorded are P_{actual}=716.25 mmHg and T_2=295.4 K

V_m = 22.4 L/mol, P_s = 760 mmHg, T_s = 273 K

Therefore, $CO_2 \text{loading} = \left(\frac{41.9}{22.4 \times 4 \times 1}\right)\left(\frac{716.25 \times 273}{760 \times 295.4}\right)$

$$= 0.407 \frac{\text{mol } CO_2}{\text{mol amine}}$$

Table A. 1: Rich loading calculations

Time, mins	Vtitre	Vexcess	Displacement	Vgas	Troom, K	Proom, mmHg	Mole of CO_2	Mole of amine	CO_2 loading
0	3.9	1	0	0	295.3	722.25	0	3.9	0
10	3.9	2	10	4.1	295.5	709.5	0.157862802	3.9	0.040477642
20	3.7	2	17	11.3	295.5	709.5	0.435085284	3.7	0.117590617
30	3.8	2	14	8.2	295.5	709.5	0.315725604	3.8	0.083085685
40	3.8	2	16	10.2	295.6	709.5	0.39259899	3.8	0.103315524
50	4	2	17.8	11.8	295.8	709.5	0.453876058	4	0.113469014

60	4	2	15.9	9.9	297.2	715.5	0.382205616	4	0.095551404
90	4.1	2	17	10.9	294.9	705.75	0.418315203	4.1	0.102028098
120	3.6	1	12.5	7.9	295.7	722.25	0.30943138	3.6	0.085953161
150	4	1	16	11	295.8	722.25	0.430708163	4	0.107677041
180	3.9	1	18.9	14	295.8	722.25	0.548174025	3.9	0.140557442
240	4	1	22.8	17.8	295.9	722.25	0.696728577	4	0.174182144
300	4	1	27.9	22.9	295.6	720	0.894467541	4	0.223616885
360	3.8	1	29.5	24.7	295.7	720	0.964448766	3.8	0.253802307

420	3.9	1	34	29.1	295.7	720	1.136253404	3.9	0.291347027
480	4	1	37.2	32.2	295.7	720	1.257297581	4	0.314324395
540	3.9	1	38.2	33.3	295.7	720	1.300248741	3.9	0.333397113
600	3.9	1	40.2	35.3	295.1	720	1.381144215	3.9	0.354139542
660	3.9	1	41	36.1	295.7	717.75	1.405174031	3.9	0.360301034
720	3.9	1	41.9	37	295.9	717.75	1.439232629	3.9	0.369034008
780	4.1	1	45	39.9	295.9	717	1.550415575	4.1	0.37815014
840	4.1	1	44.8	39.7	295.9	717	1.542644069	4.1	0.376254651

900	4	1	45.9	40.9	296	717	1.588736192	4	0.397184048
960	4	1	46.9	41.9	295.7	717	1.629231846	4	0.407307962
1020	4	1	46.9	41.9	295.4	716.25	1.6291805	4	0.407295125

Table A. 2: Lean loading calculations

Time, mins	Vtitre	Vexcess	Displacement	Vgas	Troom, K	Proom, mmHg	Mole of CO2	Mole of solvent	CO_2 loading, mol CO_2/mol amine
0	4.1	1	46.9	41.8	295.4	716.25	1.625292241	4.1	0.396412742
3.09	3.5	2	39.8	34.3	295	708	1.320098684	3.5	0.377171053
3.35	2.4	2	29	24.6	295	708	0.946776316	2.4	0.394490132
4.26	2.7	2	18	13.3	295.3	708	0.511354978	2.7	0.189390733
7	2	2	19.9	15.9	295.3	708	0.611319109	2	0.305659555
10	3.8	2	11.8	6	295.5	708	0.230530323	3.8	0.060665875
20	3.5	2	12	6.5	295.5	708	0.249741184	3.5	0.071354624
30	3.6	2	12	6.4	295.6	708	0.245815825	3.6	0.068282174
40	3.3	2	11.5	6.2	295.6	708	0.238134081	3.3	0.072161843
50.3	3.9	2	12.9	7	295.6	708	0.268861059	3.9	0.068938733
60.15	3.8	2	12.2	6.4	295.6	708	0.245815825	3.8	0.064688375

APPENDIX B: Ammonia Emissions Experimental Calculations

B.1: Evaluation of NH_3 emissions data

Using a similar approach by Dinh, 2010 and Muchan et al., 2021 ammonia emissions were calculated. The data, recorded in mg/L, indicate the amount of NH3 released over a one-hour period. The concentrations of the emitted gases were then converted to ppmV using the equation:

$$\text{Volume of } NH_3, \text{ L} = \frac{C_{NH_3} V_s V_m (0.001)}{M_w}$$

$$\text{Emission in an hr (ppmV)} = \frac{\text{Volume of } NH_3}{V_{\text{total gas}}} \times 10^6$$

Where, C_{NH_3} is the ammonia concentration in mg/L

V_s is the sample volume in $L = 0.1$

V_m is the molar volume at standard conditions = $22.4\ L/mol$

M_w is the molecular weight of NH_3 in g/mol

$V_{total\ gas}$ is the total off gas volume in an hour =$12\ L$

0.0001 is a conversion factor from mg/L to g/L

10^6 is the ppm conversion factor

The accumulation of ammonia at each sampling interval was calculated utilizing MATLAB (version R2020b) and the previously mentioned equations based on the NH3 concentration. The cumulative trapezoidal numerical integration function (cumtrapz) was employed to determine the total NH3 at each sampling point. Subsequently, the overall ammonia emission rate for each degradation cell was computed by finding the average of all the hours off gas sampling was done

Table B. 1: Ammonia emissions results for 18% O2:60°C

Degradation time (h)	NH_3 concentration in mg/L	Volume of NH_3 (L)	Rate of NH_3 emission (ppmV/h)	Accumulated amount of NH_3 (ppmV) at STD condition (273K,760 mmHg)
1	1.3	0.000183835	15.32	7.0
3	1.14	0.000161209	13.43	33.4
18	0.65	9.19176E-05	7.66	178.3
24	0.08	1.13129E-05	0.94	202.0
48	0.12	1.69694E-05	1.41	227.9
72	0.12	1.69694E-05	1.41	259.1
96	0.12	1.69694E-05	1.41	290.3
120	0.12	1.69694E-05	1.41	321.5
144	0.12	1.69694E-05	1.41	352.7
168	0.12	1.69694E-05	1.41	383.9
192	0.11	1.55553E-05	1.30	413.8
216	0.12	1.69694E-05	1.41	443.7
238	0.11	1.55553E-05	1.30	471.0
264	0.12	1.69694E-05	1.41	503.4
288	0.11	1.55553E-05	1.30	533.3
312	0.12	1.69694E-05	1.41	563.2
336	0.11	1.55553E-05	1.30	593.1

360	0.11	1.55553E-05	1.30	621.6
384	0.11	1.55553E-05	1.30	650.2
408	0.11	1.55553E-05	1.30	678.7
432	0.11	1.55553E-05	1.30	707.3
456	0.09	1.27271E-05	1.06	733.2
480	0.1	1.41412E-05	1.18	757.8
504	0.1	1.41412E-05	1.18	783.7
			2.66	

Table B. 2: Ammonia emissions results for 18% O2:40°C

Degradation time (h)	**NH_3 concentration in mg/L**	**Volume of NH_3 (L)**	**Rate of NH_3 emission (ppmV/h)**	**Accumulated amount of NH_3 (ppmV) at STD condition (273K, 760 mmHg)**
1	0.47	6.64635E-05	5.54	7.6
3	0.39	5.51506E-05	4.60	35.9
18	0.22	3.11106E-05	2.59	57.0
24	0.12	1.69694E-05	1.41	134.1
48	0.04	5.65647E-06	0.47	161.3
72	0.04	5.65647E-06	0.47	231.3
96	0.04	5.65647E-06	0.47	297.4
120	0.04	5.65647E-06	0.47	354.4

144	0.04	5.65647E-06	0.47	399.8
168	0.04	5.65647E-06	0.47	434.8
192	0.04	5.65647E-06	0.47	476.3
216	0.04	5.65647E-06	0.47	528.2
240	0.04	5.65647E-06	0.47	577.4
264	0.04	5.65647E-06	0.47	638.2
288	0.04	5.65647E-06	0.47	691.3
312	0.04	5.65647E-06	0.47	737.8
336	0.04	5.65647E-06	0.47	788.3
360	0.04	5.65647E-06	0.47	819.4
384	0.04	5.65647E-06	0.47	846.5
408	0.04	5.65647E-06	0.47	880.1
432	0.04	5.65647E-06	0.47	912.5
456	0.04	5.65647E-06	0.47	954.1
480	0.04	5.65647E-06	0.47	996.8
504	0.04	5.65647E-06	0.47	1048.5
			0.98	

Table B. 3: Ammonia emissions results for 12% O2:60°C

Degradation time (h)	NH_3 concentration in mg/L	Volume of NH_3 (L)	Rate of NH_3 emission (ppmV/h)	Accumulated amount of NH_3 (ppmV) at STD condition (273K, 760 mmHg)
1	1.61	0.000227673	18.97	8.7
3	1.33	0.000188078	15.67	40.4
18	0.21	2.96965E-05	2.47	165.2
24	0.04	5.65647E-06	0.47	173.3
48	0.04	5.65647E-06	0.47	183.6
72	0.04	5.65647E-06	0.47	193.9
96	0.04	5.65647E-06	0.47	204.2
120	0.04	5.65647E-06	0.47	214.5
144	0.04	5.65647E-06	0.47	224.9
168	0.04	5.65647E-06	0.47	235.2
192	0.07	9.89882E-06	0.82	249.5
216	0.06	8.48471E-06	0.71	266.4
238	0.08	1.13129E-05	0.94	283.0
264	0.04	5.65647E-06	0.47	299.8
288	0.07	9.89882E-06	0.82	314.0
312	0.08	1.13129E-05	0.94	333.5
336	0.05	7.07059E-06	0.59	350.3

360	0.09	1.27271E-05	1.06	368.4
384	0.04	5.65647E-06	0.47	385.2
408	0.05	7.07059E-06	0.59	396.8
432	0.05	7.07059E-06	0.59	409.8
456	0.08	1.13129E-05	0.94	426.6
480	0.04	5.65647E-06	0.47	442.1
504	0.06	8.48471E-06	0.71	455.0
			2.11	

Table B. 4: Ammonia emissions results for 6% O2:60°C

Degradation time (h)	**NH_3 concentration in mg/L**	**Volume of NH_3 (L)**	**Rate of NH_3 emission (ppmV/h)**	**Accumulated amount of NH_3 (ppmV) at STD condition (273K, 760 mmHg)**
1	1.1	0.000155553	12.96	6.8
3	0.8	0.000113129	9.43	34.3
18	0.24	3.39388E-05	2.83	157.4
24	0.15	2.12118E-05	1.77	169.7
48	0.04	5.65647E-06	0.47	194.3
72	0.04	5.65647E-06	0.47	204.6
96	0.04	5.65647E-06	0.47	214.9

120	0.04	5.65647E-06	0.47	225.3
144	0.04	5.65647E-06	0.47	235.6
168	0.04	5.65647E-06	0.47	245.9
192	0.04	5.65647E-06	0.47	256.2
216	0.04	5.65647E-06	0.47	266.5
238	0.04	5.65647E-06	0.47	276.0
264	0.04	5.65647E-06	0.47	287.2
288	0.04	5.65647E-06	0.47	297.5
312	0.04	5.65647E-06	0.47	307.8
336	0.04	5.65647E-06	0.47	318.1
360	0.04	5.65647E-06	0.47	328.5
384	0.09	1.27271E-05	1.06	345.3
408	0.04	5.65647E-06	0.47	362.1
432	0.06	8.48471E-06	0.71	375.0
456	0.08	1.13129E-05	0.94	393.1
480	0.05	7.07059E-06	0.59	409.9
504	0.12	1.69694E-05	1.41	432.0
			1.62	

Table B. 5: Ammonia emissions results for 18% O2:50°C

Degradation time (h)	NH_3 concentration in mg/L	Volume of NH_3 (L)	Rate of NH_3 emission (ppmV/h)	Accumulated amount of NH_3 (ppmV) at STD condition (273K, 760 mmHg)
1	1.44	0.000203633	16.97	7.8
3	0.81	0.000114544	9.55	32.1
18	0.25	3.53529E-05	2.95	117.9
24	0.08	1.13129E-05	0.94	128.5
48	0.04	5.65647E-06	0.47	144.0
72	0.07	9.89882E-06	0.82	158.3
96	0.07	9.89882E-06	0.82	176.5
120	0.07	9.89882E-06	0.82	194.8
144	0.07	9.89882E-06	0.82	213.0
168	0.1	1.41412E-05	1.18	235.1
192	0.1	1.41412E-05	1.18	261.0
216	0.1	1.41412E-05	1.18	286.9
238	0.1	1.41412E-05	1.18	310.7
264	0.1	1.41412E-05	1.18	338.8
288	0.1	1.41412E-05	1.18	364.7
312	0.1	1.41412E-05	1.18	390.6
336	0.1	1.41412E-05	1.18	416.5

360	0.09	1.27271E-05	1.06	441.1
384	0.09	1.27271E-05	1.06	464.4
408	0.09	1.27271E-05	1.06	487.7
432	0.09	1.27271E-05	1.06	511.0
456	0.09	1.27271E-05	1.06	534.3
480	0.09	1.27271E-05	1.06	557.5
504	0.08	1.13129E-05	0.94	579.5
			2.12	

Table B. 6: Ammonia emissions results for 6% O2:50°C

Degradation time (h)	**NH_3 concentration in mg/L**	**Volume of NH_3 (L)**	**Rate of NH_3 emission (ppmV/h)**	**Accumulated amount of NH_3 (ppmV) at STD condition (273K, 760 mmHg)**
1	0.75	0.000106059	8.84	3.8
3	0.34	0.00004808	4.01	14.9
18	0.15	2.12118E-05	1.77	51.3
24	0.04	5.65647E-06	0.47	56.8
48	0.04	5.65647E-06	0.47	67.1
72	0.05	7.07059E-06	0.59	78.8
96	0.04	5.65647E-06	0.47	90.4

120	0.06	8.48471E-06	0.71	103.4
144	0.04	5.65647E-06	0.47	116.3
168	0.04	5.65647E-06	0.47	126.6
192	0.06	8.48471E-06	0.71	139.6
216	0.04	5.65647E-06	0.47	152.6
238	0.04	5.65647E-06	0.47	162.0
264	0.06	8.48471E-06	0.71	176.1
288	0.04	5.65647E-06	0.47	189.0
312	0.04	5.65647E-06	0.47	199.3
336	0.04	5.65647E-06	0.47	209.7
360	0.04	5.65647E-06	0.47	220.0
384	0.05	7.07059E-06	0.59	231.6
408	0.06	8.48471E-06	0.71	245.9
432	0.05	7.07059E-06	0.59	260.2
456	0.04	5.65647E-06	0.47	271.8
480	0.06	8.48471E-06	0.71	284.8
504	0.07	9.89882E-06	0.82	301.7
			1.10	

Table B. 7: Ammonia emissions results for 6% O2:40°C

Degradation time (h)	NH_3 concentration in mg/L	Volume of NH_3 (L)	Rate of NH_3 emission (ppmV/h)	Accumulated amount of NH_3 (ppmV) at STD condition (273K, 760 mmHg)
1	0.42	5.93929E-05	4.95	2.3
3	0.31	4.38376E-05	3.65	9.1
18	0.23	3.25247E-05	2.71	38.2
24	0.08	1.13129E-05	0.94	45.1
48	0.04	5.65647E-06	0.47	58.0
72	0.04	5.65647E-06	0.47	68.3
96	0.04	5.65647E-06	0.47	78.7
120	0.04	5.65647E-06	0.47	89.0
144	0.04	5.65647E-06	0.47	99.3
168	0.04	5.65647E-06	0.47	109.6
192	0.04	5.65647E-06	0.47	119.9
216	0.04	5.65647E-06	0.47	130.3
238	0.04	5.65647E-06	0.47	139.7
264	0.04	5.65647E-06	0.47	150.9
288	0.04	5.65647E-06	0.47	161.2
312	0.04	5.65647E-06	0.47	171.5
336	0.04	5.65647E-06	0.47	181.9

360	0.04	5.65647E-06	0.47	192.2
384	0.04	5.65647E-06	0.47	202.5
408	0.04	5.65647E-06	0.47	212.8
432	0.04	5.65647E-06	0.47	223.1
456	0.04	5.65647E-06	0.47	233.5
480	0.04	5.65647E-06	0.47	243.8
504	0.04	5.65647E-06	0.47	254.1
			0.90	

APPENDIX C: Solvent degradation experimental calculations

In calculating the precise concentrations of the various amines, volume loss due to evaporation or volume added due to concentration was taken into account. This was determined from that fact that the initial volume was know and the final volume to remain after the 21 days of sample was known.

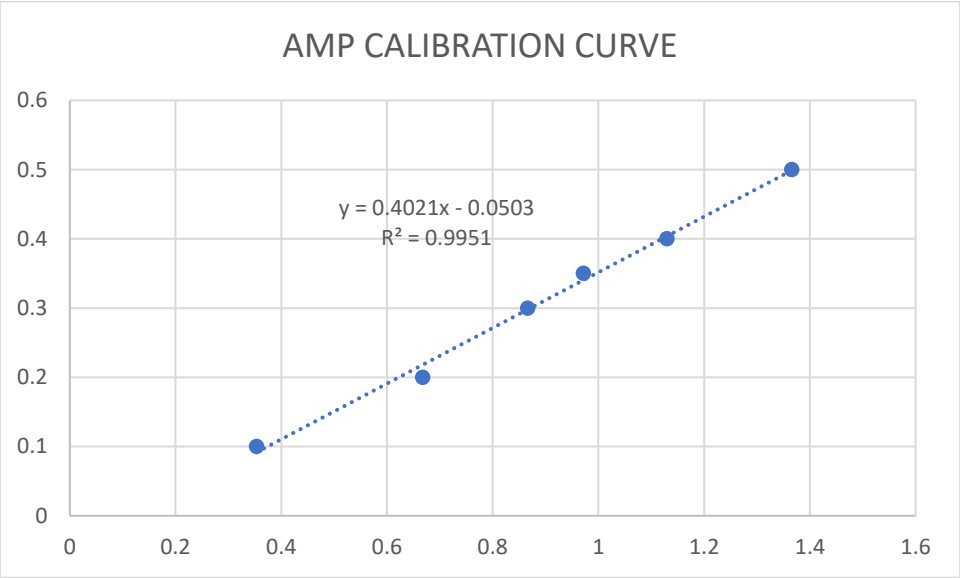

Figure C. 1: AMP calibration curve

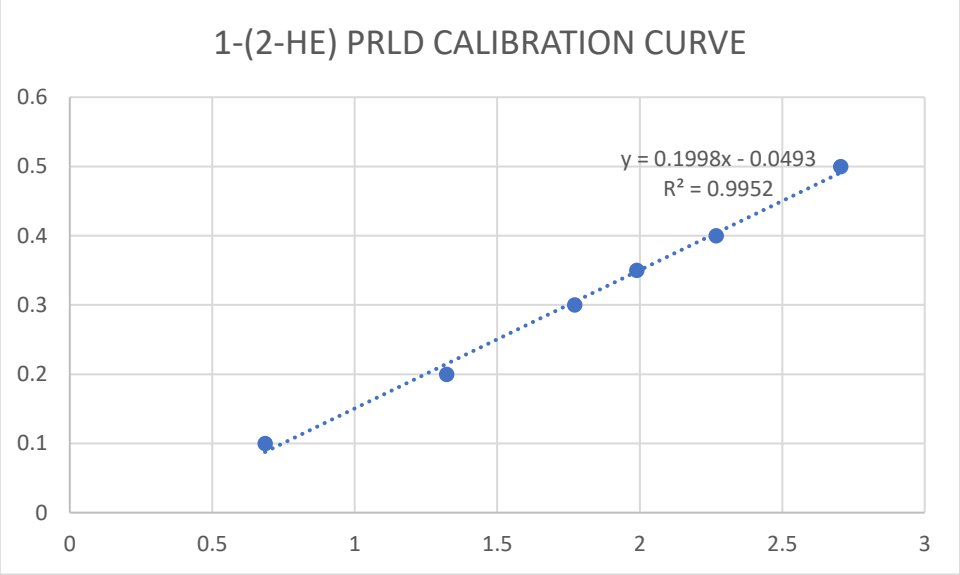

Figure C. 2:1-(2-HE) PRLD calibration curve

Table C. 1: AMP:1(2-HE) PRLD results for 18% O2:60°C

Degradation time (h)	AMP concentration after volume correction (M)	1-(2-HE) PRLD concentration after volume correction (M)	AMP:1-(2-HE) PRLD concentration after volume correction (M)
0	1.876525189	1.951409786	3.827934975
24	1.897	1.915	3.811410412
48	1.960	1.979	3.938984346
72	1.706	1.996	3.702356393
96	1.822	1.816	3.63806657
120	1.797	1.803	3.600115372
144	1.914	1.906	3.820136782
168	1.889	1.838	3.726647375
192	2.068	1.910	3.977783607
216	1.876	1.795	3.670925054
238	1.870	1.801	3.670845559
264	1.881	1.832	3.713022783
288	1.902	1.827	3.728422849
312	1.862	1.802	3.664512836
336	1.852	1.859	3.710339454
360	1.769	1.776	3.545246264
384	1.755	1.759	3.5142542

408	1.731	1.718	3.448711908
432	1.705	1.684	3.389074427
456	1.724	1.683	3.406996266
480	1.776	1.749	3.524837144
504	1.777	1.706	3.482965108
0	1.876525189	1.951409786	3.827934975
24	1.897	1.915	3.811410412

Table C. 2: AMP:1(2-HE) PRLD results for 6% 60°C

Degradation time (h)	**AMP concentration after volume correction (M)**	**1-(2-HE) PRLD concentration after volume correction (M)**	**AMP:1-(2-HE) PRLD concentration after volume correction (M)**
0	2.005350737	2.008671628	4.014022365
24	2.002124087	1.986233928	3.988358015
48	2.055396161	2.043261024	4.098657185
72	2.125091882	2.066518719	4.191610601
96	1.925590209	1.865645356	3.791235566
120	2.11682972	2.072550494	4.189380214
144	2.010018223	1.989396632	3.999414855
168	2.034451071	2.039285119	4.073736189
192	2.002432266	1.964959123	3.967391389
216	2.092078781	2.097486214	4.189564995

238	2.116838008	2.073772226	4.190610234
264	2.01066176	1.951903902	3.962565662
288	2.175320488	2.072422383	4.247742871
312	2.196178924	2.091681634	4.287860558
336	2.019659408	1.95832505	3.977984457
360	1.994146233	1.962901564	3.957047796
384	1.961281533	1.920192871	3.881474403
408	2.007720275	1.946129348	3.953849623
432	1.97656836	1.892281846	3.868850206
456	1.9695856	1.937291441	3.906877041
480	1.969548048	1.937268056	3.906816104
504	1.971616102	1.935322771	3.906938873

Table C. 3: AMP:1(2-HE) PRLD results for 18% 50°C

Degradation time (h)	**AMP concentration after volume correction (M)**	**1-(2-HE) PRLD concentration after volume correction (M)**	**AMP:1-(2-HE) PRLD concentration after volume correction (M)**
0	1.992292049	2.058277063	4.050569111
24	1.987138916	1.995874996	3.983013913
48	1.954855007	2.10843457	4.063289577
72	1.841849078	1.967095925	3.808945003
96	1.925527654	2.047535896	3.97306355

120	1.947491547	2.12352593	4.071017477
144	1.936059374	1.969638296	3.90569767
168	2.037530427	2.078960389	4.116490816
192	1.96190509	2.116321581	4.078226671
216	1.990656382	2.107465894	4.098122276
238	1.948590657	2.110142466	4.058733123
264	1.774930896	1.983530544	3.758461441
288	1.783006974	1.876610545	3.659617519
312	1.88832656	1.842919948	3.731246508
336	1.853996893	1.920687327	3.77468422
360	1.860190666	1.883369815	3.743560481
384	2.009707639	2.047010844	4.056718484
408	1.939383273	2.085158891	4.024542164
432	1.802543391	1.787190708	3.589734099
456	1.907387434	1.977804214	3.885191648
480	1.881920459	1.790594735	3.672515194
504	1.906908222	1.943915263	3.850823485

Table C. 4: AMP:1(2-HE) PRLD results for 6%:50°C

Degradation time (h)	AMP concentration after volume correction (M)	1-(2-HE) PRLD concentration after volume correction (M)	AMP:1-(2-HE) PRLD concentration after volume correction (M)
0	2.114128871	2.088215041	4.202343912
24	2.240224702	2.072119532	4.312344235
48	2.158812586	2.005605769	4.164418355
72	2.223577391	2.062884725	4.286462117
96	2.163858264	2.025191978	4.189050242
120	2.259495317	2.049076022	4.308571339
144	2.113201308	2.048870453	4.162071761
168	2.124540133	2.025682163	4.150222295
192	1.995154058	1.907946592	3.90310065
216	2.091221585	1.913835776	4.005057361
238	2.241339016	2.119879232	4.361218248
264	2.190356423	2.085989193	4.276345616
288	2.010057036	1.976816187	3.986873223
312	2.052326628	1.968651033	4.020977662
336	2.079296994	1.937914265	4.017211259
360	2.18654168	2.022958654	4.209500334
384	2.18303933	2.047553003	4.230592333
408	2.161428147	2.02367729	4.185105437

432	2.10075026	1.959463183	4.060213443
456	2.249847619	2.085580015	4.335427634
480	2.163491732	2.045604973	4.209096705
504	2.14562845	2.013097067	4.158725516

Table C. 5: AMP:1(2-HE) PRLD degradation results for 6%:40°C

Degradation time (h)	**AMP concentration after volume correction (M)**	**1-(2-HE) PRLD concentration after volume correction (M)**	**AMP:1-(2-HE) PRLD concentration after volume correction (M)**
0	2.136053516	2.066574524	4.20262804
24	2.188427401	2.080014437	4.268441837
48	2.085121587	1.989844873	4.074966459
72	2.144717453	2.029065893	4.173783346
96	2.14171947	2.019284616	4.161004086
120	2.120693542	2.045532862	4.166226404
144	2.099560605	1.982750947	4.082311552
168	2.007989011	1.935858474	3.943847485
192	2.107302952	1.982112058	4.08941501
216	2.103582638	1.990144599	4.093727237
238	2.191024299	2.022987487	4.214011785
264	2.132362021	2.004462262	4.136824283
288	2.169337427	2.072403992	4.241741419

312	2.091193788	1.982989672	4.074183459
336	2.149296506	2.042433545	4.191730052
360	2.114994731	2.053111437	4.168106168
384	2.086118134	2.062519208	4.148637342
408	2.127873594	1.990585704	4.118459298
432	2.140704319	1.990715574	4.131419893
456	2.130572408	1.998051856	4.128624264
480	2.103319488	1.993162054	4.096481541
504	2.113153094	1.990983345	4.104136439

Table C. 6: MEA:DMAE results for 12%:60°C

Degradation time (h)	MEA concentration after volume correction (M)	DMAE concentration after volume correction (M)	MEA:DMAE concentration after volume correction (M)
0	3.064	1.989	5.053
24	3.111	2.068	5.179
48	3.192	2.092	5.284
72	3.147	2.078	5.225
96	3.099	2.038	5.137
120	3.138	2.087	5.225
144	3.278	2.114	5.392
168	3.056	1.991	5.047

192	3.162	2.084	5.246
216	2.955	1.930	4.885
240	2.976	1.937	4.913
264	3.027	1.974	5.001
288	3.018	1.969	4.987
312	3.106	1.967	5.073
336	3.038	1.947	4.985
360	3.071	1.971	5.042
384	2.987	1.881	4.868
408	2.947	1.866	4.813
432	2.931	1.840	4.771
456	2.989	1.883	4.872
480	2.939	1.848	4.787
504	2.972	1.801	4.773

C.1: Ammonia Emission and Rate of Degradation Model

Table C. 7: Validation of ammonia emission and rate of degradation model

Expt. Deg. Rate AMP:1-(2-HE) PRLD	Rate of NH3 (ppmV/hr)	Pred. Deg. Rate AMP:1-(2-HE) PRLD	AD
0.0008	2.66	0.000764	0.045
0.00014	0.98	0.000092	0.342857143
0.0004	2.11	0.000544	0.36
0.00025	1.62	0.000348	0.392
0.0006	2.12	0.000548	0.086666667
0.0001	1.1	0.00014	0.4
0.00007	0.9	0.00006	0.142857143
AAD =			**0.25**

C.2: Spearman's Correlation Coefficient

The correlation was used in the comparative analysis of amine degradation. It is a descriptive statistical tool that informs on the strength on a monotonic relationship between paired data. It is usually denoted by ρ(rho). The range for determining the strength is -1≤ ρ≤1. A negative value corresponds to an indirect proportional relation between the two variables while a positive value corresponds to a direct proportional relation between the two variables.

$$\rho = 1 - \frac{6\Sigma d^2}{n(n^2-1)}$$

Where:

ρ = Spearman's correlation coefficient

d = difference between two ranks of observation

n = number of data points

Table C. 8: AMP:1(2-HE) PRLD Spearman's correlation result for 6%: 60°C

Degradation time (h)	AMP:1-(2-HE) PRLD after volume correction	Rank (Time)	Rank AMP:1-(2-HE) PRLD	d
0	4.014022365	1	14	-13
24	3.988358015	2	12	-10
48	4.098657185	3	14	-11
72	4.191610601	4	17	-13
96	3.791235566	5	1	4
120	4.189380214	6	13	-7
144	3.999414855	7	11	-4
168	4.073736189	8	11	-3
192	3.967391389	9	9	0
216	4.189564995	10	10	0
238	4.190610234	11	10	1
264	3.962565662	12	8	4
288	4.247742871	13	9	4

312	4.287860558	14	9	5
336	3.977984457	15	8	7
360	3.957047796	16	7	9
384	3.881474403	17	2	15
408	3.953849623	18	5	13
432	3.868850206	19	1	18
456	3.906877041	20	2	18
480	3.906816104	21	1	20
504	3.906938873	22	1	21

Table C. 9: MEA:DMAE Spearman's correlation result for 6%: 60°C

Degradation time (h)	**MEA/DMAE**	**Rank Time**	**Rank MEA:DMAE**	**d**
0	5.053513125	1	14	-13
24	5.179446	2	16	-14
48	5.283487399	3	19	-16
72	5.225651263	4	17	-13
96	5.13710679	5	15	-10
120	5.225150355	6	15	-9
144	5.392767194	7	16	-9
168	5.046115911	8	13	-5
192	5.245801088	9	14	-5
216	4.884527855	10	7	3

238	4.912817146	11	7	4
264	5.001413286	12	9	3
288	4.986556137	13	8	5
312	5.073116971	14	9	5
336	4.984739707	15	7	8
360	5.041138114	16	7	9
384	4.868399987	17	5	12
408	4.813425644	18	4	14
432	4.770475146	19	1	18
456	4.871890564	20	3	17
480	4.78682613	21	2	19
504	4.773625499	22	1	21

APPENDIX D: Kinetic Analysis

D.1: Rate Model Development

The NLReg software version 6.3 was used for the kinetic analysis for the rate of degradation.

The model generated was in the form of power law.

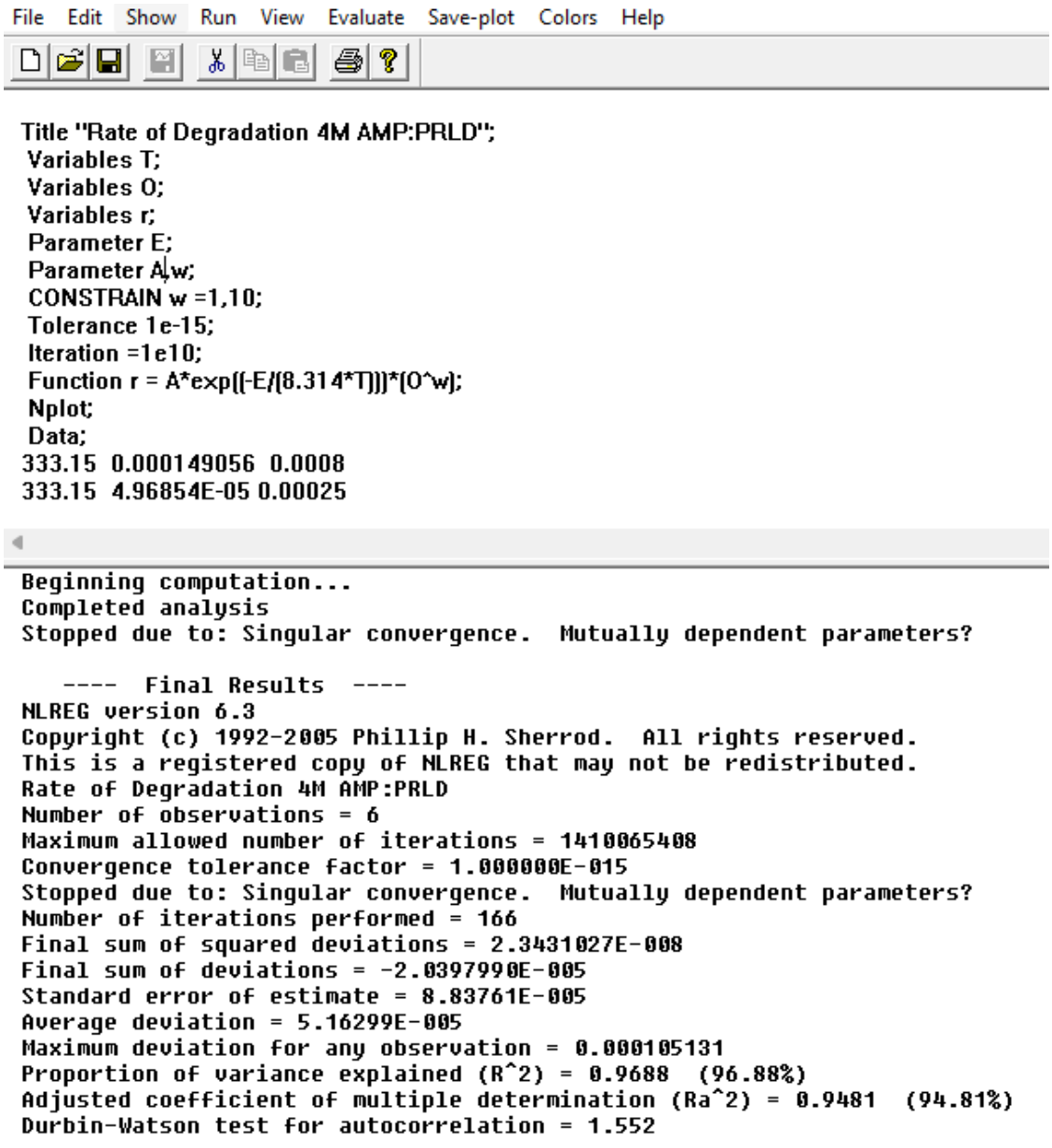

Figure D. 1: NLReg interface for rate prediction

```
Note: Parameter t-statistics and confidence intervals were not computed because
      constrain statements were used.
Analysis completed  2-Jul-2024 12:39.  Runtime = 0.06 seconds.
```

---- Descriptive Statistics for Variables ----

Variable	Minimum value	Maximum value	Mean value	Standard dev.
T	313.15	333.15	326.4833	8.164966
O	4.96854E-005	0.00016393	0.0001047342	5.439798E-005
r	7E-005	0.001	0.00047	0.0003878144

---- Calculated Parameter Values ----

Parameter	Initial guess	Final estimate
E	1	50314.08
A	1	6.82222529E+009
w	1	1.3035362

---- Analysis of Variance ----

Source	DF	Sum of Squares	Mean Square	F value	Prob(F)
Regression	2	7.28569E-007	3.642845E-007	46.64	0.00550
Error	3	2.343103E-008	7.810342E-009		
Total	5	7.52E-007			

Figure D. 2: NLReg interface for predicted parameters and statistical values

D.2: Calculation of the dissolved oxygen concentration in ppm and mol/Liter

The amount of dissolved oxygen in the amine was calculated with the equation developed by Rooney and Daniels,1998.

$$[O_2]_{ppm} = \frac{p}{K} \times \frac{32}{18} \times 10^6$$

Where $[O_2]$ is the dissolved oxygen concentration in parts per million, p is the atmosphere's partial pressure of oxygen, and 32/18 is the molecular weight of oxygen over water. K is the Henry's law constant in atm. Which can be calculated using the equation by (Xiang et al., 2016)

$$k = e^{-4.8727\times10 + 5.6026\times10^4/T - 1.7116\times10^7/T^2 + 1.6966\,10^9/T^3}$$

D.3: Validation of Kinetic Model for Degradation

Table D. 1: AMP:1-2(HE) PRLD kinetic model validation table of results

Experimental rate AMP:1-(2-HE) PRLD M/hr	**Temp (K)**	**O_2(mol/L)**	**Predicted rate AMP:1-(2-HE) PRLD (M/hr)**	**AD**
0.0008	333.15	0.000149056	0.000905132	0.131415269
0.00014	313.15	0.000186104	0.000378905	1.706462066
0.0004	333.15	9.93708E-05	0.000533545	0.333861387
0.00025	333.15	4.96854E-05	0.000216156	0.135376199
0.0006	323.15	0.00016393	0.000584022	0.026629433
0.0001	323.15	5.46433E-05	0.000139471	0.394712306
AAD =				**0.179**